

**MOISTURE DIFFUSION IN ASPHALT BINDERS AND FINE AGGREGATE
MIXTURES**

A Dissertation

by

KAMILLA LIMA VASCONCELOS

Submitted to the Office of Graduate Studies of
Texas A&M University
in partial fulfillment of the requirements for the degree of

DOCTOR OF PHILOSOPHY

May 2010

Major Subject: Civil Engineering

**MOISTURE DIFFUSION IN ASPHALT BINDERS AND FINE AGGREGATE
MIXTURES**

A Dissertation

by

KAMILLA LIMA VASCONCELOS

Submitted to the Office of Graduate Studies of
Texas A&M University
in partial fulfillment of the requirements for the degree of

DOCTOR OF PHILOSOPHY

Approved by:

Chair of Committee,
Committee Members,

Head of Department,

Dallas N. Little
Robert L. Lytton
Eyad Masad
Charles Glover
Amit Bhasin
John Niedzwecki

May 2010

Major Subject: Civil Engineering

ABSTRACT

Moisture Diffusion in Asphalt Binders and Fine Aggregate Mixtures.

(May 2010)

Kamilla Lima Vasconcelos, B.E., Universidade Federal do Ceará, (Fortaleza, Brazil);

M.Sc., Universidade Federal do Ceará (Fortaleza, Brazil)

Chair of Advisory Committee: Dr. Dallas N. Little

Moisture damage in asphalt mixtures is a complex phenomenon that involves mechanical, chemical, physical and thermodynamic processes. This damage contributes significantly to the premature deterioration of asphalt pavements, which leads to extra cost in highway maintenance and vehicle operations. One key mechanism of how moisture reaches the asphalt-aggregate interface is by its permeation or diffusion through the asphalt binder or mastic. Different techniques are available for diffusion coefficient measurement of a wide variety of polymer-solvent systems. For the asphalt-water system studied, the focus is on two techniques: (i) Fourier Transform Infrared (FTIR) – Attenuated Total Reflectance (ATR) spectrometry and (ii) Gravimetric Sorption Measurements. In the FTIR-ATR experiments, asphalt binders are under investigation. Water shows strong absorption in the infrared region and the FTIR-ATR technique has the ability to monitor both the kinetics of moisture ingress as well as any chemical changes occurring during the test. The changes in concentration can be directly related to change in the absorbance measured during the experiment. The hysteresis of water diffusion in asphalt binders is also monitored through this technique. In the gravimetric sorption experiments, cylindrical Fine Aggregate Mixtures (FAM) were investigated. The gravimetric techniques, which directly follow mass change with time, are among the most used techniques probably because of their simplicity. In this experiment, the Saturated Surface-Dry (SSD) weight of FAM samples at room temperature and at 100°F is monitored until it reaches the equilibrium. The measurements of: (i) water uptake and (ii) the diffusion coefficient were made at both temperatures. A dual mode diffusion model was shown to better represent the diffusion of water through asphalt binders. The rate of moisture diffusion in asphalt binders was proved to be dependent on the history of

exposure of the asphalt binder to the moisture. Moisture uptake and diffusivity of water through FAM is dependent on the type of aggregate and asphalt binder used to prepare the FAM.

DEDICATION

I dedicate this dissertation to my parents, Eduardo (in memoriam) and Deana, for the love and support that they always provided me to follow my dreams. It is also dedicated to my brother and sister, Lucas and Sabrina, for being the best siblings and friends. Their love gives me strength and makes my life better every day!

ACKNOWLEDGMENTS

I would like to express my gratitude to my advisor and committee chair, Dr. Dallas Little, who provide me with the opportunity and support to conduct this research. I extend my gratitude to Dr. Amit Bhasin, for his continuous support, guidance and encouragement during this entire journey. I am also grateful to my graduate committee members, Dr. Robert Lytton, Dr. Eyad Masad, and Dr. Charles Glover, for their valuable insights, and to Dr. Jorge Soares, who encouraged to pursue this dream.

Special thanks go to my parents, my grandparents, my brother and my sister for their unconditional love and continuous support in all the projects that I have pursued. I also want to thank Marcio Savasini for being such a wonderful partner and friend and for always encouraging my dreams in the past three years.

My gratitude is also expressed to my colleagues, Alex Alvarez, Belen Valdovinos, Christopher Jones, Pedro Sousa, Reza Ashtiani, SangIck Lee, Silvia Caro, Syam Nair, and Veronica Castelo Branco with whom I have shared several academic and personal conversations. Their friendship was one of the most valuable gifts I have received in College Station. Special thanks go to Veronica Castelo Branco for being the sister I have chosen and a special friend. I also want to thank the Brazilian Student Association (BRSA) at Texas A&M University for making me feel 'at home' during my almost five years in the United States. I have made friends that I will never forget. I could never forget to thank Mrs. Barbara Hein, Mrs. Cathy Bryan, and Mrs. Lupe Fattorini for their administrative assistance and affection.

I also appreciate the financial support provided by the Federal Highway Administration (FHWA) and the Western Research Institute (WRI) through the Asphalt Research Consortium (ARC) that made this research project possible and also to Capes/Fulbright for the sponsorship of my graduate studies at Texas A&M University. My appreciation is also extended to the Association of Asphalt Paving Technologists (AAPT) and to the International Road Federation (IRF) for their scholarships in 2008 and 2009, respectively.

NOMENCLATURE

A	Absorbance
AASHTO	American Association of State Highway and Transportation Officials
AFM	Atomic Force Microscopy
ANOVA	Analysis of Variance
AoI	Angle of Incidence
ASCE	American Society of Civil Engineers
CCD	Charge-Coupled-Device
CV	Coefficient of Variation
DC	Cycle of Dehydration
DMA	Dynamic Mechanical Analysis
d_p	Infrared Depth of Penetration
E_a	Activation Energy
EIS	Electrochemical Impedance Spectroscopy
FAM	Fine Aggregate Mixtures
FTIR-ATR	Fourier Transform Infrared – Attenuated Total Reflectance
HC	Cycle of Hydration
HMA	Hot Mix Asphalt
HPLC	High-performance Liquid Chromatography
IRE	Internal Reflection Element
MRL	Materials Reference Library
NMC	Non-Contact Mode
NMR	Nuclear Magnetic Resonance
PG	Performance Grade
PCSA	Polarizer-Compensator-Sample-Analyzer
RH	Relative Humidity
RoI	Region of Interest
SGC	Superpave Gyrotory Compactor
SHRP	Strategic Highway Research Program
SSD	Saturated Surface-Dry
T_g	Glass Transition Temperature

WRI	Western Research Institute
X-ray CT	X-ray Computed Tomography
ZnSe	Zinc Selenide

TABLE OF CONTENTS

	Page
ABSTRACT.....	iii
DEDICATION.....	v
ACKNOWLEDGMENTS	vi
NOMENCLATURE	vii
TABLE OF CONTENTS.....	ix
LIST OF FIGURES	xi
LIST OF TABLES.....	xv
1. INTRODUCTION.....	1
1.1 Overview.....	1
1.2 Problem Statement and Research Objectives.....	3
1.3 Dissertation Outline	4
2. MEASUREMENT OF WATER DIFFUSION IN ASPHALT BINDERS USING THE FTIR-ATR TECHNIQUE	6
2.1 Overview.....	6
2.2 Motivation and Background.....	6
2.2.1 Kinetics of Diffusion.....	7
2.2.2 Fourier Transform Infrared Spectroscopy – Attenuated Total Reflectance (FTIR-ATR).....	8
2.3 Materials and Methods.....	11
2.3.1 Sample Preparation	11
2.3.2 Film Thickness and Refractive Index Measurement.....	13
2.3.3 Measurement of Water Diffusion using FTIR-ATR.....	14
2.4 Results and Discussion.....	16
2.4.1 Analysis 1 – Fickian Diffusion Model	16
2.4.2 Analysis 2 – Dual Mode Diffusion Model.....	17
2.4.3 Statistical Analysis.....	20
2.4.4 Simplified Example to Demonstrate Implications	20
2.5 Summary and Recommendations.....	22
3. EXPERIMENTAL MEASUREMENT OF WATER DIFFUSION THROUGH FINE AGGREGATE MIXTURES	24
3.1 Introduction.....	24
3.2 Background on Kinetics of Diffusion	27

	Page
3.3 Experimental Design.....	28
3.3.1 Materials and Specimens Fabrication	28
3.3.2 Test Method	29
3.3.3 Background on Analysis	30
3.4 Results and Discussion.....	33
3.4.1 Water Uptake	33
3.4.2 Diffusivity	35
3.4.3 The Effect of Temperature on the Diffusivity of Water.....	37
3.5 Summary and Conclusions.....	39
4. HISTORY DEPENDENCE OF WATER DIFFUSION IN ASPHALT BINDERS	41
4.1 Introduction and Background.....	41
4.2 Experimental Design.....	42
4.2.1 Sample Preparation and Test Method	42
4.2.2 Analysis.....	44
4.3 Results and Discussion.....	47
4.3.1 Statistical Analysis.....	50
4.3.2 Dissolution and Loss of Asphalt Binder in Water.....	51
4.3.3 Change in Microstructure of the Asphalt Binder	52
4.3.4 Residual Moisture within the Asphalt Binder	54
4.4 Conclusions.....	56
5. CONCLUSIONS, RECOMMENDATIONS, AND FUTURE WORK	58
5.1 Detailed Conclusions and Recommendations.....	58
5.1.1 Water Diffusion in Asphalt Binders.....	58
5.1.2 Water Diffusion in Fine Aggregate Mixtures	59
5.1.3 History Dependence of Water Diffusion in Asphalt Binders.....	60
5.1.4 The Physical State of Water and the Diffusion in Asphalt Binders	62
5.2 Future Work.....	62
REFERENCES	65
APPENDIX A.....	74
APPENDIX B.....	81
APPENDIX C.....	99
VITA.....	109

LIST OF FIGURES

FIGURE		Page
2-1	Scheme of an ATR Cell and the Depth of Penetration.....	10
2-2	Chamber Designed to Hold the Water during the Test	12
2-3	Spectra of Thin Asphalt Film under Water	15
2-4	Blank Spectrum of Liquid Water.....	15
2-5	Illustration of Quantitative Analysis	16
2-6	Result Obtained by (a) Analysis 1 (Fickian Diffusion Model) and (b) Analysis 2 (Dual Mode Diffusion Model) for Asphalt AAB.....	18
2-7	Result Obtained by (a) Analysis 1 (Fickian Diffusion Model) and (b) Analysis 2 (Dual Mode Diffusion Model) for Asphalt AAD.....	19
2-8	Result Obtained by (a) Analysis 1 (Fickian Diffusion Model) and (b) Analysis 2 (Dual Mode Diffusion Model) for Asphalt AAF.....	19
2-9	Result Obtained by (a) Analysis 1 (Fickian Diffusion Model) and (b) Analysis 2 (Dual Mode Diffusion Model) for Asphalt ABD.....	19
2-10	Illustration of the Example Shown in Table 2-2.....	22
3-1	HMA and the Corresponding FAM Gradation	29
3-2	(a) 150mm (6 inches) Diameter Sample, (b) Sawing and (c) Coring Process	29
3-3	Scheme of Possible Locations Where the Water Can Be during the Gravimetric Sorption Test	30
3-4	Water Uptake by Original Mass of the FAM Samples	34
3-5	Water Uptake Measured for the Last Collected Reading and Estimated Using the Dual Mode Diffusion Model	35

FIGURE	Page
3-6	Diffusivity Results Obtained for the Samples Tested at Room Temperature and at 100°F Using the Dual Mode Diffusion Model 37
3-7	Activation Energy Obtained by the Arrhenius Law 39
4-1	System Configuration and Infrared Depth of Penetration 43
4-2	(a) Chamber (to Hold the Water above the Asphalt Film) Attached to the ATR Cell, (b) Chamber Top View (Cover Removed)..... 44
4-3	Region of Analysis Used to Quantify Change of Water Concentration into the Asphalt Binder with Time..... 45
4-4	Concentration Profile for Asphalt AAB in: (a) HC 1, (b) HC 2, and (c) HC 3..... 49
4-5	AFM Images from Asphalt AAD, (i) 25 μm^2 and (ii) 5 μm^2 53
4-6	AFM Images of Asphalt AAD after 4 Days of Water Exposure, (i) 25 μm^2 and (ii) 5 μm^2 54
4-7	Illustration of Dehydration Cycles (Asphalt AAB)..... 55
4-8	Quantification of the Presence of Water Vapor into the Asphalt Film (Peak Height at 3853 cm^{-1} for Asphalt AAB)..... 56
5-1	Overall Test Procedure Used for the Measurement of Water Diffusion in Asphalt Binder Films 59
5-2	Overall Test Procedure Used for the Measurement of Water Diffusion in Fine Aggregate Mixtures 60
5-3	Humidity Chamber Designed to Keep the Specimens at a Controlled Relative Humidity 63
B-1	Two Possible Configurations for the Film Thickness on the Top of the ATR Cell 82
B-2	(a) Spin Processor, and (b) Covered Stationary Seal..... 83

FIGURE	Page
B-3	Configuration of (a) the Glass Slide Attached to the ATR Plate on the Top of the Vacuum Chuck, and (b) the Glass Slide Covering the O-ring..... 83
B-4	Spin Coater Display with the Set Speed and Time 84
B-5	Chamber Attached to the ATR Plate..... 85
B-6	Illustration of the Dry Nitrogen Purge and Annealing at 50°C 85
B-7	Nanofilm EP3-SE and the Si Substrate Coated with Asphalt 86
B-8	Default Ellipsometer Window with the ‘Control and Live Images’ and the ‘Script Tree’ 87
B-9	Some Steps for the Ellipsometric Measurement 89
B-10	Some Steps of the Fitting Process for the Ellipsometric Measurements..... 91
B-11	FTIR-ATR – ‘Experiment Setup’ Window..... 93
B-12	FTIR-ATR – Illustration of Background Collection..... 94
B-13	FTIR-ATR – Illustration of Sample Collection with Time..... 95
B-14	Spectra after Subtraction of Asphalt without Water..... 95
B-15	Region of Analysis Used to Quantify Change of Water Concentration into the Asphalt Binder with Time 96
B-16	Data and the Dual Mode Diffusion Model 97
C-1	Potential Forms by which the Moisture Can Reach the Asphalt/Aggregate Interface: (i) Defect on Asphalt Coating, (ii) Wet Aggregates, and (iii) Diffusion through the Asphalt/Mastic 99
C-2	Arrangement Patterns of Water Molecules at Different Physical States: (a) Ice, (b) Liquid, and (c) Vapor 100
C-3	Fundamental Vibration Transitions: (i) Symmetric Stretching, (ii) Bending, and (iii) Asymmetric Stretching 101

FIGURE		Page
C-4	Comparison of Water Spectra in Vapor and Liquid Form (Source: Termo Fischer Scientific).....	102
C-5	Illustration of Water Spectra in Different Physical States, Adapted from Ewing et al. (2003).....	102
C-6	Film Thickness Configurations Used in the Experiments.....	104
C-7	Difference in Depth of Penetration in Both Regions Evaluated (ZnSe Crystal with $\theta=45^\circ$, and Refractive Index of Asphalt Assumed 1.5).....	106
C-8	Partial Results Obtained for Film Thickness in Both Configurations Presented in Figure C-6.....	107
C-9	Partial Results of Absorbance with Time for Asphalt AAD – Configuration (i), (a) Liquid Water Region, and (b) Water Vapor Region..	108
C-10	Partial Results of Absorbance with Time for Asphalt AAD – Configuration (ii), (a) Liquid Water Region, and (b) Water Vapor Region.	108

LIST OF TABLES

TABLE		Page
2-1	Summary of the Diffusivity Values.....	20
2-2	Simplified Example of Susceptibility of Adhesive Failure	21
3-1	Diffusion Coefficients for FAM with Different Characteristics.....	26
3-2	Summary of Diffusion Coefficient Values	36
4-1	Average Results Obtained for Diffusivity Values	48
4-2	Statistical Analysis	51

1. INTRODUCTION

1.1 OVERVIEW

Many forms of distress observed in asphalt pavements are caused or exacerbated by the presence of moisture. The moisture damage phenomenon is complex and involves thermodynamic, chemical, physical and mechanical process. Caro et al. (2008) reported that the moisture damage mechanism is comprised of two phases: (i) moisture transport, and (ii) response of the system. There are three main mechanisms of moisture transport into and within asphalt pavement (moisture transport) (Masad et al. 2007): (i) infiltration of surface water, (ii) permeation or diffusion of water vapor, and (iii) capillary rise of subsurface water. In addition to these processes the probability exists that residual moisture is present with the aggregate particles. The absorbed moisture may be the result of inadequate or incomplete drying in the mix plant. The problem remains a somewhat unresolved issue particularly since warm mix asphalt technology is of such interest in today's environment.

With the understanding that in the mix design process, volumetrics and the air void structure controls permeation of moisture at the 'macro-scale', the focus of the dissertation is moisture diffusion at a smaller scale: in the fine aggregate matrix (FAM) and (ultimately) in the asphalt binder.

Diffusion is the process by which matter is transported from one part of a system to another as a result of random molecular movements; result from a concentration gradient. Moisture transport in asphalt binders is similar to moisture transport in polymers. When polymers are exposed to humid environments, they absorb significant amounts of water, which adversely affects their physical and mechanical properties. Asphalt binders demonstrate similar behavior. Relative pressure, temperature, physical state of the water, and structure of the polymer are examples of the factors that influence the moisture diffusion through this type of material. Some of the documented effects caused by water diffusion are plasticization, change of physical properties, hygrothermal degradation, and swelling stress.

This dissertation follows the style of *Journal of Materials in Civil Engineering, ASCE*.

Strong localized interactions can occur between the water molecule and suitable polar groups of the polymer. Barrie (1968) have proposed that water is comprised of two species: the species that forms molecular solution and the species that are confined into areas of abnormally large free volume. The sorptive capacity of a polymer depends not only on the nature of the groups presented, but also on their position on the polymer chain. In general, a higher number of polar groups in the polymer matrix results in higher sorptive affinity with water. However, the accessibility of these groups, the degree of crystallinity of the matrix and the relative strengths of water-water and water-polymer bonds are important factors in deciding the total water absorption.

Fick's law is generally used for the mathematical model of the diffusion process. It assumes constant pressure and temperature throughout the sample and no long-range electrostatic interactions. Assuming that Fick's law is relevant to modeling diffusion, the diffusion coefficient may be treated in different ways, such as (Karlsson and Isacson 2003a):

- a single diffusion coefficient;
- a concentration-dependent diffusion coefficient; and
- a diffusion coefficient distributed by a probability function.

Fickian diffusion of a single solute in a polymer film can be described by the one-dimensional continuity equation:

$$\frac{\partial C}{\partial t} = D \frac{\partial^2 C}{\partial z^2} \quad (1-1)$$

where, C is the penetrant concentration, t is the time, and D is the diffusion coefficient. The analytical solution to the Equation (1-1) will depend on the initial and boundary conditions. For more complex systems this equation can be modified to incorporate diffusion constants that depend on concentration, inhomogeneity of the media, and a host of boundary conditions which can take many forms.

There are also some cases where the diffusion behavior departs from the Fickian criteria. The following anomalous sorption behaviors have been reported (Frisch 1980):

- pseudo-Fickian behavior in which the sorption curve plotted versus $t^{1/2}$ shows an anomalous small initial linear region, but departs from film thickness scaling;
- sigmoidal behavior of the sorption curve that is encountered when M_t/M_∞ is plotted against $t^{1/2}$;

- two-stage sorption: after an initial rapid uptake, the sorption curve as a function of $t^{1/2}$ approaches a quasi-equilibrium, followed by a slow approach to a final true equilibrium; and
- time dependent surface concentration.

Different techniques are available for diffusion coefficient measurement of a wide variety of polymer-solvent systems. Some of them are found in the literature: conventional gravimetric sorption (Artamendi and Khalid 2006; Doumenc et al. 2005; Gonzalez et al. 2007; Hong et al. 1997; Larobina et al. 2007), FTIR-ATR spectroscopy (Doppers et al. 2006; Hong et al. 1997; Karlsson and Isacsson 2003a; Karlsson and Isacsson 2003b; Larobina et al. 2007; McKnight and Gillespie Jr. 1997), magnetic suspension balance (Schabel et al. 2007), quartz crystal microbalance/heat conduction calorimeter (Smith et al. 2006), laser interferometer (Tong et al. 1989), capillary column inverse gas chromatography (Pawlisch et al. 1987), nuclear magnetic resonance (NMR) spectroscopy (Korsmeyer et al. 1986), soaking test (Kassem et al. 2006) and dynamic shear rheometer (Karlsson and Isacsson 2003b). Two of these techniques will be addressed in this dissertation: (i) FTIR-ATR spectroscopy, and (ii) gravimetric sorption.

1.2 PROBLEM STATEMENT AND RESEARCH OBJECTIVES

The highway system connects people with a wide range of opportunities available across the country and also provides a vital link to a country's economic development. In the USA, approximately 85% of the pavements are flexible. Moisture damage contributes significantly to the premature deterioration of asphalt pavements, which results in substantial costs to maintain, repair and rehabilitate the highway infrastructure system. Among the mechanisms of moisture transport within the asphalt pavements is the process of diffusion. It is the process by which moisture reaches the asphalt-aggregate interface, and is the focus of this research. The main objectives of this study are:

- determine the water diffusion coefficient of asphalt binders using the FTIR-ATR technique;
- determine the water diffusion coefficient in fine aggregate mixtures using gravimetric sorption measurements at different temperatures; and
- determine the history dependence of water diffusion in asphalt binders using the FTIR-ATR technique.

1.3 DISSERTATION OUTLINE

This dissertation combines three papers, presented according to the style and format of the Journal of Materials in Civil Engineering, ASCE, as well as the guidelines provided in the Texas A&M University Thesis Manual. The dissertation is organized in five sections as subsequently described.

Section 1 presents an introduction that includes overview, problem statement and research objectives, and the dissertation outline. A relevant literature review is included in the appropriate section of each paper according to the corresponding topic treated in the paper.

Section 2 presents a paper related to the measurement of water diffusion in asphalt binders using the FTIR-ATR technique. This paper was accepted for presentation at the Transportation Research Board Meeting in Washington, DC, 2010. The revised paper is being reviewed for possible publication in the Journal of the Transportation Research Board. The authors of this paper are Kamilla L. Vasconcelos, Amit Bhasin and Dallas N. Little.

Section 3 presents a paper related to the measurement of water diffusion in fine aggregate mixture using gravimetric sorption. This paper was submitted for publication in the Journal of Materials in Civil Engineering (ASCE), and the authors are Kamilla L. Vasconcelos, Amit Bhasin, Dallas N. Little and Robert L. Lytton.

Section 4 presents a paper that addresses the history dependence of water diffusion in asphalt binders. This paper will be submitted for publication in the International Journal of Pavement Engineering and the authors are Kamilla L. Vasconcelos, Amit Bhasin and Dallas N. Little.

Section 5 presents the conclusions and recommendations of the dissertation. In addition, topics for further research are suggested in this section.

Appendix A has the detailed development of the FTIR-ATR diffusion model, originally proposed by Fieldson and Barbari (1993).

Appendix B has the detailed procedure used for the diffusion measurements using the FTIR-ATR. Focus was established in: sample preparation using the spin coater, film thickness and refractive index measurement by the ellipsometer; and the test procedure used in the FTIR-ATR.

Appendix C has the literature review and some preliminary results obtained in the comparison between water diffusion in the liquid state with the moisture (or vapor) state, both at

room temperature. This section is part of an ongoing research conducted by Kamilla L. Vasconcelos, Amit Bhasin, Dallas N. Little and Charles Glover.

2. MEASUREMENT OF WATER DIFFUSION IN ASPHALT BINDERS USING THE FTIR-ATR TECHNIQUE*

2.1 OVERVIEW

The presence of moisture in asphalt mixtures deteriorates its structural integrity. Moisture also acts as a catalyst to promote other forms of pavement distresses. Two critical factors influence the rate and intensity of moisture induced damage: the speed of moisture transport within the asphalt mixture and binder, and the influence of moisture on the cohesive and adhesive properties of the constituent materials. Quantifying these two factors is essential in order to understand, model, and mitigate moisture-induced damage in asphalt mixtures. This paper presents the experimental and analytical procedures used to measure water diffusivity in asphalt binders. Fourier Transform Infrared-Attenuated Total Reflectance (FTIR-ATR) spectroscopy was used to monitor the diffusion of water into thin films of asphalt binder. The diffusion process was characterized by changes in the portions of the spectra that correspond to the presence of water. Two models were used to fit the data obtained: (i) a diffusion model that follows Fick's second law, and (ii) a dual mode diffusion model with two diffusion coefficients (D_1 and D_2) and weighting factor X_1 . Four asphalt binders were evaluated (AAB, AAD, AAF, and ABD), and the diffusion characteristics of all four were better represented by the dual mode diffusion model. The diffusivity of asphalt binders AAB, AAD and AAF were statistically similar, while the diffusivity of asphalt binder ABD was different from all other three.

2.2 MOTIVATION AND BACKGROUND

Several damage mechanisms in asphalt pavements are caused by or their severity increased due to the presence of moisture. The moisture damage phenomenon is complex and involves chemical, physical, thermodynamic, and mechanical processes. These processes can be grouped into two broad categories that dictate the rate and intensity of moisture-induced in mixtures. First is the speed with which moisture migrates to the interior of the mixture. Second is the influence of moisture on the adhesive and cohesive properties of the constituent materials in the mixture. Both these factors are equally important when quantifying and seeking to mitigate

* Accepted for presentation "Measurement of Water Diffusion in Asphalt Binders using the FTIR-ATR Technique" by Kamilla L. Vasconcelos, Amit Bhasin, and Dallas N. Little. *Transportation Research Board Meeting*, 2010, Washington, DC.

moisture-induced damage in asphalt mixtures. Ideally for a mix to be resistant to moisture-induced damage it is desirable that its constituent materials are inherently resistant to the influence of moisture. Further, it is also desirable to produce a mixture with material constituents and a microstructure that is resistant to damage from moisture. Despite inherent moisture sensitivity of the materials used in asphalt mixtures, the mixture may demonstrate reasonable resistance to moisture-induced damage provided that the diffusivities of moisture through the mixture and binder are very low.

Few references were found reporting the water diffusion coefficient of asphalt binders. The results vary significantly depending on the experimental method, plate substrate, and equipment used. Nguyen et al. (2005) measured the apparent diffusion coefficient on thin asphalt binder films on siliceous ATR plates using the FTIR-ATR technique. The results reported were in the range from 1.4×10^{-14} to 3.3×10^{-14} m²/s. Wei (2009) measured the water diffusion coefficient in asphalt binders using the Electrochemical Impedance Spectroscopy (EIS). He used thin films of asphalt on aluminum plate substrate and the results ranged from 1.5×10^{-17} to 4.2×10^{-17} m²/s.

The focus of this study was to use spectroscopic techniques to determine the diffusivity of water through thin films of asphalt binder. This paper summarizes the findings from this study. Measurements for four different binders are reported. A simplified example to demonstrate the importance of combining diffusivity with material properties to assess moisture sensitivity is also presented.

2.2.1 Kinetics of Diffusion

Fick's second law is generally used to model diffusion driven by concentration gradients in different materials. It assumes constant pressure and temperature throughout the sample and the absence of any long-range electrostatic interactions. The Fickian diffusion of a single solute in a polymer film can be described by the one-dimensional continuity equation:

$$\frac{\partial C}{\partial t} = D \frac{\partial^2 C}{\partial z^2} \quad (2-1)$$

where, C is the penetrant concentration, t is the time, and D is the diffusion coefficient. The analytical solution to the Equation (2-1) depends on the initial and boundary conditions. For more complex systems, this equation can be modified to incorporate diffusion constants that

depend on concentration, inhomogeneous media, and a host of boundary conditions which can take many forms.

Schlotter and Furlan (1992) presented a concise explanation of three different cases of solvent diffusion in polymers. While asphalt binders are chemically different from polymers, these three cases provide useful insight into understanding the characteristics of moisture diffusion.

- Case I – Fickian diffusion occurs when the rate of diffusion is much less than the relaxation rate of the polymer. This is based on a simple diffusion model in which the Fickian solution shows a linear mass sorption increase relative to $t^{1/2}$ (where t is time).
- Case II – diffusion is very rapid compared to the polymer relaxation process. Frequently a sharp solvent front, which propagates into the polymer at a constant velocity, is associated with Case II diffusion. Thomas and Windle (1982) mention that Case II is characteristic of systems in which the permeating substance substantially swells the polymer.
- Case III – non-Fickian or anomalous diffusion occurs when the diffusion and relaxation process rates are similar.

2.2.2 Fourier Transform Infrared Spectroscopy – Attenuated Total Reflectance (FTIR-ATR)

Fourier Transform Infrared (FTIR) – Attenuated Total Reflectance (ATR) spectroscopy is a robust and accurate noninvasive in-situ method that can provide short-time data identifying the various functional groups present in the material. This technique has also been used to examine diffusion in polymers, with investigations covering a diverse range of applications. Elabd and coworkers (2003) provide an extensive literature review on different applications of the FTIR-ATR, especially on the technique's ability to identify unique chemical species arising from molecular interaction. Harrick (1965) presents a detailed description of the quantitative aspects of internal reflection spectroscopy, particularly when infrared absorbing species are uniformly distributed in either a thin film or an infinitely thick sample. A series of papers and reports were also published by Nguyen and coworkers about the use of this technique to address water at the interface between different organic coatings, including asphalt binder, and substrates (Nguyen et al. 1994; Nguyen et al. 1995a; Nguyen et al. 1995b; Nguyen et al. 1996a; Nguyen et al. 1996b; Nguyen et al. 2005; Nguyen et al. 1991a; Nguyen et al. 1991b).

ATR spectroscopy differs from normal transmission spectroscopy in the nature of the incident light path. When total reflection of a light beam or electromagnetic field occurs at the boundary between the internal reflection element (IRE) surface (ATR cell) and a rarer medium (e.g., a polymer or asphalt binder film), penetration of the electromagnetic field into the rarer medium occurs (Figure 2-1). This electromagnetic field forms an evanescent wave caused by the interference of the incident and reflected waves. The magnitude of the evanescent wave can be expressed as follows (Griffiths and de Haseth 2007):

$$E = E_0 e^{-\gamma z} \quad (2-2)$$

where, E is the strength of the electric field, E_0 is the field strength at the interface, γ

$\left(\gamma = \frac{1}{d_p}\right)$ and z are the decay coefficient and the distance from the reflecting surface of the evanescent wave, respectively.

In FTIR-ATR, the depth of penetration of the infrared (d_p), illustrated in Figure 2-1, is defined as the distance from the IRE surface, over which the magnitude of the penetrating electric field diminishes by a factor of $\frac{1}{e}$ and is given by the following expression (Griffiths and de Haseth 2007):

$$d_p = \frac{\lambda}{2\pi n_2 \left(\sin^2 \theta - \left(\frac{n_2}{n_1} \right)^2 \right)^{1/2}} \quad (2-3)$$

where, λ is the wavelength of the radiation in vacuum, θ is the angle of incidence, and n_1 and n_2 are the refractive indices of the IRE and the sample respectively.

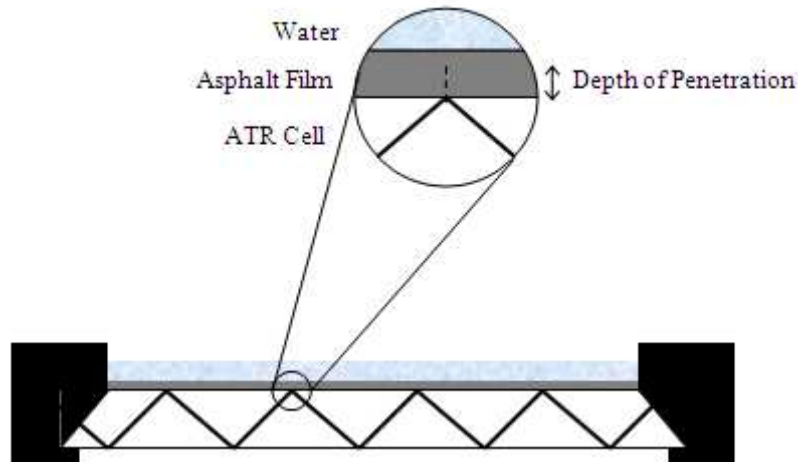


Figure 2-1. Scheme of an ATR Cell and the Depth of Penetration

Although the probing depth can be up to three times of d_p (Mirabella Jr. 1990), because of the rapid decay of the evanescent wave, more than 85% of the total absorption intensity corresponds to the material within d_p (Iwamoto and Ohta 1984). The use of a thinner prism, a longer prism, a smaller angle of incidence, or a combination of these factors would increase the ability to detect of water at the coating/substrate interface by the FTIR-ATR technique.

The advantage of using the FTIR-ATR technique is that it has the ability to monitor both the kinetics of moisture ingress as well as any chemical changes that occur during the test. The changes in concentration can be directly related to change in absorbance measured during the experiment. The physics of FTIR-ATR can be incorporated with a suitable diffusion model to evaluate the kinetics of the diffusion process. Some of the challenges associated with the use of this technique are that the FTIR spectra can be affected by (a) gel formation; (b) swelling of the material; and (c) rapid exchange of protons between the solvent and the material. However, according to Doppers et al. (2006), the exchange of protons is probably too slow to have a very significant effect. Further, Elabd et al. (2003) mentioned that spectroscopically, water is considered to be one of the most difficult molecules to interpret with a broad OH stretching vibration between $3,800$ and $3,000\text{ cm}^{-1}$, revealing a distribution of self-associated clusters that are sometimes difficult to de-convolute.

2.3 MATERIALS AND METHODS

In this study, four asphalt binders were selected from the Strategic Highway Research Program (SHRP) Materials Reference Library (MRL): AAB is a PG 58-22 grade binder from Wyoming, AAD is a PG 58-22 grade California Coastal, AAF is a PG 64-10 from W Texas, and ABD is a PG 58-10 California Valley (Jones IV 1993). The procedure used to determine the diffusivity of water through these binders is described in the following subsections.

The following subsection details the procedure that was used to prepare the sample for testing.

2.3.1 *Sample Preparation*

Stock solutions for different asphalt binders were prepared using 1.5 g of asphalt dissolved in 11 mL of HPLC grade toluene to facilitate the production of thin films. Previous studies conducted at the Western Research Institute (WRI) indicate that asphalt binder in a toluene solution does not compromise the physio-chemical characteristics of the binder after the toluene is removed. These previous studies also indicate that bitumen molecules in a toluene solution have similar kinetics to those of molecules in liquid bitumen at elevated temperatures (WRI 2001).

The asphalt solutions were prepared approximately 12h before use to guarantee that the solvent had dissolved all the asphalt in the container. A spin coater (Laurell WS-650S) was used to produce thin and homogeneous films of asphalt. The equipment supports rotation speed from 100 to 8000 rpm, with a repeatability of ± 0.5 rpm. The processor is equipped with a 44 mm vacuum chuck for substrates with diameters ranging from 50 to 100 mm. The MultiBounce ATR ZnSe (Zinc Selenide) flat plate was used as the substrate, and the spin coater was adjusted to rotate at 1000 rpm for 10 s. The substrate was spin coated two times to ensure complete coverage of the ATR plate by the asphalt solution. The rotation speed, time, and number of layers were obtained after conducting several trials to obtain an optimal film thickness.

After spin coating, the sample was placed in a chamber connected to a dry nitrogen purge for 2 h to eliminate the solvent (toluene) that was used to prepare the film. Afterwards, to eliminate possible micro capillaries in the asphalt film that might have been created due to the vaporization of toluene under nitrogen purge, the sample was annealed for 1 h at 50°C. A chamber was designed to be attached to the ATR cell and contain the water over the thin film during the test (Figure 2-2).

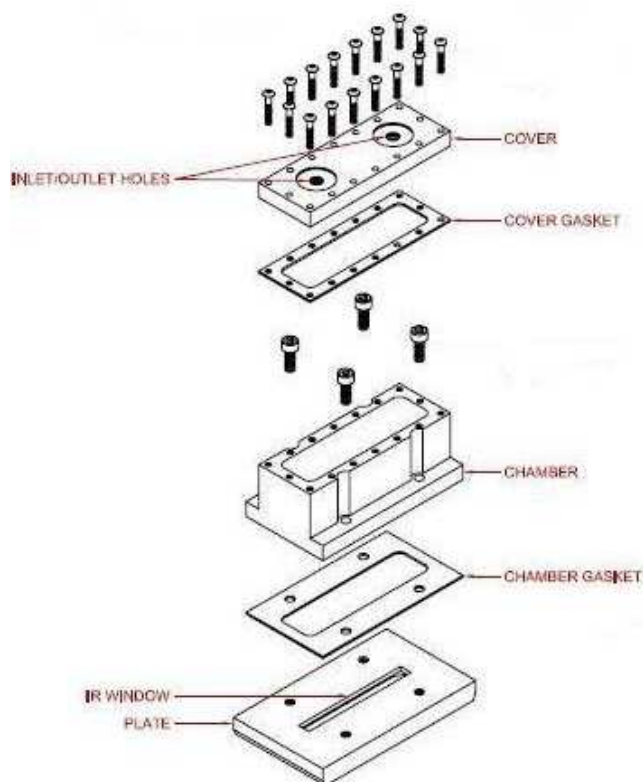


Figure 2-2. Chamber Designed to Hold the Water during the Test

The target film thickness was an important consideration while preparing specimens. There are two possible cases for the specimen film thickness. The first case is when the film thickness is much greater than the effective depth of penetration, d_p . In this case when a constant boundary condition (100% saturation) is achieved by adding water to the top of the film, water diffusion starts from the upper surface of the film that is beyond the detection range of the FTIR spectra. Therefore, one would have to wait for an undefined and perhaps experimentally unreasonable amount of time until moisture diffuses to within the effective depth of penetration and is detected in the spectra. Change in concentration of water within the film over time is quantified by correcting for the time of arrival of moisture and film thickness. The second case is when the film thickness is less than the effective depth of penetration, d_p . In this case when water is added to the top of the film, a portion of the water over the film as well as the entire film is immediately detected in the spectra. Change in concentration of water within the film over time is quantified by subtracting the initial spectra at time $t = 0$ s from the spectra detected at a

specific point in time. In this study, both approaches were used for trial experiments but the later was preferred due to practical considerations.

Another important consideration was not to have a very thin and homogeneous film. Other research studies have shown that the diffusivity of liquids through very thin polymer films is not representative of diffusivity through the bulk (Vogt et al. 2004). However, the limit at which diffusivity changes as a function of film thickness was in the order of tens of nanometers. This study ensured that all films were in the one micron range. Once the thin film samples were prepared, the next important step was to accurately measure the thickness of the thin film. The following section details the procedure that was used to measure the thin film thickness.

2.3.2 Film Thickness and Refractive Index Measurement

Film thickness and refractive index of the material are inputs required to calculate diffusivity of water through thin films of asphalt binder. In this study an ellipsometer was used to determine the thickness and optical properties of the film. Upon reflection from a plane surface, linearly polarized radiation generally becomes elliptically polarized. Its polarization state can be described by two ellipsometric parameters: amplitude ratio ($\tan\psi$) and phase shift difference (Δ) of two mutually orthogonal polarized components of the reflected wave (r_s and r_p) (Hinrichs et al. 2005). The complex reflectance ratio ρ is defined as:

$$\rho = R_p / R_s = \tan \Psi e^{i\Delta} \quad (2-4)$$

where, R_p and R_s are the complex reflection coefficients of light polarized parallel and perpendicular, respectively, to the plane of incidence. In this study, the Nanofilm EP3-SE model ellipsometer was used to measure values of amplitude ratio ($\tan\psi$) and phase shift difference (Δ) for the film. The ellipsometric data was evaluated modeling the sample as a layered structure: air / asphalt film / substrate. The data were used with three-parameter Cauchy function using built-in software to determine the thickness and refractive index of the film.

The ATR cell is transparent and therefore could not be used with the ellipsometer as a substrate to measure the thickness of the asphalt film. Instead, the same procedure was used to cast thin films on silica wafers as substrates. The Si wafer substrate produces more accurate results because of its reflectivity and known optical properties. The roughness of Si wafer and ZnSe crystal and differences in the thickness of the film casted on both surfaces were unlikely to be significant.

Each time a thin film specimen was prepared by spin coating the ATR cell, the same asphalt solution was subjected to exactly the same procedure to immediately spin coat a Si wafer. The thickness of the film as well as optical properties were measured using the ellipsometer. The film thickness and refractive index of specimens varied from 0.66 micron to 1.3 microns, and 1.22 to 1.65, respectively. This variation does not affect the final results since the model for diffusion incorporates these parameters.

After preparing the sample and establishing the film thickness, the next step was to measure the diffusion of water through the thin films of asphalt binder using the FTIR. The following two sections discuss the test procedure that was followed to collect the relevant data and the concomitant analysis to determine diffusivity of water through the asphalt binder.

2.3.3 Measurement of Water Diffusion Using FTIR-ATR

The Thermo Scientific Nicolet 6700 FTIR was used to collect the IR spectra. All spectra were the result of 32 scans and were collected at a 4 cm^{-1} resolution in the $900\text{-}4000 \text{ cm}^{-1}$ range. Unpolarized light at an incident angle of 45° was used and all spectra plotted in the absorbance (A) mode. Data were collected at periodic intervals for at least 15 days, with the final spectrum serving as a reference for the final saturation values (A_{eq}) of the absorption band.

The FTIR-ATR technique does not directly measure mass of the diffusant at a given depth, but provides absorbance at any time t (A_t). The absorbance is proportional to the total instantaneous mass of the diffusant (M_t) within the film. When a polymer film of thickness $2l$ on an ATR plate is exposed to an infinite reservoir, assuming weak absorption and constant polymer refractive index, the following equation can be derived in terms of absorbance (Fieldson and Barbari 1993):

$$\frac{A_t - A_0}{A_{eq} - A_0} = 1 - \frac{8\gamma}{\pi[1 - \exp(2l\gamma)]} \sum_{n=0}^{\infty} \left[\frac{\exp\left(\frac{-D(2n+1)^2 \pi^2 t}{4l^2}\right) \left[\frac{(2n+1)\pi}{2l} \exp(-\gamma 2l) + (-1)^n (2\gamma) \right]}{(2n+1) \left(4\gamma^2 + \left(\frac{(2n+1)\pi}{2l} \right)^2 \right)} \right] \quad (2-5)$$

where, γ is the evanescent field decay coefficient (inverse of the depth of penetration and previously described in Equation 2-3), A_0 is the absorbance at time zero, and D is the diffusivity. Equation 2-5 is similar to the mass uptake equation used in gravimetric sorption experiments, with the main difference being that the Fickian concentration profile is convoluted with the FTIR-ATR absorption equation before it is integrated (Fieldson and Barbari 1993).

As mentioned before, in this study thin films were used so that the electric field did not decay completely inside the asphalt sample (Figure 2-3). The same concept was reported by Pereira and Yarwood (1996a), and in order to obtain the ATR spectrum of water absorbed by thin films it is necessary to subtract the spectra of pure liquid water from the spectra of the film-water composite. However, the OH stretching band for pure liquid water is more intense than the OH band intensity for the film-water system, because the film is an absorbing material and works as a barrier. Therefore, the subtraction would produce negative bands. In order to avoid this problem, we subtracted the spectra of the film-water composite for the first hydration time from the spectra of the film-water composite at subsequent times. Figure 2-4 illustrates the blank spectrum of liquid water at room temperature.

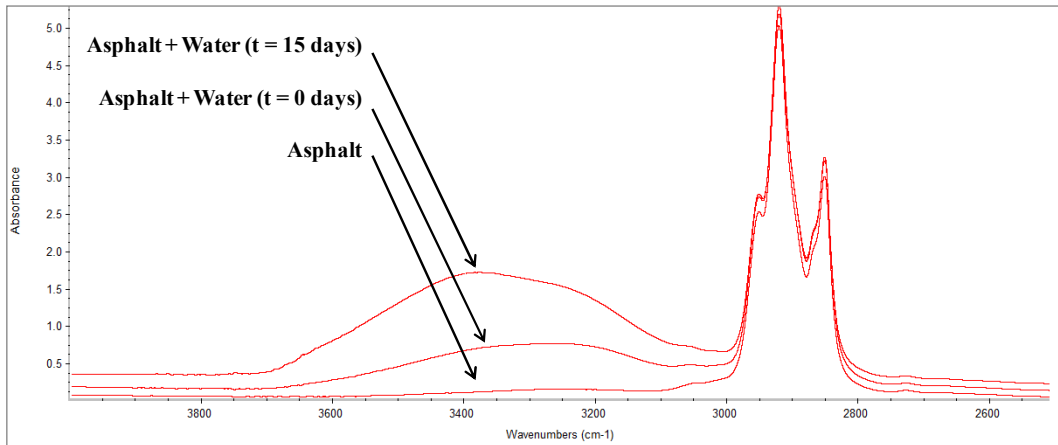


Figure 2-3. Spectra of Thin Asphalt Film under Water

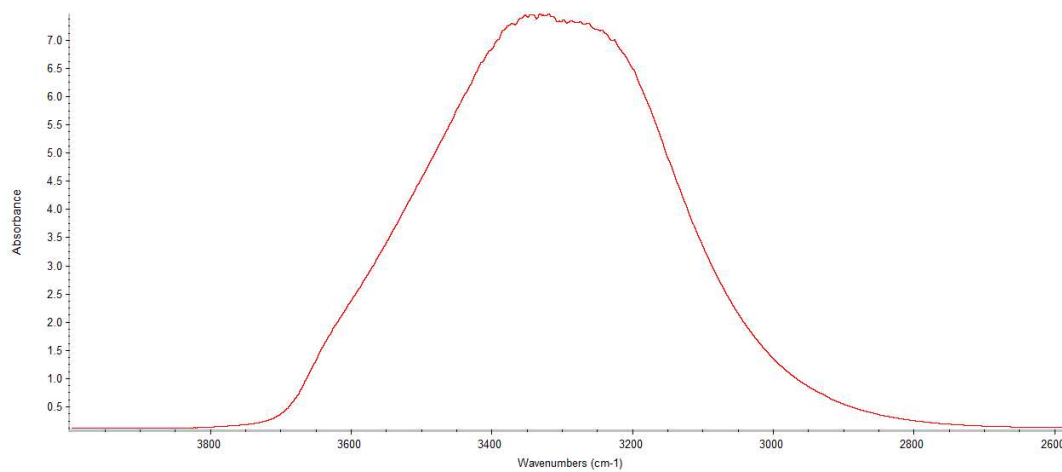


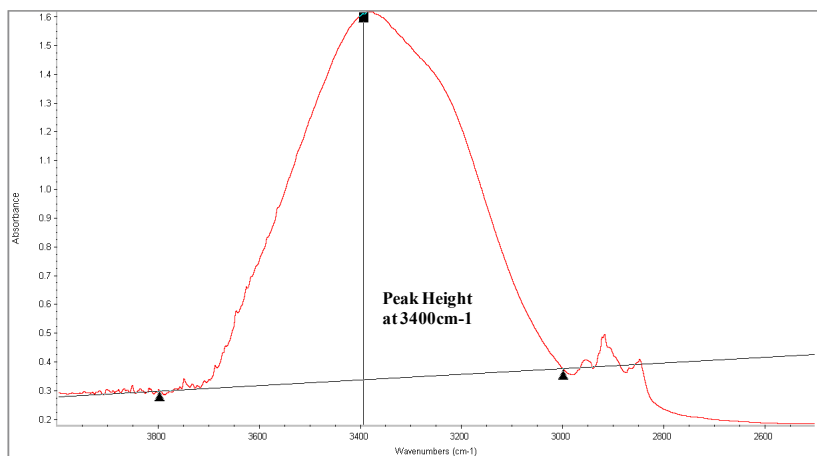
Figure 2-4. Blank Spectrum of Liquid Water

2.4 RESULTS AND DISCUSSION

Quantitative analyses were performed using the Fickian diffusion model described by Equation 2-5, referred to as Analysis 1, and a dual mode diffusion model, referred to as Analysis 2.

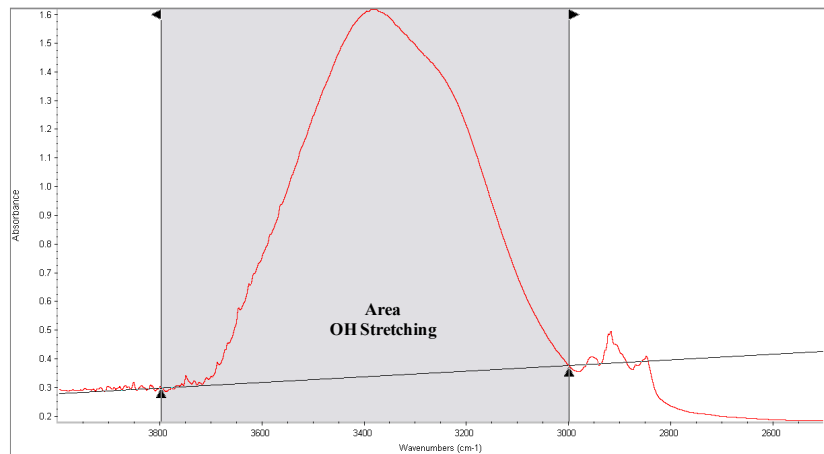
2.4.1 Analysis 1 – Fickian Diffusion Model

For the Fickian diffusion model, quantitative analyses were performed using: (i) the peak height at 3400 cm^{-1} , (ii) the area between $3000\text{--}3800\text{ cm}^{-1}$, and (iii) using an internal benchmark, where the area of the OH stretching was divided by the area of the CH stretching ($2750\text{--}3000\text{ cm}^{-1}$), illustrated in Figure 2-5. The third method was included because for some samples there was a shift on the CH stretching area during the course of the test. The results obtained with all three methods were very similar and only the results from the second method are presented in this paper.

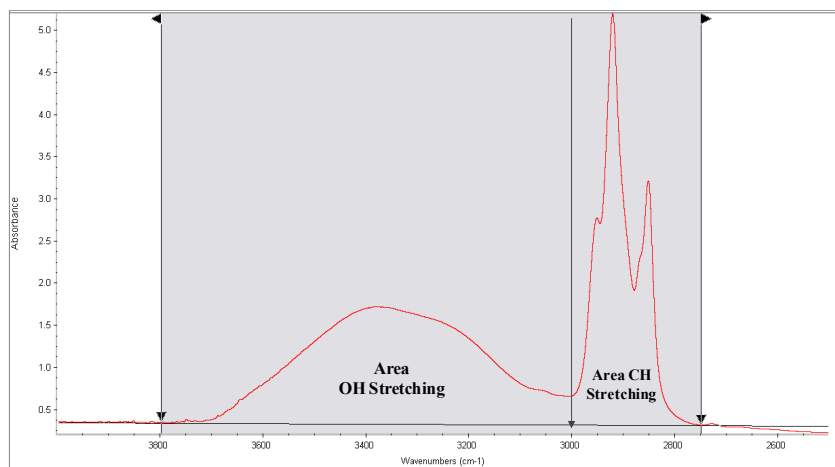


(i)

Figure 2-5. Illustration of Quantitative Analysis



(ii)



(iii)

Figure 2-5. Continued

2.4.2 Analysis 2 – Dual Mode Diffusion Model

Localized interactions can occur between the water molecule and suitable polar groups of the asphalt binder. Several authors have proposed that diffused water can be categorized into two species: those forming a molecular solution and those confined into areas of abnormally large free volume. Barrie (1968) also mentioned two forms of sorbed water, the first represents water that is initially absorbed with little perturbation of the matrix and appears to be attached firmly to specific sites. The second is water that usually promotes swelling of the matrix.

This analysis considers that the cumulative diffusion of water through thin films of asphalt binder does not follow Fick's law. Instead, water diffuses following a dual sorption mode, where each mode of sorption individually follows Fick's law. In this model it is assumed

that a fraction of the water molecules (x_1) is partially mobile (rapid absorption onto the surface sites), and the other fraction ($1 - x_1$) is completely mobile and can diffuse into the asphalt matrix freely (subsequent diffusion into the bulk materials). Thus the expression for describing this model contains two diffusion coefficients (Pereira and Yarwood 1996b):

$$\frac{A_1 - x_1 A_0}{x_1 (A_{eq} - A_0)} = 1 - \frac{8\gamma}{\pi [1 - \exp(2l\gamma)]} \sum_{n=0}^{\infty} \left[\frac{\exp\left(\frac{-D_1(2n+1)^2 \pi^2 t}{4l^2}\right) \left[\frac{(2n+1)\pi}{2l} \exp(-\gamma 2l) + (-1)^n (2\gamma) \right]}{(2n+1) \left(4\gamma^2 + \left(\frac{(2n+1)\pi}{2l} \right)^2 \right)} \right] \quad (2-6)$$

$$\frac{A_2 - x_2 A_0}{x_2 (A_{eq} - A_0)} = 1 - \frac{8\gamma}{\pi [1 - \exp(2l\gamma)]} \sum_{n=0}^{\infty} \left[\frac{\exp\left(\frac{-D_2(2n+1)^2 \pi^2 t}{4l^2}\right) \left[\frac{(2n+1)\pi}{2l} \exp(-\gamma 2l) + (-1)^n (2\gamma) \right]}{(2n+1) \left(4\gamma^2 + \left(\frac{(2n+1)\pi}{2l} \right)^2 \right)} \right] \quad (2-7)$$

where, D_1 and D_2 are the diffusivities (or diffusion coefficients) components of the dual mode diffusion model. After rearranging Equations 2-6 and 2-7 as a function of A_1 and A_2 , they can be added to produce the total absorbance at time t ($A_1 + A_2 = A_t$). The values of x_1 and x_2 are related to the proportion of the partially and totally mobile molecules ($x_1 + x_2 = 1$). The value of x_1 and two separate diffusion coefficients (D_1 and D_2) are then derived from the absorbance data. Figures 2-6, 2-7, 2-8 and 2-9 present examples of the fitting obtained by Analyses 1 and 2 for asphalt binder AAB, AAD, AAF and ABD, respectively.

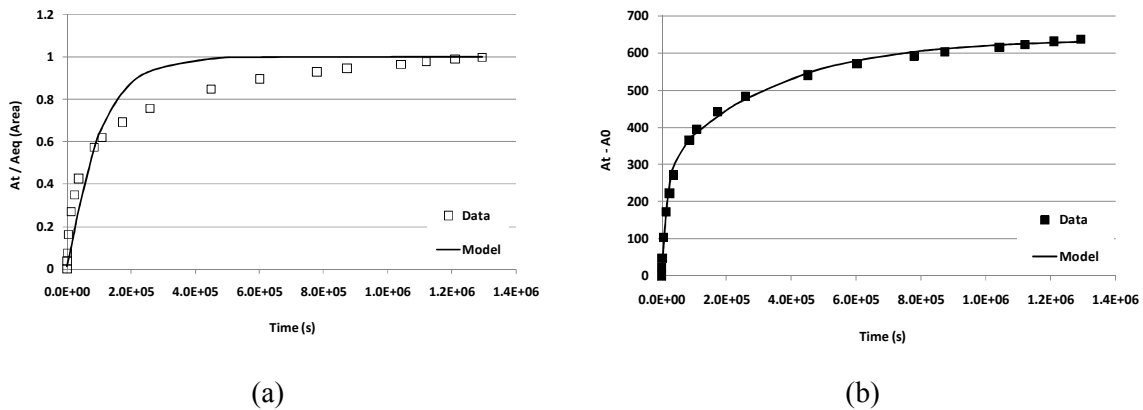
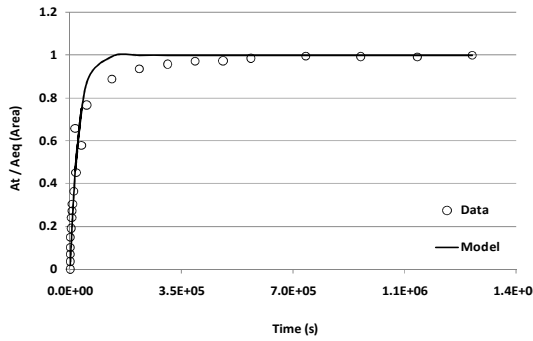
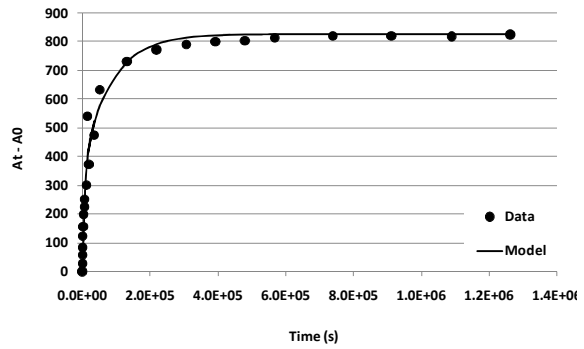


Figure 2-6. Result Obtained by (a) Analysis 1 (Fickian Diffusion Model) and (b) Analysis 2 (Dual Mode Diffusion Model) for Asphalt AAB

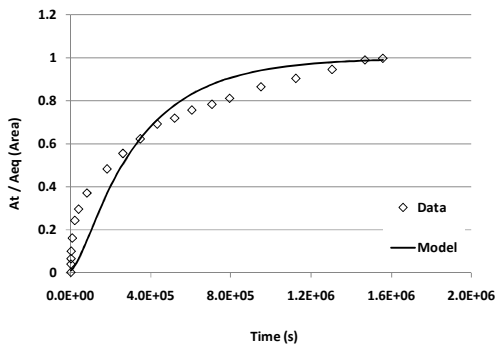


(a)

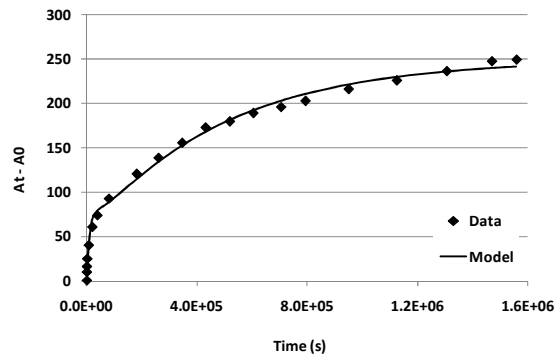


(b)

Figure 2-7. Result Obtained by (a) Analysis 1 (Fickian Diffusion Model) and (b) Analysis 2 (Dual Mode Diffusion Model) for Asphalt AAD

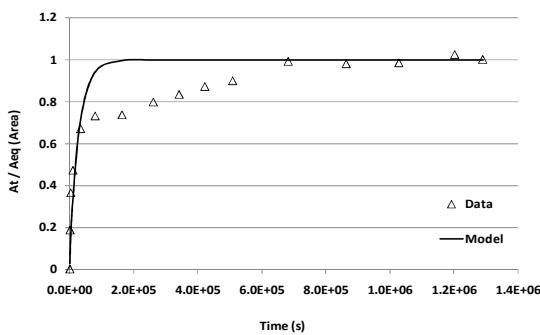


(a)

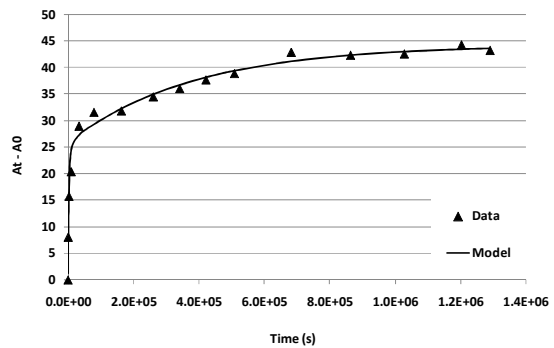


(b)

Figure 2-8. Result Obtained by (a) Analysis 1 (Fickian Diffusion Model) and (b) Analysis 2 (Dual Mode Diffusion Model) for Asphalt AAF



(a)



(b)

Figure 2-9. Result Obtained by (a) Analysis 1 (Fickian Diffusion Model) and (b) Analysis 2 (Dual Mode Diffusion Model) for Asphalt ABD

2.4.3 Statistical Analysis

Table 2-1 shows the average of the results obtained by Analysis 1 and Analysis 2, with the coefficient of variation (CV) for both methods and the four asphalts. Results from the dual mode diffusion model presented a better fit for all the samples. A level of significance of 0.05 was used in the analysis of variance (ANOVA) for the dual mode diffusion model values. According to the statistical analysis, asphalts AAB, AAD and AAF have the same D_{eff} value, while the other three asphalt combinations (AAB-ABD, AAD-ABD and AAF-ABD) presented statistically different values using the same level of significance.

Table 2-1. Summary of the Diffusivity Values

Asphalt	Number of Replicates	Analysis 1		Analysis 2				
		Average $D(\text{nm}^2/\text{s})$ [CV]	R^2 (fitting with the model)	$D_1(\text{nm}^2/\text{s})$	$D_2(\text{nm}^2/\text{s})$	x_1	Average $D_{\text{eff}}(\text{nm}^2/\text{s})$ [CV]	R^2 (fitting with the model)
AAB	6	3.76 [71%]	0.826	23.02	0.79	0.51	12.17 [49%]	0.989
AAD	4	9.39 [36%]	0.921	38.26	1.75	0.57	16.79 [37%]	0.978
AAF	3	0.96 [6.3%]	0.928	36.29	0.67	0.25	9.69 [17.5%]	0.995
ABD	6	6.99 [168%]	0.722	75.07	0.40	0.53	39.82 [45%]	0.969

2.4.4 Simplified Example to Demonstrate Implications

The rate at which water diffuses through the bulk of the asphalt binder as well as the inherent sensitivity of the binder and the binder-aggregate interface to the presence of moisture dictates the rate and intensity of moisture-induced damage. Rigorous computational or analytical models are available that combine binder and mixture diffusivity with their propensity for cohesive or adhesive damage (Caro et al. 2009; Kringos and Scarpas 2005). Although detailed modeling of moisture damage is beyond the scope of this paper, a simplified example is presented here to demonstrate the implication of binder diffusivity on adhesive damage.

Bhasin et al. (2007) demonstrate the use of an energy parameter based on the surface free energy to differentiate the moisture susceptibility of adhesive bonds between binders and aggregates. However, the energy parameter can only be used to compare the moisture susceptibility of different binder-aggregate interfaces at the same level of saturation. For

different levels of saturation, it can be hypothesized that the product of percent saturation (governed by the diffusivity of water through the binder) and the energy parameter reflects the susceptibility of the adhesive bond to moisture damage. For this simplified example, Table 2-2 and Figure 2-10 present three different combinations of asphalt binders AAD and ABD with the same basalt aggregate. In each case the aggregate is coated with a binder film and a boundary condition with 100% saturation is applied to the surface of the binder. The percent saturation at the interface shown in the Table was computed using the values and dual mode diffusion model described in this paper. The Table clearly illustrates the influence of material property, coating thickness and diffusivity on the moisture susceptibility of the interface.

Table 2-2. Simplified Example of Susceptibility of Adhesive Failure

Binder – Aggregate combination	Thickness of binder coating the aggregate	Energy parameter for the interface (A)*	% Saturation @interface after 24 hours (B)	(A)×(B)	Rank order (from most to least susceptible to adhesive failure after 24 hours)**
AAD-basalt	5 μm	1	6	6	2
ABD-basalt	5 μm	0.8	17	13.6	1
ABD-basalt	7 μm	0.8	5	4	3

* From Bhasin et al.(2007); reciprocal of the energy parameter is used such that lower values indicate more moisture susceptibility

** Moisture susceptibility of the mix must also include influence of moisture on deterioration of the binder or cohesive failure

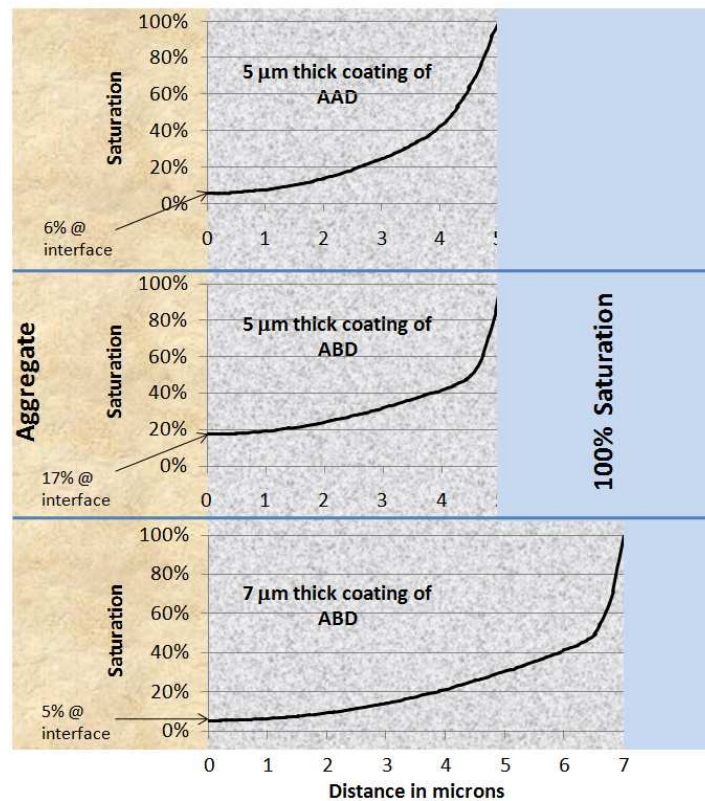


Figure 2-10. Illustration of the Example shown in Table 2-2

2.5 SUMMARY AND RECOMMENDATIONS

Moisture transport through an asphalt mixture is an integral part of the moisture damage mechanism. Moisture damage in an asphalt mixture is a complex process that represents the cumulative effect of moisture transport processes (e.g. diffusion through binder) and moisture deterioration processes (e.g. loss in mechanical properties of the binder due to the presence of moisture). In this study a procedure was developed and used to measure the diffusivity of water through thin films of asphalt binder using the FTIR-ATR. The technique was largely based on similar approaches used in the field of polymer technology. The major conclusions of this study are:

- The diffusivity of water through asphalt was significantly higher for (at least) one asphalt binder than it was in the other three binders (from the set of four tested) indicating that diffusivity may be an important material variable that influences the rate of moisture damage.

- A dual mode diffusion model was shown to better represent the diffusion of water through asphalt binders. This model suggests that water molecules may be diffusing at two different rates within the asphalt binder with the slower rate being associated with interaction between water molecules and polar functional groups within the material. The implication of this mode of diffusion through asphalt binders in terms of performance and asphalt chemistry requires further investigation. However, these results do suggest that future efforts related to modeling of moisture damage should consider the use of a dual mode diffusion model rather than simple diffusion based on Fick's second law.
- The values of diffusivity reported in this study are much smaller than the values reported by Arambula et al. (2009) and Kassem et al. (2006). However, the values reported in this paper pertain to the diffusion of liquid water through thin films of asphalt binder which is different from diffusion of moisture through mixtures or mastics. The latter is dictated by macroscopic properties including interconnected air voids that allow moisture to travel much faster through the bulk. In contrast, the results shown in this study are relevant to the diffusion of moisture through the binder as in the case of microstructural entities that interconnect voids to the binder-aggregate interface. The impact of this could be that binders that develop a tenacious bond with aggregate surfaces and also resist moisture diffusion to the binder-aggregate interface may be more resistant to moisture damage. Further study is under investigation to evaluate the difference in diffusivity values when water is under liquid or vapor form.
- The results obtained in this study are in the same order of magnitude of the results presented by Wei (2009) using the Electrochemical Impedance Spectroscopy (EIS). Wei used thin binder film on aluminum plate substrate.

Researchers are currently conducting further studies using the FTIR-ATR technique to address different issues related to the diffusivity in asphalt binders including: (i) rates of diffusion at the binder-substrate interface in addition to the rates of diffusion through thin films of asphalt binder as presented in this paper, (ii) diffusivity of polymer modified binders (including considerations such as casting of thin homogenous films), and (iii) differences between the diffusion of liquid water versus water vapor.

3. EXPERIMENTAL MEASUREMENT OF WATER DIFFUSION THROUGH FINE AGGREGATE MIXTURES

3.1 INTRODUCTION

Approximately 85% of the pavements in the United States are flexible with a hot mix asphalt (HMA) surface. In the late 1970s and early 1980s, a significant number of pavements in the United States began to experience distress associated with moisture sensitivity of HMA (Epps 2000).

Moisture damage in asphalt mixtures or HMA can be defined as the loss of strength and durability due to the influence of moisture. HMA is a composite material comprised of asphalt binder, aggregates and air voids. Consequently moisture damage in this type of material is a complex phenomenon that involves chemical, physical, thermodynamic, and mechanical processes. The moisture damage mechanism can be divided into two stages (Caro 2008): (i) the transport of moisture into the mixture, and (ii) the interaction of moisture with the mixture constituents. The four main modes of moisture transport are: (i.1) infiltration of surface water, (i.2) capillary rise of subsurface water (i.3) water diffusion due to relative humidity gradients, and (i.4) migration of residual moisture from within the bulk of the aggregate particle to the surface. The interaction of moisture results in three main types of degradation: (ii.1) loss of cohesion of the asphalt binder/mastic, (ii.2) adhesive failure at the asphalt and aggregate interface, and possibly (ii.3) degradation of individual aggregate particles when subjected to freezing.

The transport of small molecules through a material such as polymer, asphalt cement or asphalt mastic (asphalt cement and mineral filler smaller than 0.075 mm) is a very complex process that is influenced by factors such as, temperature, chemistry of the diffusing molecules, physical properties of the mineral filler or modifier (normally a polymer), interaction of the solvent molecules with the polymer, external mechanical deformation, and complex internal structure of the polymer (De Kee et al. 2005). No single model provides a complete explanation of the transport process for polymeric composites due to their complex internal structure.

Different modes of moisture transport have been used to characterize or quantify the sensitivity of asphalt mixtures to moisture damage. Some examples are permeability (Al-Omari et al. 2002; Huang et al. 1999; Masad et al. 2004; Mohammad et al. 2003), hydraulic conductivity (Kutay 2005), capillary rise (Masad et al. 2007), and diffusivity (Kassem et al. 2006; Sasaki et al. 2006). Kringos and Scarpas (2008) considered two different phenomena in the simulation of water infiltration into an asphalt mixture. The first phenomenon they considered was infiltration of moisture into the 'macro-pores', which is primarily dependent on hydraulic suction and flow velocity. The second phenomenon is a follow-on to the first where, after moisture has already entered the macro-pores, it continues to infiltrate within the bulk of the aggregate-binder matrix. This infiltration is, in contrast to the first phenomenon (pressure driven), a molecular diffusion process which is driven by a moisture concentration gradient within the material. A few studies were also conducted for the measurement of water/moisture diffusion in fine aggregate mixtures (FAM). Table 3-1, updated from (Arambula et al. 2009), shows the results of the measurements and the details of the experimental setup and specimen configuration for three studies.

Table 3-1. Diffusion Coefficients for FAM with Different Characteristics

Reference	Blend Proportions	Average Diffusion Coefficients (m ² /s)	Specimens Characteristics and Experimental Conditions
(Kassem et al. 2006)	<u>Aggregate:</u> 52.4% sandstone 35.0% igneous screening 4.6% hydrated lime <u>Asphalt:</u> 8.0% PG 76-22	1.03x10 ⁻¹¹	<ul style="list-style-type: none"> - Cylindrical specimens with 50mm diameter and 50mm height sitting in a shallow water bath at 25°C while measuring the change in the logarithm of total suction using a psychrometer embedded in the middle of the specimen and placed 5mm above the bottom end of the specimen. - Aggregate size passing sieve No 16. - Air voids not specified.
	<u>Aggregate:</u> 66.2% natural sand 25.8% limestone sand <u>Asphalt:</u> 8.0% PG 64-22	9.72x10 ⁻¹²	
	<u>Aggregate:</u> 46% natural sand 46% limestone sand <u>Asphalt:</u> 8.0% PG 64-28	2.43x10 ⁻¹¹	
(Kringos et al. 2008b)	<u>Aggregate:</u> 50% crushed sand 25% lime <u>Asphalt:</u> 25% Pen 70/100	1.31x10 ⁻¹³	<ul style="list-style-type: none"> - Gravimetric sorption method on 30mm x 30mm and 1mm thick specimens placed inside an 85% relative humidity chamber at 25°C. - Aggregate size not specified. - Air voids not specified.
	<u>Aggregate:</u> 50% crushed sand 25% hydrated lime <u>Asphalt:</u> 25% Pen 70/100	3.08x10 ⁻¹³	
	<u>Aggregate:</u> 50% crushed sand 25% hydrated lime <u>Asphalt:</u> 25% Cariphalte XS	3.64x10 ⁻¹³	
	<u>Aggregate:</u> 50% crushed sand 25% hydrated lime <u>Asphalt:</u> 25% Sealoflex 5-50(PA)	3.17x10 ⁻¹³	
(Arambula et al. 2009)	<u>Aggregate:</u> 51.7% Diabase 46.5% Sand 1.8% Dust <u>Asphalt:</u> 8.5% PG 70-22	2.54x10 ⁻¹⁰	<ul style="list-style-type: none"> - Gravimetric method on cylindrical ensembles containing 70mm diameter and 4mm – 5mm thick specimens, where the ensembles were placed in a chamber with 15% relative humidity at 35°C. - Aggregate size passing sieve No 4. - Air voids between 11-13%

The objective of this study was to experimentally determine the diffusion of water in different FAMs using simple gravimetric sorption measurements. In this study FAM is defined as a blend of aggregate fractions smaller than sieve No 16 (1.18mm) with asphalt binders. The air void distribution in FAM specimens is considered to be more uniform than the air void distribution in hot mix asphalt (HMA) (Kim et al. 2006; Masad et al. 2006). In this study, the FAM is regarded as a homogenous representative volume of the HMA for the purposes of measuring diffusivity of water. This assumption is considered as reasonable and relevant because analytical or computational models of the performance of full asphalt mixtures typically treat the full mix as a composite of coarse aggregate, air and FAM (Caro et al. 2010). Because of practical limitations in defining microstructural details, asphalt binder and fine aggregates are not considered separately. Consequently, the mechanical and material properties of the FAM phase, such as the diffusivity of water, form the critical inputs for such modeling.

3.2 BACKGROUND ON KINETICS OF DIFFUSION

Fick's law expresses the proportionality of solute flux with respect to concentration gradient. Similar relations are Darcy's law for fluid flow in porous media, Ohm's law for electric flux and Fourier's law for heat transfer. The mathematical theory of diffusion in isotropic substances is based on the hypothesis that the steady state rate of transfer of a diffusing substance through a unit area cross section is proportional to the concentration gradient measured normal to the section (Fick's first law):

$$F = -D \frac{\partial C}{\partial z} \quad (3-1)$$

where, F is the rate of transfer per unit area of section (flux), C is the concentration of the penetrant, and D is the diffusion coefficient, or diffusivity.

Fick's second law is generally used to model diffusion driven by concentration gradients in different materials. It assumes constant pressure and temperature throughout the sample and the absence of any long-range electrostatic interactions. The Fickian diffusion of a single substance in another substance can be described by the one-dimensional continuity equation:

$$\frac{\partial C}{\partial t} = D \frac{\partial^2 C}{\partial z^2} \quad (3-2)$$

where, t is the time. The analytical solution to the Equation 3-2 will depend on the geometry, initial and boundary conditions. For more complex systems, this equation can be modified to

incorporate diffusion constants that depend on concentration, inhomogeneous media, and a diversity of boundary conditions which can take many forms.

3.3 EXPERIMENTAL DESIGN

This section presents the experiment design for this study, which includes materials and specimen fabrication, test method, and the background on analysis.

3.3.1 Materials and Specimens Fabrication

Three asphalt binders and two aggregates selected from the Strategic Highway Research Program (SHRP) Materials Reference Library (MRL) were evaluated. The three asphalt binders include AAB, which is a PG 58-22 grade binder from Wyoming; AAD, which is a PG 58-28 grade California Coastal asphalt; and ABD, which is a PG 58-10 California Valley asphalt (Jones IV 1993). The experiment design includes two aggregates: RK is a basalt and RA is a granite (Robl et al. 1991).

The fine aggregate mixture (FAM) design was the same as that used by Zollinger (2005), and the specimen fabrication followed the same procedure as that used by Zollinger to fabricate cylindrical specimens prepared for the Dynamic Mechanical Analysis (DMA). The four main steps of this procedure are briefly described below.

- The gradation for the FAM followed the gradation of the fine aggregate portion of the full asphalt mixture (Figure 3-1).
- FAM samples 150 mm in diameter and 70 mm in height were compacted using the Superpave Gyrotory Compactor (SGC) (Figure 3-2a). The standard procedure described in AASHTO T 316 was used as a reference. The criterion of termination was the percent of air voids specified for the design.
- The upper and lower part of the cylindrical sample was sawed to obtain a new cylinder with the same diameter (150 mm) but with 50 mm in height (Figure 3-2b). Finally, cylindrical specimens of 50 mm height and 12 mm diameter were obtained (Figure 3-2c) by coring the larger specimen.
- The volumetric properties of each small cylindrical sample were obtained following procedures similar to those used for full asphalt mixtures.

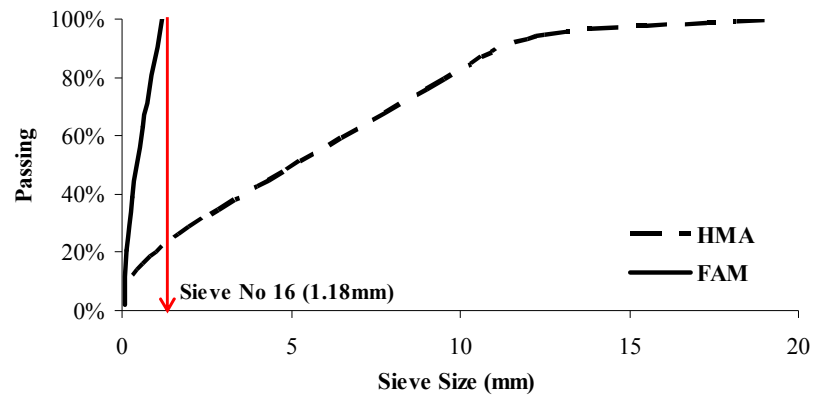


Figure 3-1. HMA and the Corresponding FAM Gradation

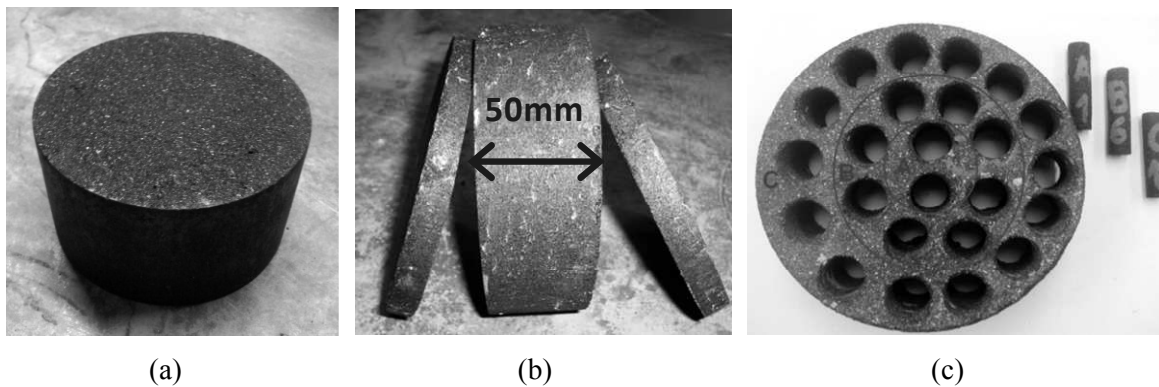


Figure 3-2. (a) 150 mm (6 inches) Diameter Sample, (b) Sawing and (c) Coring Process

3.3.2 Test Method

The test method for gravimetric sorption measurements is simple and inexpensive and the only equipment required is a sensitive mass balance. The dry weight of each FAM specimen was recorded. Following this the specimens were placed in a distilled water bath of 100mL with approximately 5mm of water above the surface of the sample to ensure that the diffusion was mostly concentration driven. Subsequently, the weight of each specimen at saturated surface-dry (SSD) condition was measured (as in AASHTO T 166) at periodic intervals. The specimens were placed back in the water bath immediately after recording the weight of the specimen. The time intervals varied along the test, since the rate of water absorption was not constant. In the first three days of the test, the SSD weight of the samples was measured three to six times per day. By the end of the test, the measurements were made only once every two weeks. Two groups of samples were evaluated, one at room temperature, and another at 100°F.

The main objective of the test method was to measure the amount of water that was absorbed by the sample as a function of time required to reach equilibrium. Figure 3-3 illustrates four possible locations of water inside the FAM sample during the test: (i) in the ‘Macro’ voids, (ii) absorbed by the asphalt binder, (iii) at the binder-aggregate interface, and (iv) within the aggregates. One disadvantage of the gravimetric method is that it is difficult to separate the amount of water sorbed by contribution due to these four mechanisms, since they probably happen simultaneously. Accordingly, the recorded measurements and deduced values correspond to an average or homogenized material comprised of these four mechanisms.

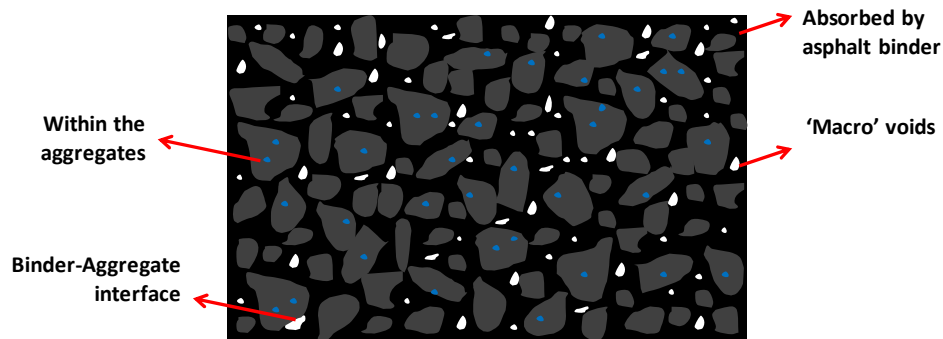


Figure 3-3. Scheme of Possible Locations where the Water can be During the Gravimetric Sorption Test

3.3.3 Background on Analysis

This subsection presents a brief background regarding the analytical solution that was used to back calculate the diffusivity of the FAM. General solutions to the diffusion equation can be obtained for a variety of initial and boundary conditions provided the diffusion coefficient is constant. As stated by Crank (1975), such a solution usually has one of two standard forms. Either it is comprised of a series of error functions or related integrals (both are most suitable for numerical evaluation at small times), or it is in the form of a trigonometric series that converges more satisfactorily for large values of time. For diffusion in samples with cylindrical geometries the trigonometric series is replaced by a series of Bessel functions.

The FAM samples were considered as long circular cylinders in which radial diffusion was predominant. Thus, concentration in the specimen (C) can be described as a function of radius and time only. The diffusion equation then becomes:

$$\frac{\partial C}{\partial t} = \frac{1}{r} \frac{\partial}{\partial r} \left(rD \frac{\partial C}{\partial r} \right) \quad (3-3)$$

For the case presented in this paper, the boundary condition relates to the rate of transfer of water (the diffusing substance) across the surface of the FAM specimen, with the sample initially in a dry condition. A simple and reasonable assumption is that the rate of exchange is directly proportional to the difference between the actual concentration C_s just within the cylinder at any time and the concentration C_0 which would be the one required to maintain equilibrium with the surrounding atmosphere. Mathematically this means that the condition at the surface is:

$$-D \frac{\partial C}{\partial r} = \alpha(C_s - C_0) \quad (3-4)$$

If the cylinder is initially at a uniform concentration C_2 , the required solution is:

$$\frac{C - C_2}{C_0 - C_2} = 1 - \sum_{n=1}^{\infty} \frac{2LJ_0\left(r \frac{\beta_n}{a}\right)}{(\beta_n^2 + L^2)J_0(\beta_n)} \exp\left(\frac{-\beta_n^2 Dt}{a^2}\right) \quad (3-5)$$

where, the β_n is the n^{th} root of

$$\beta J_1(\beta) - LJ_0(\beta) = 0 \quad (3-6)$$

and

$$L = \frac{a\alpha}{D} \quad (3-7)$$

is a dimensionless parameter, with a being the radius of the sample.

The total amount of diffusing substance M_t entering or leaving the cylinder, depending on whether C_0 is greater or smaller than C_2 , is expressed as a fraction of M_∞ , the corresponding quantity after infinite time (or equilibrium), by

$$\frac{M_t}{M_\infty} = 1 - \sum_{n=1}^{\infty} \frac{4L^2 \exp\left(\frac{-\beta_n^2 Dt}{a^2}\right)}{\beta_n^2 (\beta_n^2 + L^2)} \quad (3-8)$$

In a previous study, Pereira and Yarwood (1996b) considered a cumulative diffusion of water through thin films of asphalt binder that does not follow Fick's law. Instead, water diffuses following a dual sorption mode, where each mode of sorption individually follows Fick's law. In this model it is assumed that a fraction of the water molecules (x_1) is partially

mobile (rapid absorption onto the surface sites), and the other fraction ($x_2 = 1 - x_1$) is completely mobile and can diffuse into the asphalt matrix freely (subsequent diffusion into the bulk materials).

The concept of the dual mode diffusion proposed by Pereira and Yarwood (1996b) was investigated for the FAM cylindrical samples. Although the FAM samples have three components (asphalt binder, aggregates, and air voids), without considering the interface between asphalt binder and aggregate, the dual mode is an attempt to represent the diffusion process only by two stages that occur in parallel (simultaneously): (i) in the first one, the water molecules are completely mobile (roughly representing the free volume), and (ii) in the second one, the water molecules are partially mobile. Equation 3-8 is then represented as follows:

$$\frac{M_1}{x_1 M_\infty} = 1 - \sum_{n=1}^{\infty} \frac{4L^2 \exp\left(\frac{-\beta_n^2 D_1 t}{a^2}\right)}{\beta_n^2 (\beta_n^2 + L^2)} \quad (3-9)$$

$$\frac{M_2}{x_2 M_\infty} = 1 - \sum_{n=1}^{\infty} \frac{4L^2 \exp\left(\frac{-\beta_n^2 D_2 t}{a^2}\right)}{\beta_n^2 (\beta_n^2 + L^2)} \quad (3-10)$$

After rearranging Equations 3-9 and 3-10 as a function of M_1 and M_2 , they can be added to produce the total water absorbed at time t (M_t), Equation 3-11. The values of x_1 and x_2 are related to the proportion of the partially and totally mobile molecules. The value of x_1 and two separate diffusion coefficients (D_1 and D_2) are then derived from the gravimetric data.

$$M_t = \left[(x_1 \times M_\infty) \times \left(1 - \sum_{n=1}^{\infty} \frac{4L^2 \exp\left(\frac{-\beta_n^2 D_1 t}{a^2}\right)}{\beta_n^2 (\beta_n^2 + L^2)} \right) \right] + \left[(x_2 \times M_\infty) \times \left(1 - \sum_{n=1}^{\infty} \frac{4L^2 \exp\left(\frac{-\beta_n^2 D_2 t}{a^2}\right)}{\beta_n^2 (\beta_n^2 + L^2)} \right) \right] \quad (3-11)$$

A similar approach was used by Cheng et al. (2003) to divide the sorption of water into asphalt or mastic in two stages. In the first stage, both adsorption at the asphalt surface and absorption within the asphalt occur simultaneously. In the second stage, adsorption on the surface of the asphalt comes to equilibrium, but absorption (considered a diffusion process) continues and eventually becomes constant. However, the approach used by Cheng et al. (2003) was to differentiate between absorption and adsorption in asphalt binders unlike the approach by

Pereira and Yarwood, which was to differentiate between different rates of absorption or diffusion.

3.4 RESULTS AND DISCUSSION

All combinations of asphalt binders and aggregates contain 8.9% (by weight) of asphalt binder and air voids varying from 7% to 11%, determined by the standard method AASHTO T 166. Their internal structure is, however, unknown. Resolution limitations of the X-ray CT prevent us from capturing the air voids in the size they happen in the FAM specimens.

3.4.1 Water Uptake

The capacity of sand-asphalt or FAM specimens to absorb water in its internal structure is an important factor for the moisture damage. One of the parameters used in computing diffusivity using Equation 3-11 is M_{∞} , which is the amount of moisture absorbed by the specimen at saturation. In a gravimetric test, saturation is evident when there is no further change in mass of the specimen with time. In this study FAM specimens were immersed in water at room temperature (75°F) and 100°F for 21 months and 14 months respectively. Figure 3-4 illustrates typical mass absorption data for specimens at 75°F and 100°F. This figure indicates that mass absorption has clearly not reached an asymptote representative of a saturated specimen for the specimens at 100°F, whereas the specimens at room temperature appear to be closer to saturation. In any case, since M_{∞} was not clearly established for these test specimens, this parameter was also treated as an unknown in Equation 3-11. A similar approach was used by Pereira and Yarwood (1996b) to analyze results from water diffusion in sulfonated poly(ether sulfone) membranes.

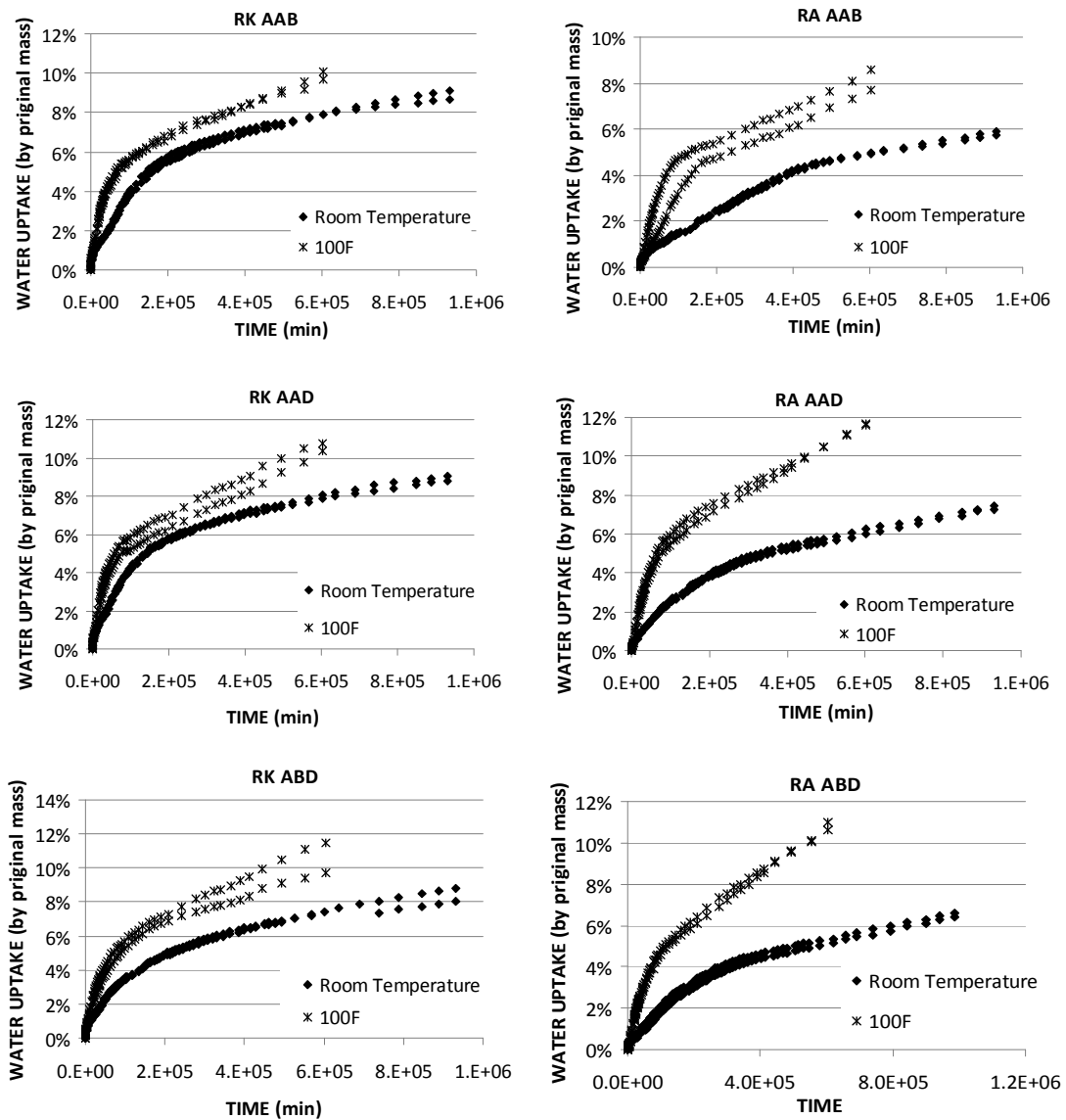


Figure 3-4. Water Uptake by Original Mass of the FAM Samples

From the data presented in Figure 3-4 one can observe that some samples were still far from reaching an asymptote. Therefore, a considerable error exists when trying to predict M_{∞} . The room temperature data offer a better estimate of M_{∞} compared with the samples at 100°F since they are closer to saturation, reaching an asymptote. These data do, however, clearly establish that water uptake is greater and continues longer at higher temperatures.

Figure 3-5 illustrates the difference of the water uptake considering both conditions: (i) the last water uptake measurement as M_{∞} , and (ii) the estimated value using the dual mode

diffusion model. For a given binder type, FAM mixes with RK aggregate absorbed more water than mixes with RA aggregate. Aggregate RK and RA are both siliceous aggregates. However, RK has a much higher SSA compared to RA (Little et al. 2005), and this is an indirect evidence that water is being adsorbed at the binder aggregate interface causing stripping as it diffuses into the FAM specimen. Aggregate RK has a much higher SSA and therefore will adsorb more water at the binder-aggregate interface compared to RA. From the data presented in Figure 3-5 it is clear that the difference between estimated and measured levels of moisture uptake is greater for 100°F than for room temperature.

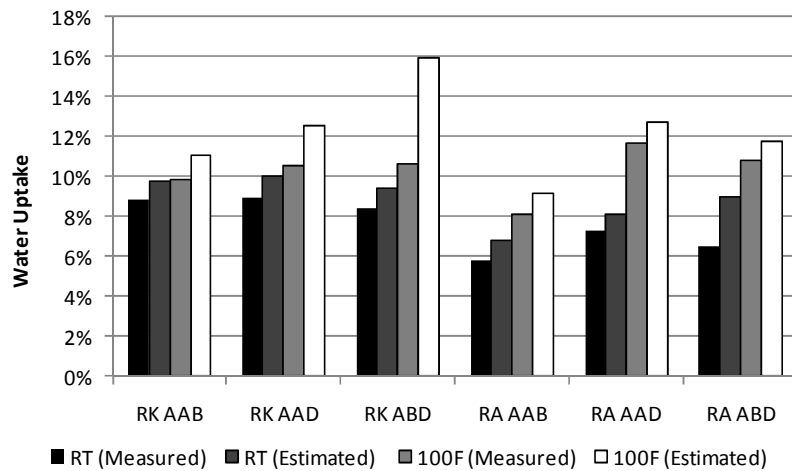


Figure 3-5. Water Uptake Measured for the Last Collected Reading and Estimated using the Dual Mode Diffusion Model

3.4.2 Diffusivity

The diffusivity, or diffusion coefficient, values were obtained using Equation 3-11. Table 3-2 presents the results of D_{eff} for all 24 samples evaluated (2 aggregates x 3 asphalt binders x 2 temperatures x 2 replicates). The effective diffusivities (D_{eff}) were obtained by the following equation, and the average values illustrated in Figure 3-6:

$$D_{eff} = (D_1 \times x_1) + [D_2 \times (1 - x_1)] \quad (3-12)$$

Table 3-2. Summary of Diffusion Coefficient Values

	Agg.	Asphalt	Sample	D_{eff} ($10^{-12} \text{ m}^2/\text{s}$)	R^2 (%)	$D_{\text{eff average}}$ (m^2/s)
Room Temperature (75°F)	RK	AAB	1	2.00	99.7	1.85E-12
			2	1.70	99.7	
		AAD	1	2.20	99.8	2.23E-12
			2	2.26	99.8	
		ABD	1	1.82	99.9	2.04E-12
			2	2.26	99.9	
	RA	AAB	1	0.785	99.6	7.83E-13
			2	0.781	99.6	
		AAD	1	1.36	99.8	1.34E-12
			2	1.33	99.8	
		ABD	1	1.15	99.8	1.22E-12
			2	1.29	99.9	
100°F	RK	AAB	1	4.76	99.5	4.90E-12
			2	5.04	99.7	
		AAD	1	4.81	99.4	4.46E-12
			2	4.11	99.1	
		ABD	1	3.50	99.6	3.20E-12
			2	2.91	99.9	
	RA	AAB	1	3.46	98.7	2.75E-12
			2	2.05	99.2	
		AAD	1	2.83	98.8	3.10E-12
			2	3.37	99.0	
		ABD	1	2.12	98.6	2.21E-12
			2	2.31	99.0	

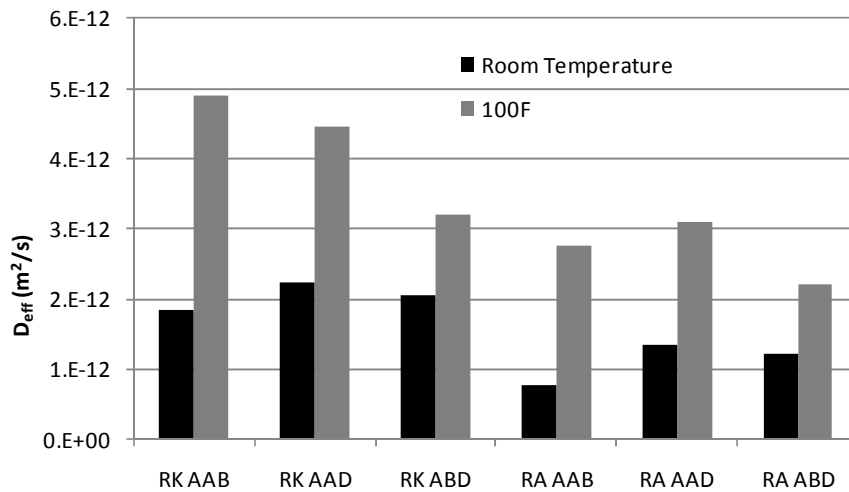


Figure 3-6. Diffusivity Results Obtained for the Samples Tested at Room Temperature and at 100°F using the Dual Mode Diffusion Model

From Table 3-2 it is important to mention the influence of the predicted M_{∞} on the diffusivities results. If the predicted M_{∞} were underestimated, the effective diffusivity values can perhaps be conservative.

3.4.3 The Effect of Temperature on the Diffusivity of Water

The temperature dependence of the diffusion coefficient can be described with the activation energy (E_a) such that:

$$D_{eff}(T) = D_0 \exp\left(-\frac{E_a}{RT}\right) \quad (3-13)$$

where, D_0 is the diffusion coefficient when the temperature goes to infinity (m^2/s), E_a is the activation energy (J/mol), R the universal gas constant (8.314J/mol-K) and T is the absolute temperature (K).

The temperature dependence of the hydration rate has been quantitatively described, in terms of the sample diffusivities by the Arrhenius law. Plots of the diffusivity of water into the FAM samples at two test temperatures were used to calculate the activation energy. Two samples of each asphalt-aggregate combination were tested at each temperature. Extension of the temperature range towards higher temperatures was limited by the stability of the asphalt binder.

The term activation energy means the energy that a system must acquire before a process can occur. The molecular interactions in a complex molecular system such as asphalt are extensive, and at any given temperature, these interactions will tend to control the molecular motions of the constituents in asphalt (Netzel 2006). The concept of activation energy has been applied for different properties and parameters of asphaltic materials, such as viscosity (Salomon and Zhai), oxidation/aging (Ait-Kadi et al. 1996; Liu et al. 1996), and crack growth process (Jacobs et al. 1996). It was also previously used to rank the relative compaction effort of asphalt mixtures in the field (Salomon and Zhai 2009).

Artamendi and Khalid (2006) studied the absorption/diffusion of bitumen from different sources and grades into waste truck and car-tire rubber by weight gain experiments. The temperature dependence of the diffusion coefficient has been observed to follow the Arrhenius relationship characteristic of an activation energy process. Karlsson et al. (2007) reported that by their experience, most bitumens show close to log-linear relationships between diffusion coefficients and temperatures for the range as used in their study (60-100°C). The use of the activation energy was also applied for water diffusion in mineral materials. Simonyan et al. (2009) evaluated the $\text{H}_2\text{O} \rightarrow \text{D}_2\text{O}$ exchange process in porous feldspar in the temperature range from 11°C to 44°C. The activation energy ranged from 7.8 to 18.8 kJ/mol, and the authors concluded that the effective diffusivity of water was mainly controlled by physical properties of the feldspar (i.e. porosity, pore connectivity, pore geometry and distribution).

Figure 3-7 illustrates the E_a results obtained in this study for water diffusion in FAM samples. They varied from 0.36 to 0.98 kJ/mol. Different asphalt binders and aggregates resulted in different activation energies for diffusion. A higher E_a value indicates greater temperature sensitivity of the diffusion coefficient. Comparing the results of activation energy with the water uptake illustrated in Figure 3-5, one can observe that both parameters are inversely proportional.

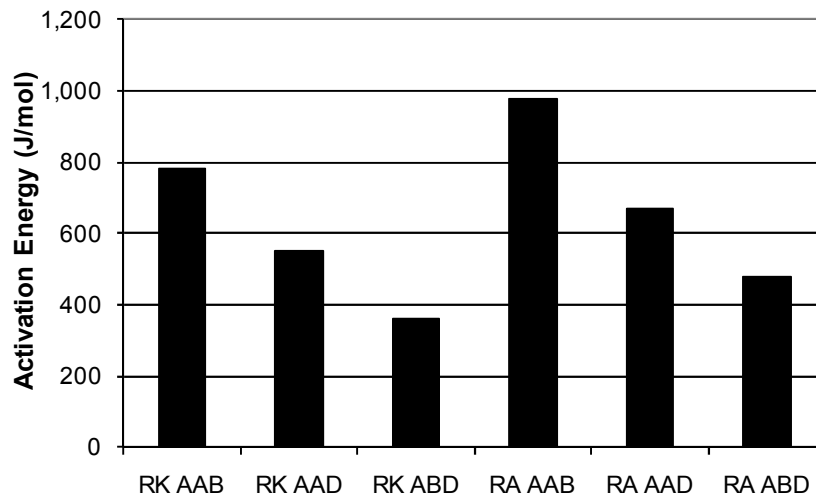


Figure 3-7. Activation Energy Obtained by the Arrhenius Law

3.5 SUMMARY AND CONCLUSIONS

Moisture transport through an asphalt mixture is an integral part of the moisture damage mechanism. Moisture damage in an asphalt mixture is a complex process that represents the cumulative effect of the moisture transport and the deterioration processes. In this study the water uptake and the diffusivity of water in FAM was determined using a simple gravimetric sorption technique. The major conclusions of this study are:

- Diffusivity of several different FAMs was measured using a simple gravimetric approach. Results indicate that the diffusivity of water through FAM is in the order of 10^{-12} m²/s. These results are in the same order of magnitude as those reported by Kringos et al. (2008a).
- Moisture uptake and diffusivity of water through FAM is dependent on the type of aggregate and asphalt binder. For any given asphalt binder, FAM specimens with aggregates having a significantly higher specific surface area such as RK had higher moisture uptake and higher diffusivity when compared to FAM specimens with aggregates having a significantly lower specific surface area. Since both aggregates are siliceous with low porosity, this indicates that a portion of the diffused water is probably trapped at the binder-aggregate interface.
- At room temperature, the rank order of diffusivity and moisture uptake for the three binders was the same irrespective of the type of aggregate. However, this rank order

changed at higher temperatures suggesting that at elevated temperatures different binders may be undergoing a different level of change in the free volume.

4. HISTORY DEPENDENCE OF WATER DIFFUSION IN ASPHALT BINDERS

4.1 INTRODUCTION AND BACKGROUND

Moisture transport through an asphalt mixture is an integral part of the moisture damage mechanism. Material properties and system configuration control the modes of moisture transport into the bulk of the mixture and the response of the system. The water has the ability to weaken the mastic and displaces the asphalt binder from the aggregate. The moisture diffusion through the asphalt binder, or through the mastic, is presented as one of the moisture damage mechanisms. Previous studies (Vasconcelos et al. 2010; Wei 2009) have measured the diffusivity of moisture through asphalt binders to be of the order of 10^{-17} m²/s. Based on these numbers, a 10 micron thick binder film continuously exposed to 100% relative humidity or water at one end would have 50% saturation on the other end of the film after a period of 15 months. In field conditions, it is not very likely that such boundary condition would exist over such sustained periods of time. The main objective of this study was to investigate the effect of cycling moisture boundary conditions on the diffusivity of moisture through asphalt binders. In other words, the objective of this research was to quantify the influence of hysteresis on diffusivity of moisture through asphalt binders.

Hysteresis of a physical property is observed in many fields of science. Examples include magnetic hysteresis, ferroelectric hysteresis, mechanical hysteresis, superconducting hysteresis, adsorption hysteresis, optical hysteresis, and electron beam hysteresis (Mayergoyz 1991). It is a phenomenon in which the response of a physical system to an external influence depends not only on the present magnitude of that influence but also on the previous history of the system. Bertotti and Mayergoyz (2006) defined it in modern science as ‘the collective name for a class of strongly nonlinear physical phenomena’.

Despite the importance of hysteresis (or any type of history dependence) of water diffusion in polymeric materials, there is only limited literature available on this subject. Frisch (1964) suggested that a polymer below its glass transition temperature (T_g) must possess history-dependent diffusion coefficients and experience time-dependent changes in surface concentrations in order to maintain sorption-equilibrium at its boundaries. These time dependencies are intrinsically related to the relaxation times for molecular rearrangement in the polymers. Naumov et al. (2007) used the pulse gradient NMR method to study molecular diffusion of adsorbate molecules in mesoporous materials with different pore morphologies. The

experimental results revealed that in line with the adsorption hysteresis, the measured diffusivities exhibited a history-dependent behavior, and diffusivities on the adsorption branch did not follow those measured on the desorption branch. The authors also found that the porous structure strongly influences the resultant patterns of the experimentally obtained diffusivities. Apicella and coworkers (1981) evaluated the water uptakes in sorption experiments made on thin sheets of an epoxy resin. The authors used a quartz microbalance placed in a temperature and humidity controlled cell. The sorption behaviors, under the same temperature and humidity conditions, have been successively compared for samples with different hygrothermal histories. Equilibrium moisture sorptions have been found to be dependent upon the humidity history to which the system had been previously subjected.

In this paper, the history dependence of water diffusion in asphalt binders was monitored using the FTIR-ATR technique with each sample passing through three hydration cycles, and two dehydration cycles. This paper validates the existence of hysteresis of moisture diffusivity in asphalt binders. The authors believe that the history dependence of this property is an important factor in characterizing asphalt binders especially in the modeling of moisture damage with fluctuating boundary conditions.

4.2 EXPERIMENTAL DESIGN

In this study, three asphalt binders were selected from the Strategic Highway Research Program (SHRP) Materials Reference Library (MRL): AAB, which is a PG 58-22 grade binder from Wyoming; AAD, which is a PG 58-22 grade California Coastal; and ABD, which is a PG 58-10 California Valley (Jones IV 1993). The procedure used to determine the history dependence of water diffusion in the asphalt binders is described in the following subsections.

4.2.1 Sample Preparation and Test Method

The detailed procedure for the sample preparation followed the same described in a previous publication (Vasconcelos et al. 2010). Asphalt binder solutions were prepared with toluene in the concentration of 1.5g of asphalt to 11mL of solvent (WRI 2001). The solution was spin coated in the ZnSe (Zinc Selenide) ATR crystal, followed by: (i) 2h under dry nitrogen purge to eliminate residual solvent presented in the film, and (ii) 1h period at 50°C in order to anneal micro cavities that might have been created due to solvent vaporization. Spin coating of the asphalt film was carried out such that the film thickness was less than the effective depth of penetration of the

infrared, d_p (Figure 4-1). In this case when water is added to the top of the film, a portion of the water over the film as well as the entire film is immediately within the effective detection range of the spectra. Change in concentration of water within the film over time is quantified by subtracting the initial spectra at time $t = 0$ s from the spectra detected at any subsequent point in time.

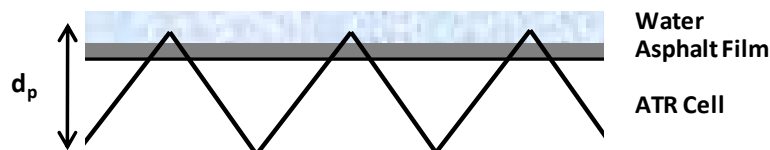


Figure 4-1. System Configuration and Infrared Depth of Penetration

The detailed test procedure to determine the rate of moisture absorption in asphalt binders is presented by Vasconcelos et al. (2010). However, in this study instead of only one cycle, the samples passed through three cycles of hydration (HC) followed by dehydration (DC). The duration of each HC was fixed at 15 days. The key steps of this procedure are briefly described below:

- A thin film of asphalt binder is prepared on a ZnSe ATR crystal using spin coating. The specially designed chamber is attached to the ZnSe crystal in order to deposit any liquid or allow passage of vapors over the film.
- The FTIR spectra of the asphalt binder are collected.
- 10mL of distilled water is added into the chamber (Figure 4-2) to initiate the first hydration cycle HC1. The chamber is sealed during the HC1 to avoid loss of water. Readings of asphalt/water spectrum are collected for 15 days using the FTIR.
- Water is removed from the chamber with a syringe at the end of HC1, and the film is allowed to come to equilibrium with the ambient atmosphere without disturbing of the system (no vacuum applied). An important observation here was that after 24 hours of dehydration, the FTIR spectra for the asphalt binder was very similar to the spectra obtained before the addition of water. This indicates that the 24 hour period was adequate to significantly complete the dehydration process. This was the first dehydration cycle or DC1. The relative humidity of the room was monitored during the DC and was found to be 40-45%.

- After DC1, the second hydration cycle or HC2 was initiated following the same procedure described for HC1.
- Three hydration cycles and two dehydration cycles comprised the complete procedure.

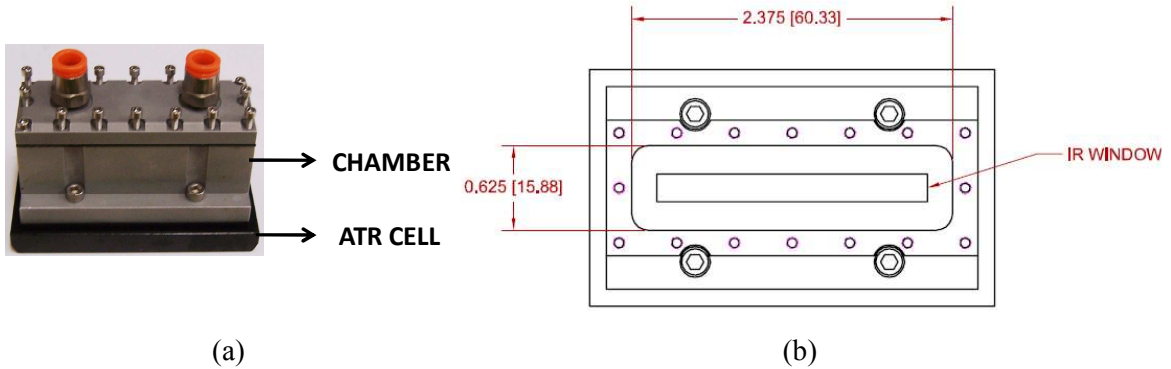


Figure 4-2. (a) Chamber (to Hold the Water above the Asphalt Film) Attached to the ATR cell, (b) Chamber Top View (Cover Removed)

4.2.2 Analysis

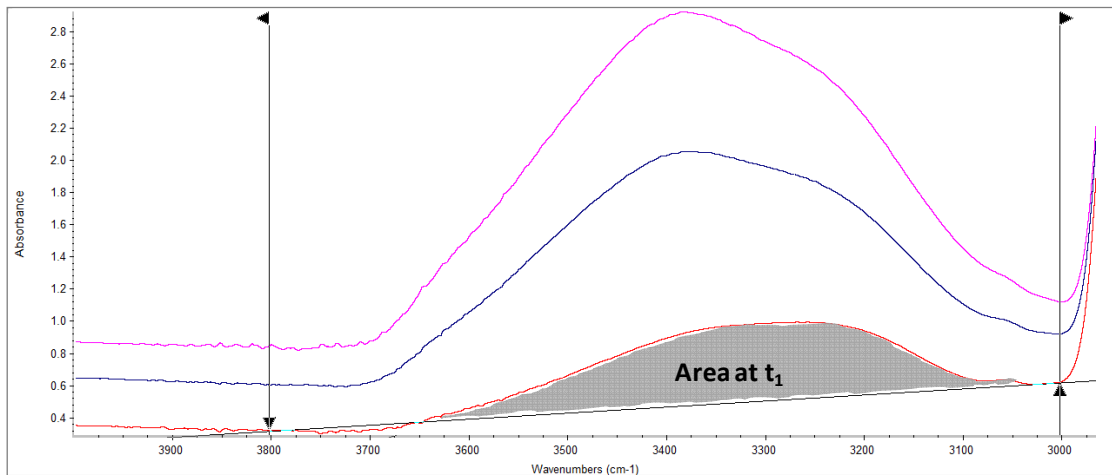
The FTIR-ATR technique does not directly measure mass of the diffusant at a given depth, but provides total absorbance in the entire film at any time t (A_t). The absorbance is proportional to the total instantaneous mass of the diffusant (M_t) within the film. When a polymer film of thickness $2l$ on an ATR plate is exposed to an infinite reservoir, assuming weak absorption and constant polymer refractive index, the following equation can be derived in terms of absorbance (Fieldson and Barbari 1993):

$$\frac{A_t - A_0}{A_{eq} - A_0} = 1 - \frac{8\gamma}{\pi[1 - \exp(2l\gamma)]} \sum_{n=0}^{\infty} \frac{\exp\left(\frac{-D(2n+1)^2 \pi^2 t}{4l^2}\right) \left[\frac{(2n+1)\pi}{2l} \exp(-\gamma 2l) + (-1)^n (2\gamma) \right]}{(2n+1) \left(4\gamma^2 + \left(\frac{(2n+1)\pi}{2l} \right)^2 \right)} \quad (4-1)$$

where, γ is the evanescent field decay coefficient (inverse of the depth of penetration), A_0 is the absorbance at time zero, D is the diffusivity, and A_{eq} is the absorbance value at saturation. In the FTIR-ATR test, saturation is evident when there is no further change in absorbance of the specimen with time. Since A_{eq} was not clearly established in all the specimens and all the

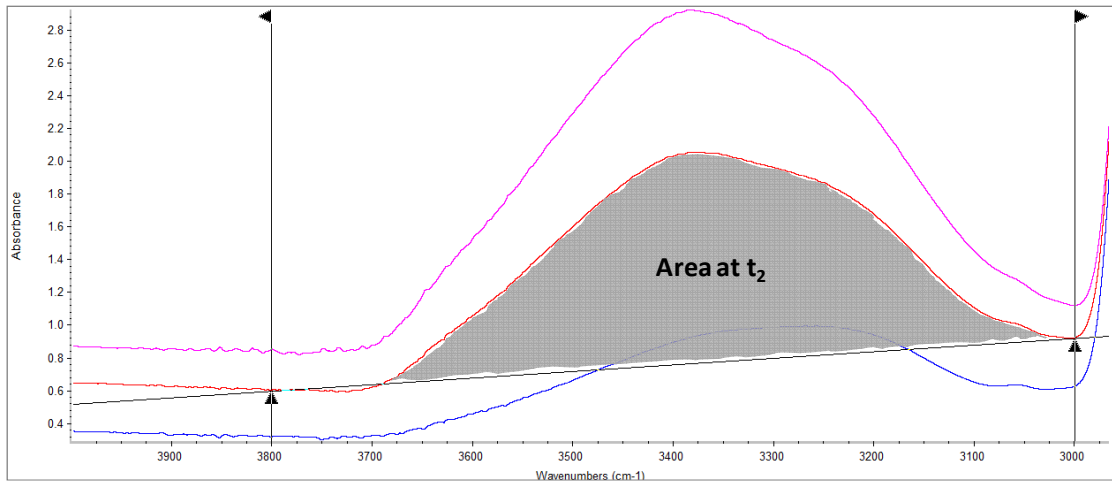
hydration cycles, this parameter was also treated as an unknown in Equation 4-1. A similar approach was used by Pereira and Yarwood (1996b) to analyze results from water diffusion in sulfonated poly(ether sulfone) membranes.

Equation 4-1 is similar to the mass uptake equation used in gravimetric sorption experiments, with the main difference being that the Fickian concentration profile is convoluted with the FTIR-ATR absorption equation before it is integrated (Fieldson and Barbari 1993). The quantitative analyses were performed using the corrected area between 3000 and 3800 cm^{-1} , as illustrated in Figure 4-3. The increase of the area with time was used to quantify the increase in water concentration into the asphalt binder.

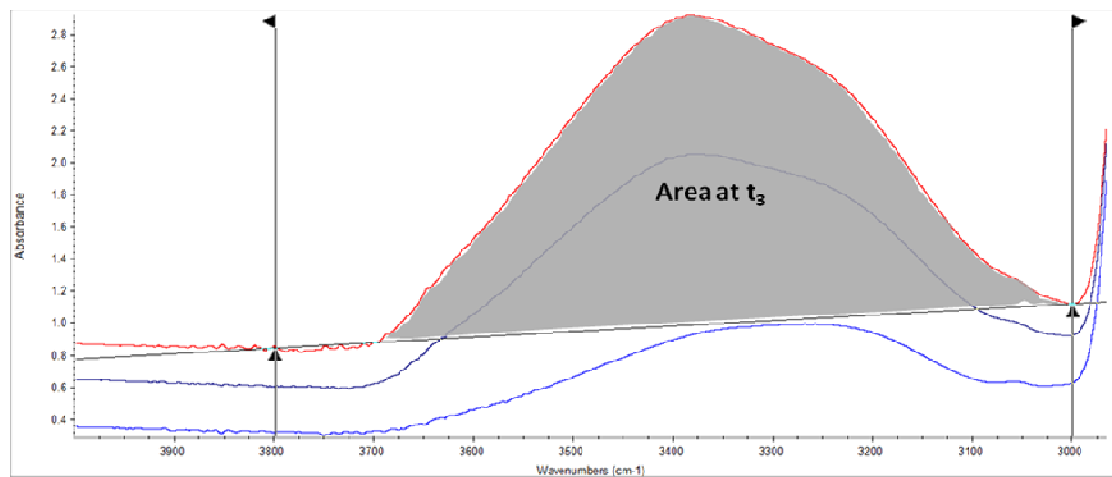


(i)

Figure 4-3. Region of Analysis used to Quantify Change of Water Concentration into the Asphalt Binders with Time



(ii)



(iii)

Figure 4-3 Continued

As reported by Vasconcelos et al (2010), the water diffusion in thin (less than 1 μm) films of asphalt binders did not follow the simple Fick's second law. Instead, water diffuses following a dual sorption mode, where each mode of sorption individually follows Fick's law. In this model it is assumed that a fraction of the water molecules is partially mobile, and the other fraction is completely mobile and can diffuse into the asphalt matrix freely. Thus the expression for describing this model contains two diffusion coefficients (Pereira and Yarwood 1996b):

$$\frac{A_1 - x_1 A_0}{x_1 (A_{eq} - A_0)} = 1 - \frac{8\gamma}{\pi [1 - \exp(2l\gamma)]} \sum_{n=0}^{\infty} \left[\frac{\exp\left(\frac{-D_1(2n+1)^2 \pi^2 t}{4l^2}\right) \left[\frac{(2n+1)\pi}{2l} \exp(-\gamma 2l) + (-1)^n (2\gamma) \right]}{(2n+1) \left(4\gamma^2 + \left(\frac{(2n+1)\pi}{2l} \right)^2 \right)} \right] \quad (4-2)$$

$$\frac{A_2 - x_2 A_0}{x_2 (A_{eq} - A_0)} = 1 - \frac{8\gamma}{\pi [1 - \exp(2l\gamma)]} \sum_{n=0}^{\infty} \left[\frac{\exp\left(\frac{-D_2(2n+1)^2 \pi^2 t}{4l^2}\right) \left[\frac{(2n+1)\pi}{2l} \exp(-\gamma 2l) + (-1)^n (2\gamma) \right]}{(2n+1) \left(4\gamma^2 + \left(\frac{(2n+1)\pi}{2l} \right)^2 \right)} \right] \quad (4-3)$$

where, D_1 and D_2 are the diffusivities (or diffusion coefficients) components of the dual mode diffusion model. After rearranging Equations 4-2 and 4-3 as a function of A_1 and A_2 , they can be added to produce the total absorbance at time t ($A_1 + A_2 = A_t$). The values of x_1 and x_2 are related to the proportion of the partially and totally mobile molecules ($x_1 + x_2 = 1$). The value of x_1 and two separate diffusion coefficients (D_1 and D_2) are then derived from the absorbance data. The same analysis procedure was used for the three hydration cycles, and the D_{eff} of each cycle were compared.

4.3 RESULTS AND DISCUSSION

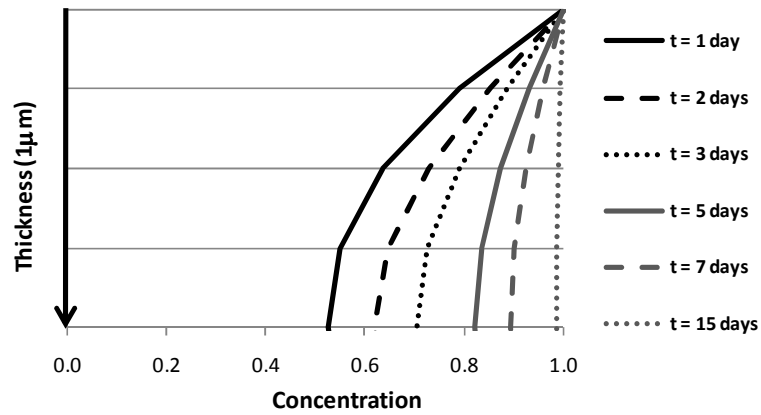
Quantitative analyses were performed using the Dual Mode diffusion model for the three hydration cycles, in each asphalt binder. Recall that the moisture content in the asphalt binder prior to the start of each hydration cycle was verified to be the same as that of the original binder prior to the start of the test sequence. Four replicates of each asphalt were evaluated and the average results are presented in Table 4-1.

Table 4-1. Average Results Obtained for Diffusivity Values

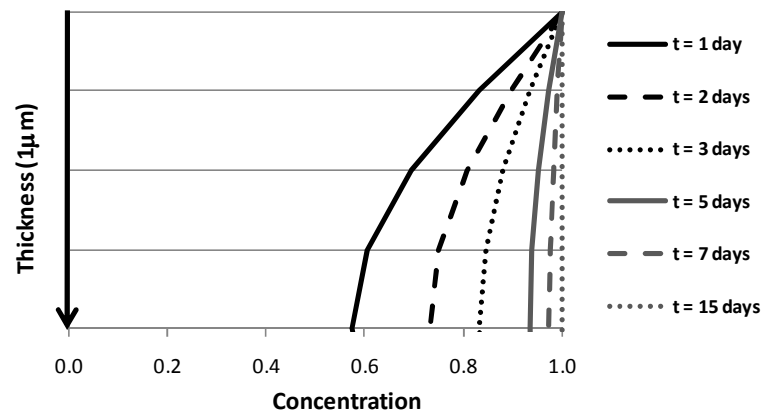
Asphalt	Cycle	$D_1(\text{nm}^2/\text{s})$	$D_2(\text{nm}^2/\text{s})$	x_1	Average D_{eff} (nm^2/s) [CV]	R^2 (fitting with the model)
AAB	1	29.0	1.2	0.50	15.0 [29.8%]	0.992
	2	167.9	2.2	0.46	80.8 [47.3%]	0.984
	3	194.7	2.8	0.47	92.1 [20.5%]	0.984
AAD	1	41.7	1.8	0.41	16.2 [40.6%]	0.988
	2	59.9	1.0	0.48	28.2 [33.5%]	0.991
	3	103.0	1.5	0.43	41.3 [34.2%]	0.992
ABD	1	102.7	0.5	0.55	52.0 [34.6%]	0.974
	2	371.8	1.4	0.62	178.3 [50.3%]	0.906
	3	571.5	2.3	0.44	244.4 [21.6%]	0.946

The difference in the diffusivity after each hydration cycle under the same environmental conditions may be attributed to a progressive change in microstructure. For example, a previous study attributed the history dependence of moisture damage in epoxy resins to a microcavitation damage in the form of localized solvent crazing (Apicella et al. 1981). This damage process has been associated with the presence of network inhomogeneities, which, on sorption, may favor localized crazing by differential swelling stresses. The authors concluded that the moisture by itself was not effective in producing the microcavitation in the resin but the synergistic effect of moisture and temperature was effective in the damaging process. In general, the diffusivity of moisture through the asphalt binder significantly increased after the first

hydration cycle. Figure 4-4 illustrates the concentration profile for asphalt AAB for hydration cycles 1, 2 and 3.

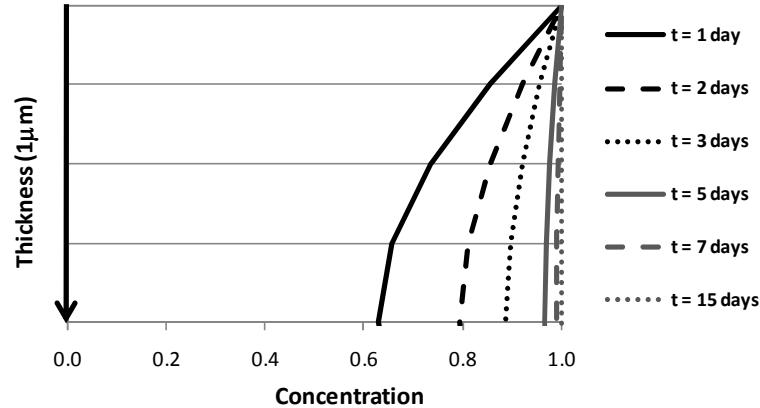


(a)



(b)

Figure 4-4. Concentration Profile for Asphalt AAB in: (a) HC 1, (b) HC 2, and (c) HC3



(c)

Figure 4-4 Continued

4.3.1 Statistical Analysis

Table 4-1 shows the average of the results obtained using the Dual Mode diffusion model, with the coefficient of variation (CV) for all three hydration cycles and asphalt binders. Two types of statistical analyses were carried out, (i) comparison of the same hydration cycle for different asphalts, and (ii) comparison of the different hydration cycles for the same asphalt. The analyses were conducted using the SPSS Statistics 17.0 software and included all the replicates for each cycle and each asphalt binder.

The null hypothesis of equal diffusivity values was assessed by applying Analysis of Variance (ANOVA) at a significance level of 0.05. Corresponding results showed that: (i) the moisture diffusivity for all three asphalt binders was statistically different, and (ii) for any given asphalt binder the moisture diffusivity was statistically different from one cycle to another. Tukey's HSD (honestly significant difference), and Bonferroni t test were used for identification of significant different means. Both methods presented the same classification for the different asphalts and hydration cycles. Table 4-2 presents the results obtained by the Tukey's HSD test.

Table 4-2. Statistical Analysis*

Part (i)					Part (ii)				
	ANOVA (Sig.)	Multiple Comparisons (Sig.)				ANOVA (Sig.)	Multiple Comparisons (Sig.)		
HC1	0.002	AAB	AAD	0.987	AAB	0.003	HC1	HC2	0.011
		AAB	ABD	0.003			HC1	HC3	0.004
		AAD	ABD	0.004			HC2	HC3	0.797
HC2	0.013	AAB	AAD	0.422	AAD	0.025	HC1	HC2	0.289
		AAB	ABD	0.086			HC1	HC3	0.020
		AAD	ABD	0.011			HC2	HC3	0.236
HC3	0.000	AAB	AAD	0.133	ABD	0.005	HC1	HC2	0.040
		AAB	ABD	0.000			HC1	HC3	0.004
		AAD	ABD	0.000			HC2	HC3	0.321

*The results in bold were considered statistically different

The difference in the diffusivity values for different hydration cycle may be attributed to the following causes:

- i) Dissolution and loss of asphalt binder in water that was removed using a syringe,
- ii) Change in the microstructure of the asphalt binder due to hydration/dehydration cycles, and
- iii) Residual water within the asphalt binder between the hydration cycles.

Additional tests and analysis were conducted to further evaluate the contribution of the above mentioned causes on the history dependence of water diffusion in asphalt binders. The following subsections discuss the findings from these tests.

4.3.2 Dissolution and Loss of Asphalt Binder in Water

All forms of spectroscopy give spectra that may be described in terms of frequency, intensity, and shape of spectral lines and bands. Nuclear Magnetic Resonance (NMR) is a spectroscopy technique that relies on the magnetic properties of the atomic nucleus. When placed in a strong magnetic field, certain nuclei resonate at a characteristic frequency in the radio frequency range of the electromagnetic spectrum. Slight variations in this resonant frequency give us detailed

information about the molecular structure in which the atom resides. A detailed description of NMR spectroscopy is beyond the scope of this paper.

In this study NMR spectroscopy was used to detect traces of bitumen that may have dissolved while the water was in contact with the bitumen. Two samples of asphalt AAD were prepared following the same procedure described for the FTIR-ATR test and submerged under a thin layer of water. The water remained in contact with the asphalt binder for 30 days, when it was removed for testing with the NMR. Results indicated that only signals characteristic of water molecules were observed, 2.5 to 3.0 ppm, with no signal of organic compounds pronounced in both samples analyzed. Based on this information, one can eliminate the possibility of cause i) presented above.

4.3.3 Change in Microstructure of Asphalt Binder

New techniques are being developed to evaluate the microstructure of asphalt binders. Among these are microscopic techniques such as the atomic force microscopy (AFM). The AFM, introduced by Binnig et al. (1986), provides insight into the surface topography with a powerful three-dimensional spatial resolution in the angstrom range. This technique was previously used to quantify the relative stiffness of different phases in asphalt binders (Jäger et al. 2004), to test asphalts at low temperatures (Masson et al. 2007), to evaluate the influence of aging of modified binders (Wu et al. 2008), and also to quantify its surface energy (Pauli et al. 2003).

The AFM was applied in this study to investigate potential influence of water on the microstructure or surface morphology of thin films of asphalt binder. The implicit assumption in this approach is that surface morphology also reflects changes within the bulk of the binder. The same substrate (ZnSe crystal), and procedure for sample preparation (spin coating and annealing) used for the FTIR-ATR measurements were also used for the AFM imaging (Vasconcelos et al. 2010). The specimens were scanned by a cantilever with a small tip placed near its free end, with the deflection of the cantilever describing the interaction between the AFM tip and the sample surface. The non-contact mode (NCM) was used to scan the surface topography of the asphalt binder without disturbing the specimen due to contact with the cantilever. The detailed test procedure can be found in other publications (Pauli 1999; Pauli et al. 2001).

Asphalt AAD was selected as result of its poor performance in the presence of water reported in previous publication (Bhasin et al. 2007). Figure 4-5 and 4-6 display the AFM images (topography and amplitude) of asphalt binder AAD before, and after 4 days of exposure

to water, respectively. Figure 4-5 clearly shows the ‘bee’ structure previously observed in different asphalt binders (Dourado and Simao 2009; Loeber et al. 1996; Pauli 1999; Pauli et al. 2001), and reported as being related to the asphaltenes or waxes in asphalt binders.

After subjecting the binder to water and dehydration, Figure 4-6 did not show the same surface morphology as seen in Figure 4-5. Based on these preliminary results it is very likely that water in contact with thin films of asphalt AAD altered its surface morphology. Therefore, a change in the microstructure of the asphalt binder could be a plausible explanation for the history dependence of moisture diffusivity in asphalt binders. However, further investigation may be required to quantify this effect and possibly correlate it with the chemical constituents of asphalt binder.

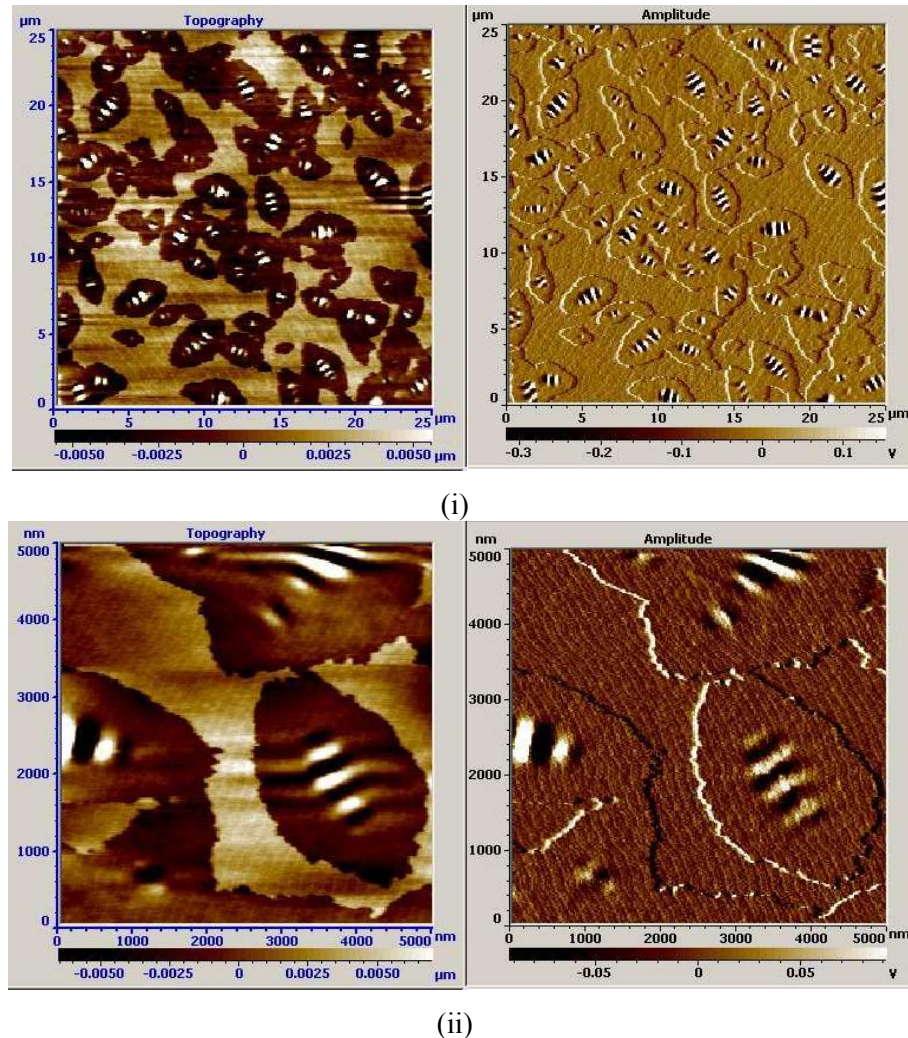


Figure 4-5. AFM Images from Asphalt AAD, (i) 25 μm² and (ii) 5 μm²

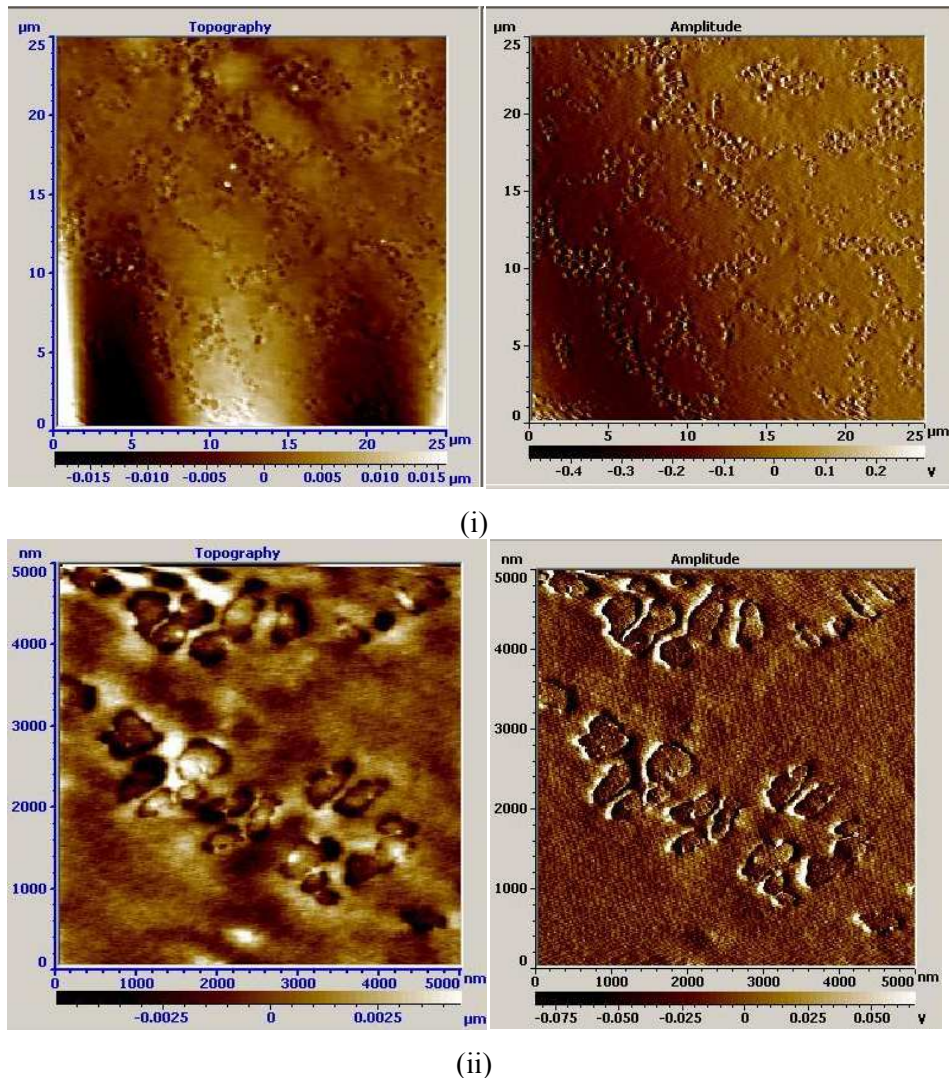


Figure 4-6. AFM Images of Asphalt AAD after 4 Days of Water Exposure, (i) 25µm² and (ii) 5µm²

4.3.4 Residual Moisture within the Asphalt Binder

As described in the test method section, the dehydration cycles followed a 24h period after the liquid water was removed from the chamber. It was observed that at the end of the dehydration cycles, some interference fringes appeared in the region from 3600-4000cm⁻¹ of the spectra (Figure 4-7). This is the fingerprint for water in the vapor or molecular form, as reported by Ewing et al. (2003). In the mentioned publication the authors show the different absorption spectra of water as (i) vapor at 25°C, (ii) liquid at 25°C, and (iii) ice at 190K.

From Figure 4-7 one can observe an increase in the appearance of the interference fringes in the region from 3600-4000 cm^{-1} from cycle 1 to cycle 3. The region of manifestation of water vapor (or molecular water) is not as simple to quantify as the region of liquid water (that has a broad peak area from 3000-3800 cm^{-1}). However, a tentative quantification was done by measuring the peak height at 3853 cm^{-1} , once it was observed that this point in the spectra had a constant increase over time. Figure 4-8 presents the results of this quantification for the three hydration cycles of one specimen of asphalt AAB.

Although the liquid water had been removed from the chamber during the dehydration cycles, it seems that there is still some residual water in the vapor state trapped into the asphalt binder film. The consequence of the residual moisture in the history dependence of diffusivity, and ultimately to the debonding of asphalt binder from aggregate is still unknown. Further analyses and tests are still necessary to arrive in conclusive data. The topic is still under investigation by this research group.

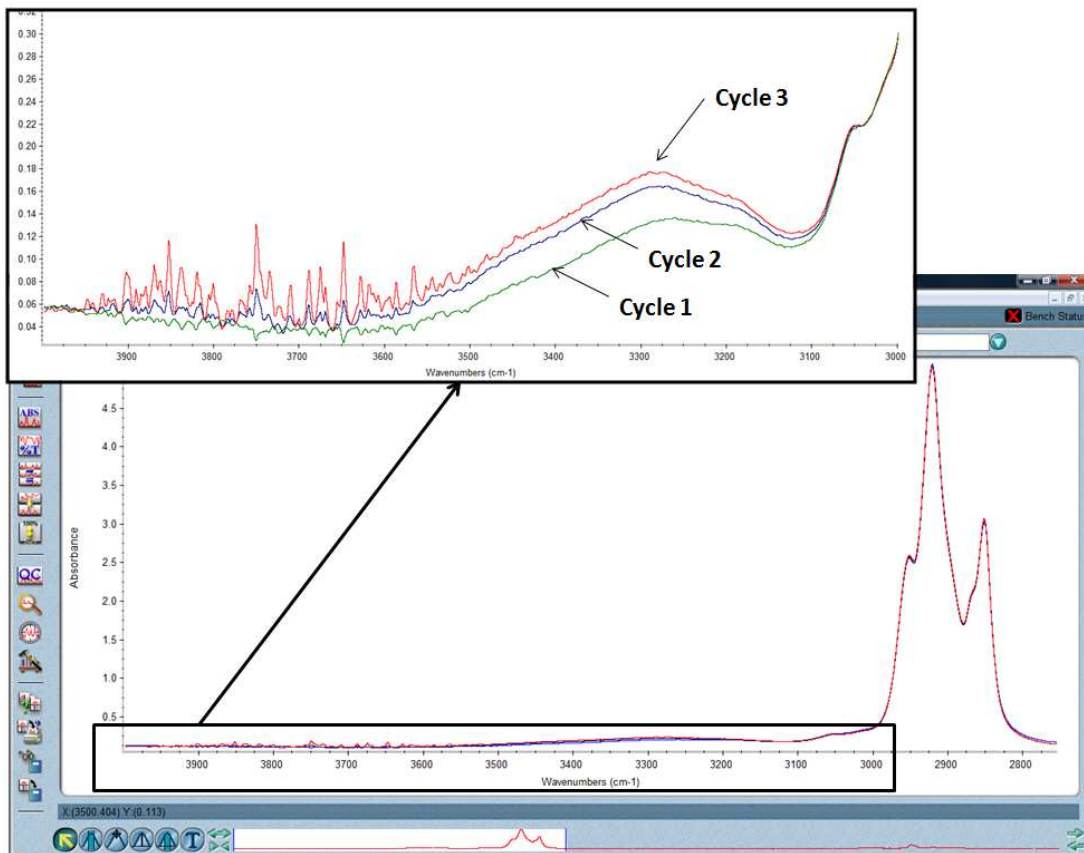


Figure 4-7. Illustration of Dehydration Cycles (Asphalt AAB)

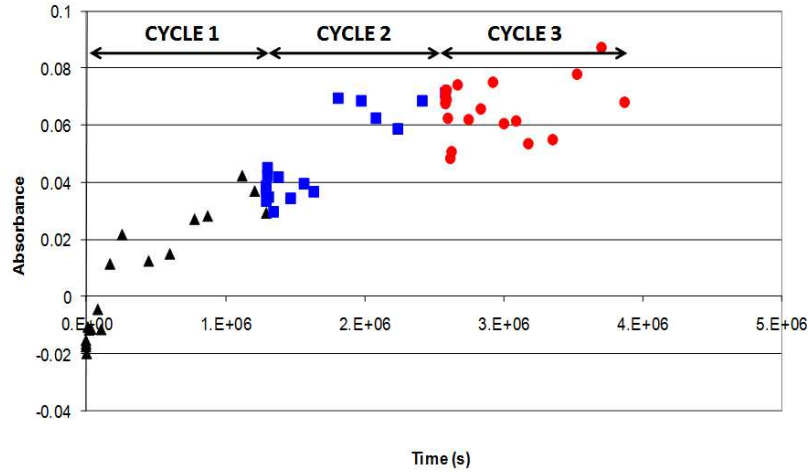


Figure 4-8. Quantification of the Presence of Water Vapor in the Asphalt Film (Peak Height at 3853cm^{-1} for Asphalt AAB)

4.4 CONCLUSIONS

Despite the importance of hysteresis of water diffusion in polymeric materials, there is only limited literature available on this subject. The FTIR-ATR spectroscopy technique was used to investigate the effect of cycling moisture boundary conditions on the diffusivity of moisture through three asphalt binders (SHRP reference library). The samples passed through three cycles of hydration (HC) followed by dehydration (DC) and the major conclusions of this study follows:

- The rate of moisture diffusion in asphalt binders was proved to be dependent on the history of exposure of the asphalt binder to the moisture. The phenomenon was observed in the three asphalt binders investigated.
- In most cases, the diffusivity of moisture increased with every subsequent cycle of exposure to moisture. The increase in diffusivity was most significant after the first cycle, and the change in diffusivity was dependent on the type of asphalt binder.
- The NMR spectroscopy technique was used to analyze the water exposed to the bitumen film for a 30 days period. No signal of organic compounds was observed in the samples analyzed, reducing the possibility of dissolution or loss of asphalt binder in water.
- The increase in moisture diffusivity was attributed mostly to the change in microstructure of the asphalt binder after being exposed to the moisture. This was

supported by AFM images of asphalt binder before and after being exposed to water. Further investigation is still necessary to quantify this effect and possibly correlate it with the chemical constituents of asphalt binder.

- There was some evidence of increase in moisture trapped in the form of vapor even after dehydration that could also contribute to the increase in diffusivity. The consequence of the residual moisture in the history dependence of diffusivity, and ultimately to the debonding of asphalt binder from aggregate is still unknown. Further analyses and tests are still necessary to arrive in conclusive data. The topic is still under investigation by this research group.

5. CONCLUSIONS, RECOMMENDATIONS, AND FUTURE WORK

5.1 DETAILED CONCLUSIONS AND RECOMENDATIONS

This section summarizes the main findings of this research study and corresponding recommendations to the measurement of water diffusion in asphalt materials, and related topics to further improve the aspects treated in this study. The following subsections have the detailed conclusions and recommendations obtained in each section of this manuscript.

5.1.1 *Water Diffusion in Asphalt Binders*

The detailed procedure for the measurement of water diffusion in asphalt binder films was presented. Figure 5-1 illustrates the three main steps in the procedure: sample preparation using stock asphalt solution and spin coating; film thickness and refractive index measurement by the ellipsometer, and the test method used in the FTIR-ATR. The homogeneity of the asphalt film was carefully evaluated, since the thickness is an important parameter in the analytical model used. Following are the main findings of this study:

- The diffusivity of water through asphalt was significantly higher for (at least) one asphalt binder than it was in the other three binders (from the set of four tested) indicating that diffusivity may be an important material variable that influences the rate of moisture damage.
- A dual mode diffusion model was shown to better represent the diffusion of water through asphalt binders. This model suggests that water molecules may be diffusing at two different rates within the asphalt binder with the slower rate being associated with interaction between water molecules and polar functional groups within the material. The implication of this mode of diffusion through asphalt binders in terms of performance and asphalt chemistry requires further investigation. However, these results do suggest that future efforts related to modeling of moisture damage should consider the use of a dual mode diffusion model rather than simple diffusion based on Fick's second law.
- The values of diffusivity reported in this study are smaller than the values reported by Arambula et al. (2009) and Kassem et al. (2006). The values reported in this paper pertain to the diffusion of liquid water through thin films of asphalt binder which is different from diffusion of moisture through mixtures or mastics. The latter is dictated by macroscopic properties including interconnected air voids that allow moisture to travel much faster

through the bulk. In contrast, the results shown in this study are relevant to the diffusion of moisture through the binder as in the case of microstructural entities that interconnect voids to the binder-aggregate interface. The impact of this could be that binders that develop a tenacious bond with aggregate surfaces and also resist moisture diffusion to the binder-aggregate interface may be more resistant to moisture damage.

- The results obtained in this study are in the same order of magnitude of the results presented by Wei (2009) using the Electrochemical Impedance Spectroscopy (EIS). Wei used thin binder film on aluminum plate substrate.

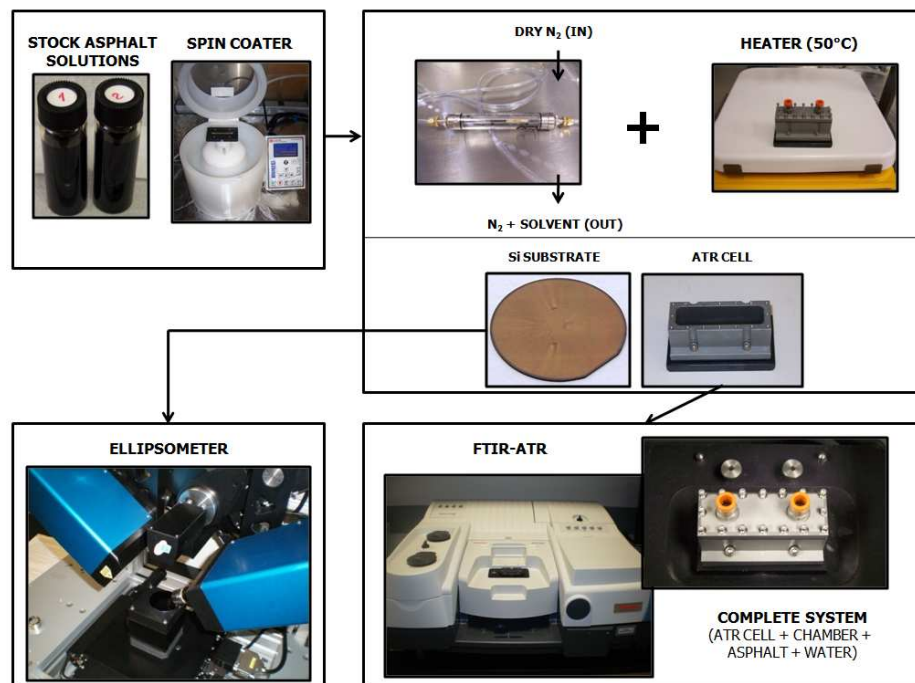


Figure 5-1. Overall Test Procedure used for the Measurement of Water Diffusion in Asphalt Binder Films

5.1.2 Water Diffusion in Fine Aggregate Mixtures

A simple gravimetric sorption procedure for the measurement of water diffusion in fine aggregate mixtures was presented. Figure 5-2 illustrates the two main steps in the procedure: specimen fabrication, and the test method. The specimens were comprised of fine aggregates (passing sieve No 16), asphalt binder and air voids. Three asphalt binders and two aggregates were combined and tested at two different temperatures. Following are the main findings of this study:

- Diffusivity of several different FAMs was measured using a simple gravimetric approach. Results indicate that the diffusivity of water through FAM is in the order of 10^{-12} m²/s. These results are in the same order of magnitude as those reported by Kringos et al. (2008a).
- Moisture uptake and diffusivity of water through FAM is dependent on the type of aggregate and asphalt binder. For any given asphalt binder, FAM specimens with aggregates having a significantly higher specific surface area such as RK had higher moisture uptake and higher diffusivity when compared to FAM specimens with aggregates having a significantly lower specific surface area. Since both aggregates are siliceous with low porosity, this indicates that a portion of the diffused water is probably trapped at the binder-aggregate interface.
- At room temperature, the rank order of diffusivity and moisture uptake for the three binders was the same irrespective of the type of aggregate. However, this rank order changed at higher temperatures suggesting that at elevated temperatures different binders may be undergoing a different level of change in the free volume.

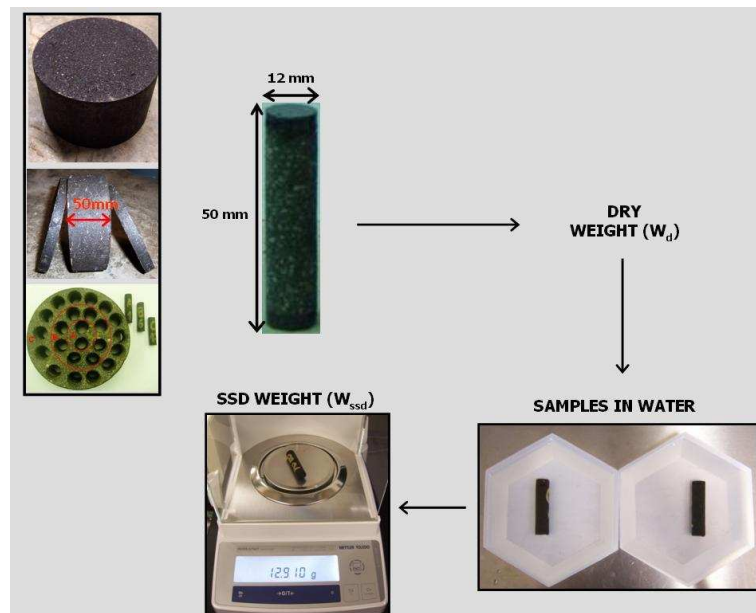


Figure 5-2. Overall Test Procedure used for the Measurement of Water Diffusion in Fine Aggregate Mixtures

5.1.3 History Dependence of Water Diffusion in Asphalt Binders

In this study, the history dependence of water diffusion in asphalt binders was monitored using the FTIR-ATR technique with each sample passing through three hydration cycles, and two

dehydration cycles. The paper validates the existence of hysteresis of water diffusivity in asphalt binders. The authors believe that the history dependence of this property is an important factor in characterizing asphalt binders especially in the modeling of moisture damage with fluctuating boundary conditions. The major conclusions of this study follow:

- The rate of moisture diffusion in asphalt binders was proved to be dependent on the history of exposure of the asphalt binder to the moisture. The phenomenon was observed in the three asphalt binders investigated.
- In most cases, the diffusivity of moisture increased with every subsequent cycle of exposure to moisture. The increase in diffusivity was most significant after the first cycle, and the change in diffusivity was dependent on the type of asphalt binder.
- NMR spectroscopy was used to analyze the water exposed to the bitumen film for a 30 day period. No signal of organic compounds was observed in the samples analyzed, reducing the possibility of dissolution or loss of asphalt binder in water.
- The increase in moisture diffusivity was attributed mostly to the change in microstructure of the asphalt binder after being exposed to the moisture. This was supported by AFM images of asphalt binder before and after being exposed to water. Further investigation is still necessary to quantify this effect and possibly correlate it with the chemical constituents of asphalt binder.
- There was some evidence of increase in moisture trapped in the form of vapors even after dehydration that could also contribute to the increase in diffusivity. The consequence of the residual moisture in the history dependence of diffusivity, and ultimately to the debonding of asphalt binder from aggregate is still unknown. Further analyses and tests are still necessary to arrive in conclusive data. The topic is still under investigation by this research group.

5.1.4 The Physical State of Water and the Diffusion in Asphalt Binders

It is known that the water molecule has distinct arrangement patterns as the physical state change from ice to water to vapor. The FTIR-ATR technique has the ability to differentiate water in different physical states, and this technique is being used to quantify molecular water movement into asphalt films. Based on the partial results obtained until now, one can observe that the detection of water vapor by the FTIR occurred before the detection of liquid water. These preliminary results give an insight about the influence of the physical state of water in rate of diffusion into the asphalt films. The study is still under investigation by this research group.

5.2 FUTURE WORK

The analysis conducted allowed identification of the aspects subsequently discussed, not included in this study, that require additional study to further investigate the process of moisture diffusion in asphalt materials.

- Further investigation of the differences between the diffusion of liquid water versus water vapor is recommended. A simple and not expensive way to have the relative humidity (RH) controlled at high levels (above 95%) is through the use of saturated salt solutions. In previous studies (Carotenuto and Dell'Isola 1996; Martin 1962; O'Brien 1948) one can find a list of different salts and the equilibrium relative humidity values for each salt at different temperatures. The same FTIR-ATR technique previously described can be used. A chamber was designed for this investigation (Figure 5-3). In case different results are observed for the diffusivity of liquid water and water vapor in asphalt binders, the consequences of this difference should also be addressed.

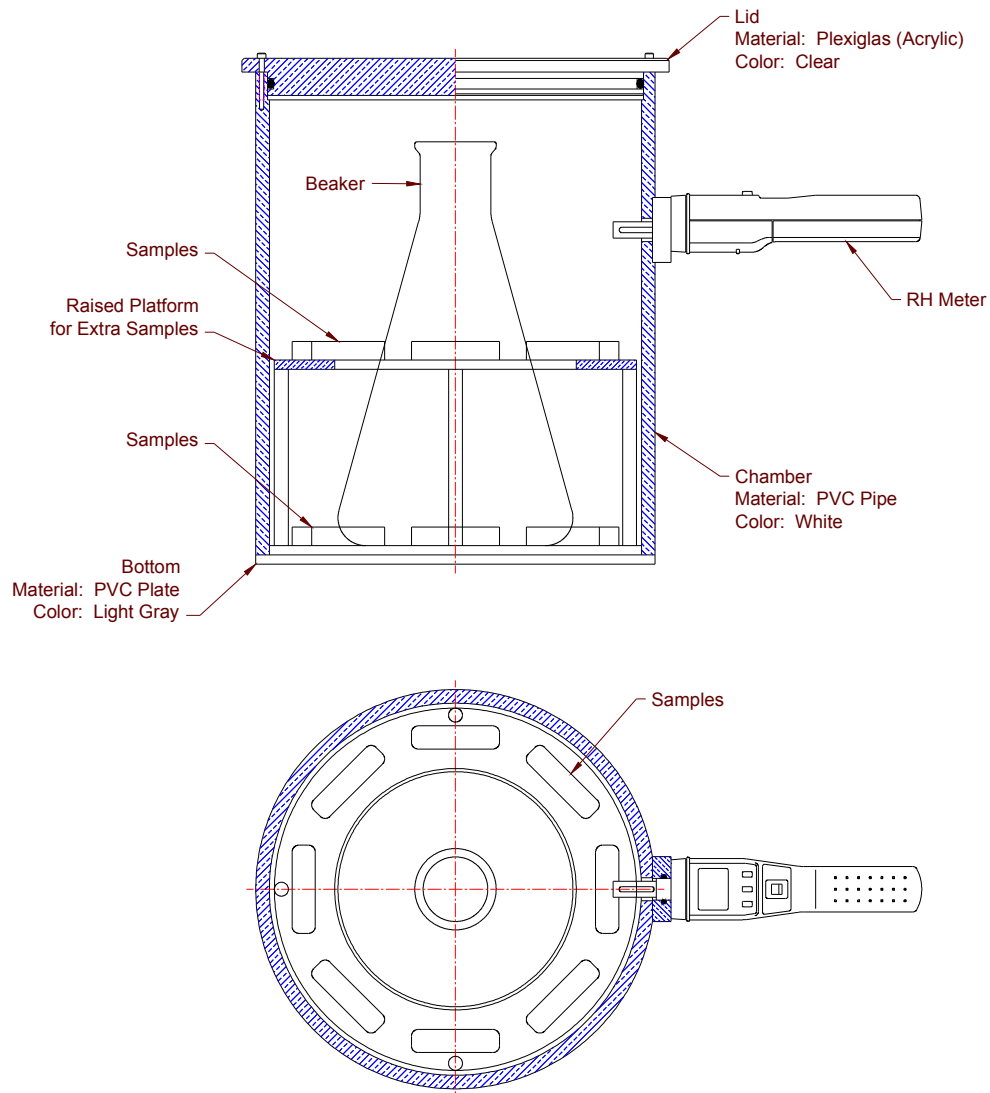


Figure 5-3. Humidity Chamber Designed to Keep the Specimens at a Controlled Relative Humidity

- Use of the FTIR-ATR to quantify water and moisture diffusivity through polymer modified binders, and also mastic (asphalt binder and material passing sieve No 200). Considerations such as casting of thin homogenous films are important when using this technique.
- Determine the rate of diffusion at the binder-substrate interface in addition to the rates of diffusion through thin films of asphalt binder. The kinetics of debonding, or rate of debonding, at the binder-aggregate is mostly influenced by the thermodynamic potential for water to cause debonding (determined using the surface free energy components) and micro texture of the aggregate surface.

- The gravimetric sorption setup can also be applied for measurements at different scales and also to different samples and test configurations. Sample geometry, test temperature, aggregate sizes, and different specimen air voids are some examples of potential topics for further investigation.

REFERENCES

- Ait-Kadi, A., Brahimi, B., and Bousmina, M. (1996). "Polymer blends for enhanced asphalt binders." *Polymer Engineering and Science*, 36(12), 1724-1733.
- Al-Omari, A., Tashman, L., Masad, E., Cooley, A., and Harman, T. (2002). "Proposed methodology for predicting HMA permeability." *Journal of the Association of Asphalt Paving Technologists*, 71, 30-58.
- Apicella, A., Nicolais, L., Astarita, G., and Drioli, E. (1981). "Hygrothermal history dependence of equilibrium moisture sorption in epoxy resins." *Polymer*, 22(8), 1064-1067.
- Arambula, E., Caro, S., and Masad, E. (2009). "Experimental measurement and numerical simulation of water vapor diffusion through asphalt pavement materials." *Journal of Materials in Civil Engineering, ASCE*, submitted for evaluation.
- Artamendi, I., and Khalid, H. A. (2006). "Diffusion kinetics of bitumen into waste tyre rubber." *Journal of the Association of Asphalt Paving Technologists*, 75, 133-164.
- Barrie, J. A. (1968). "Water in polymers" *Diffusion in Polymers*, J. Crank and G.S. Park, eds., Academic Press, New York.
- Benjamin, I. (1994). "Vibrational spectrum of water at the liquid/vapor interface." *Physical Review Letters*, 73(15), 2083.
- Bertie, J. E., Labbe, H. J., and Whalley, E. (1969). "Absorptivity of ice I in the range 4000--30 cm^[sup - 1]." *The Journal of Chemical Physics*, 50(10), 4501-4520.
- Bertotti, G., and Mayergoz, I. D. (2006). *The Science of Hysteresis, Volume II: Physical Modeling, Micromagnetics, and Magnetization Dynamics*, Elsevier Inc., Oxford, UK.
- Bhasin, A., Little, D. N., Vasconcelos, K. L., and Masad, E. (2007). "Surface free energy to identify moisture sensitivity of materials for asphalt mixes." *Transportation Research Record*(2001), 37-45.
- Binnig, G., Quate, C. F., and Gerber, C. (1986). "Atomic force microscope." *Physical Review Letters*, 56(9), 930.
- Caro, S., Masad, E., Bhasin, A. and Little, D. N. (2008). "Moisture susceptibility of asphalt mixtures, Part 1: mechanisms." *International Journal of Pavement Engineering*, 9(2), 81-98.

- Caro, S., Masad, E., Bhasin, A., and Little, D. N. (2009). "A coupled micromechanical model of moisture induced damage in asphalt mixtures." *Journal of Materials in Civil Engineering*, posted online ahead of print.
- Caro, S., Masad, E., Bhasin, A., Little, D. N., and Sanchez-Silva, M. (2010). "Probabilistic modeling of the effect of air voids on the mechanical performance of asphalt mixtures subjected to moisture diffusion." *Journal of the Association of Asphalt Paving Technologists (AAPT)*, submitted for evaluation.
- Carotenuto, A., and Dell'Isola, M. (1996). "An Experimental verification of saturated salt solution-based humidity fixed points." *International Journal of Thermophysics*, 17(6), 1423-1439.
- Cheng, D. X., Little, D. N., Lytton, R. L., and Holste, J. C. (2003). "Moisture damage evaluation of asphalt mixtures by considering both moisture diffusion and repeated-load conditions." *Bituminous Paving Mixtures 2003(1832)*, 42-49.
- Crank, J. (1975). *The Mathematics of Diffusion*, Oxford University Press, Oxford, UK.
- Crank, J. (1979). *The Mathematics of Diffusion*, Oxford University Press, Oxford, UK.
- De Kee, D., Liu, Q., and Hinestroza, J. (2005). "Viscoelastic (non-fickian) diffusion." *The Canadian Journal of Chemical Engineering*, 83(December 2005), 913-929.
- Doppers, L.-M., Sammon, C., Breen, C., and Yarwood, J. (2006). "FTIR-ATR studies of the sorption and diffusion of acetone/water mixtures in poly(vinyl alcohol)." *Polymer*, 47, 2714-2722.
- Doumenc, F., Guerrier, B., and Allain, C. (2005). "Coupling between mass diffusion and film temperature evolution in gravimetric experiments." *Polymer*, 46, 3708-3719.
- Dourado, E. R., and Simao, R. (2009). "Analysis of the Asphaltic Binder by Atomic Force Microscopy (AFM)." *11th International Conference on Advanced Materials*, Rio de Janeiro, Brazil.
- Du, Q., Superfine, R., Freysz, E., and Shen, Y. R. (1993). "Vibrational spectroscopy of water at the vapor/water interface." *Physical Review Letters*, 70(15), 2313.
- Elabd, Y. A., Baschetti, M. G., and Barbari, T. A. (2003). "Time-resolved Fourier transform infrared/attenuated total reflection spectroscopy for the measurement of molecular diffusion in polymers." *Journal of Polymer Science Part B-Polymer Physics*, 41, 2794-2807.

- Epps, J. A., Sebaaly, P.E., Penaranda, J., Maher, M.R., McCann, M.B. and Hand, A.J. (2000). "Compatibility of a Test for Moisture-Induced Damage with Superpave Volumetric Mix Design." *NCHRP Report 444*, Transportation Research Board - National Research Council, Washington, D.C.
- Ewing, G. E., Foster, M., Cantrell, W., and Sadtchenko, V. (2003). "Thin film water on insulator surfaces." *Water in Confining Geometries*, V. Buch and J. P. Devlin, eds., Springer-Verlag, Berlin, p. 179-211.
- Falk, M., and Ford, T. A. (1966). "Infrared spectrum and structure of liquid water." *Canadian Journal of Chemistry*, 44, 1699-1707.
- Fieldson, G. T., and Barbari, T. A. (1993). "The use of FTIR-ATR spectroscopy to characterize penetrant diffusion in polymers." *Polymer*, 34(6), 1146-1153.
- Frisch, H. L. (1964). "Isothermal diffusion in systems with glasslike transitions." *J. Chem. Phys.*, 41, 3379-3683.
- Frisch, H. L. (1980). "Sorption and transport in glassy polymers-a review." *Polymer Engineering & Science*, 20(1), 2-13.
- Gonzalez, A., Eceolaza, A., Etxeberria, J., and Iruin, J. (2007). "Diffusivity of ethylene and propylene in atactic and isotactic polypropylene: morphology effects and free-volume simulations." *Journal of Applied Polymer Science*, 104, 3871-3878.
- Griffiths, P. R., and de Haseth, J. A. (2007). *Fourier Transform Infrared Spectrometry*, Wiley-Interscience, USA.
- Harrick, N. J. (1965). "Field strengths at a totally reflecting interfaces." *Journal of the Optical Society of America*, 55(7), 851-857.
- Hinrichs, K., Gensch, M., Nikonenko, N., Pioteck, J., and Eichhom, K.-J. (2005). "Spectroscopy ellipsometry for characterization of thin films of polymer blends." *Macromol. Symp.*, 230, 26-32.
- Hong, S. U., Barbari, T. A., and Sloan, J. M. (1997). "Diffusion of methyl ethyl ketone in polyisobutylene: comparison of spectroscopy and gravimetric techniques." *J. Polymer Sci., Part B: Polym. Phys.*, 35, 1261-1267.
- Huang, B., Mohammad, L., Raghavendra, A., and Abadie, C. (1999). "Fundamentals of permeability in asphalt mixtures." *Journal of the Association of Asphalt Paving Technologists*, 68, 479-500.

- Iwamoto, R., and Ohta, K. (1984). "Quantitative surface analysis by Fourier transform attenuated total reflection infrared spectroscopy." *Applied Spectroscopy*, 38(3), 359-365.
- Jacobs, M. M. J., Hopman, P. C., and Molenaar, A. A. A. (1996). "Characterization of fracture in asphaltic mixes based on a molecular approach." *Transportation Research Record: Journal of the Transportation Research Board*, 1535, 22-28.
- Jäger, A., Lackner, R., Eisenmenger-Sittner, C., and Blab, R. (2004). "Identification of microstructural components of bitumen by means of atomic force microscopy (AFM)." *PAMM*, 4(1), 400-401.
- Jones IV, D. R. (1993). "SHRP Materials Reference Library: Asphalt Cements: A Concise Data Compilation." *Report SHRP-A-645, Contract A-001*, Strategic Highway Research Program, National Research Council, Washington, DC.
- Karlsson, R., and Isacson, U. (2003a). "Application of FTIR-ATR to characterization of bitumen rejuvenator diffusion." *Journal of Materials in Civil Engineering*, 15(2), 157-165.
- Karlsson, R., and Isacson, U. (2003b). "Investigation on bitumen rejuvenator diffusion and structural stability." *Journal of the Association of Asphalt Paving Technologists*, 73, 463-501.
- Karlsson, R., Isacson, U., and Ekblad, J. (2007). "Rheological characterisation of bitumen diffusion." *Journal of Materials Science*, 42(1), 101-108.
- Kassem, E. A., Masad, E., Bulut, R., and Lytton, R. L. (2006). "Measurements of moisture suction and diffusion coefficient in hot mix asphalt and their relationships to moisture damage." *Transportation Research Record: Journal of the Transportation Research Board*, 1970, 45-54.
- Kim, Y., Lee, H. J., Little, D. N., and Kim, Y. R. (2006). "A simple testing method to evaluate fatigue fracture and damage performance of asphalt mixtures." *Journal of the Association of Asphalt Paving Technologists*, 75, 755-787.
- Korsmeyer, R. W., Meerwall, E. V., and Peppas, N. A. (1986). "Solute and penetrant diffusion in swellable polymers. II. Verification of theoretical models." *Journal of Polymer Science: Polymer Physics Edition*, 24, 409-434.
- Kringos, N., and Scarpas, A. (2005). "Raveling of asphaltic mixes due to water damage - computational identification of controlling parameters." *Bituminous Paving Mixtures 2005*(1929), 79-87.

- Kringos, N., and Scarpas, A. (2008). "Physical and mechanical moisture susceptibility of asphaltic mixtures." *International Journal of Solids and Structures*, 45, 2671-2685.
- Kringos, N., Scarpas, A., and deBondt, A. (2008). "Determination of moisture susceptibility of mastic-stone bond strength and comparison to thermodynamical properties." *Journal of the Association of Asphalt Paving Technologists*, 77, 435-478.
- Kringos, N., Scarpas, A., and Selvadurai, A. P. S. (2008). "Simulation of mastic erosion from open-graded asphalt mixes using a Hybrid Lagrangian-Eulerian finite element approach." *Cmes-Computer Modeling in Engineering & Sciences*, 28(3), 147-159.
- Kutay, M. E. (2005). "Modeling Moisture Transport in Asphalt Pavements," Ph.D. dissertation, University of Maryland, College Park.
- Larobina, D., Lavorgna, M., Mensitieri, G., Musto, P., and Vautrin, A. (2007). "Water diffusion in glassy polymers and their silica hybrids: an analysis of state of water molecules and of the effect of tensile stress." *Macromol. Symp.*, 247, 11-20.
- Little, D. N., Bhasin, A., Lytton, R. L., and Hefer, A. (2005). "Using Surface Energy Measurements to Select Materials for Asphalt Pavements." *NCHRP 9-37*, National Cooperative Highway Research Program, Transportation Research Board, National Research Council.
- Liu, M., Lunsford, K. M., Davison, R. R., Glover, C. J., and Bullin, J. A. (1996). "The kinetics of carbonyl formation in asphalt." *Aiche Journal*, 42(4), 1069-1076.
- Loeber, L., Sutton, O., Morel, J., Valleton, J. M., and Muller, G. (1996). "New direct observations of asphalts and asphalt binders by scanning electron microscopy and atomic force microscopy." *Journal of Microscopy*, 182, Pt 1, April 1996, 32-39.
- Martin, S. (1962). "The Control of Conditioning Atmospheres by Saturated Salt Solutions." *Journal of Scientific Instruments*, 7, 370-372.
- Masad, E., Arambula, E., Ketcham, R. A., Abbas, A. R., and Epps Martin, A. (2007). "Nondestructive Measurement of Moisture Transport in Asphalt Mixtures." *Journal of the Association of Asphalt Paving Technologists*, 76, 919-952.
- Masad, E., Birgisson, B., Al-Omari, A., and Cooley, A. (2004). "Analytical derivation of permeability and numerical simulation of fluid flow in hot-mix asphalt." *Journal of Materials in Civil Engineering, ASCE*, 16(5), 487-496.
- Masad, E., Castelo Branco, V. T. F., Little, D. N., and Lytton, R. L. (2006). "An Improved Method for the Dynamic Mechanical Analysis of Fatigue Failure of Sand Asphalt

Mixtures." *Federal Highway Administration FHWA/473630*, Texas Transportation Institute, Texas A&M University, College Station, TX.

- Masson, J.-F., Leblond, V., Margeson, J., and Bundalo-Perc, S. (2007). "Low-temperature bitumen stiffness and viscous paraffinic nano- and micro-domains by cryogenic AFM and PDM." *Journal of Microscopy*, 227 Pt 3(September 2007), 191-202.
- Mayergoyz, I. D. (1991). *Mathematical Models of Hysteresis*, Springer-Verlag Inc., New York.
- McKnight, S. H., and Gillespie Jr., J. W. (1997). "In situ examination of water diffusion to the polypropylene-silane interface using FTIR-ATR." *J. Appl. Polym. Sci.*, 64(10), 1971-1985.
- Mirabella Jr., F. M. (1990). "Quantitative internal reflection spectroscopy." *Spectroscopy*, 5(8), 20-30.
- Mohammad, L. N., Herath, A., and Huang, B. (2003). "Evaluation of permeability of superpave asphalt mixtures." *Transportation Research Record: Journal of the Transportation Research Board*, 1832, 50-58.
- Naumov, S., Valiullin, R., Galvosas, P., Kärger, J., and Monson, P. A. (2007). "Diffusion hysteresis in mesoporous materials." *The European Physical Journal - Special Topics*, 141(1), 107-112.
- Netzel, D. A. (2006). "Apparent activation energies for molecular motions in solid asphalts." *Energy & Fuels*, 20, 2181-2188.
- Nguyen, T., Bentz, D., and Byrd, E. (1994). "A Study of water at the organic coating/substrate interface." *Journal of Coatings Technology*, 66(834), 39-50.
- Nguyen, T., Bentz, D., and Byrd, E. (1995a). "Method for measuring water diffusion in a coating applied to a substrate." *Journal of Coatings Technology*, 67(844), 37-46.
- Nguyen, T., Byrd, E., and Bentz, D. (1995b). "Quantifying water at the organic film/hydroxylated substrate interface." *J. Adhesion*, 48, 169-194.
- Nguyen, T., Byrd, E., Bentz, D., and Lin, C. (1996a). "In situ measurement of water at the organic coating/substrate interface." *Progress in Organic Coatings*, 27, 181-193.
- Nguyen, T., Byrd, E., Bentz, D., and Seiler, J. (1996b). "Development of a Method for Measuring Water-Stripping Resistance of Asphalt/Siliceous Aggregate Mixtures." *National Institute of Standards and Technology (NISTIR) Report 5865*, Transportation Research Board, National Research Council, Washington, D.C., USA.

- Nguyen, T., Byrd, E. W., Bentz, D., and Martin, J. (2005). "In situ spectroscopy study of water at the asphalt/siliceous substrate Interface and its implication in stripping." *The Journal of Adhesion*, 81, 1-28.
- Nguyen, T., Byrd, E. W., and Lin, C. (1991a). "A spectroscopy technique for in situ measurement of water at the coating/metal interface." *J. Adhesion Sci. Technol.*, 5(9), 697-709.
- Nguyen, T., Byrd, W. E., Lin, C., and Bentz, D. (1991b). "A novel spectroscopy technique for in-situ studies of water at the interface between a metal and an opaque polymeric film." *Advanced Composite Materials*, 19, 1051-1060.
- O'Brien, F. E. M. (1948). "The control of humidity by saturated salt solutions." *Journal of Scientific Instruments*, 3, 73-76.
- Pauli, A. T. (1999). "Lateral force microscopy of SHRP asphalts and modified asphalts." *36th Annual Petersen Asphalt Research Conference*, Laramie, Wyoming.
- Pauli, A. T., Branthaver, J. F., Robertson, R. E., and Grimes, W. (2001). "Atomic force microscopy - investigation of SHRP asphalts." *Symposium on Heavy Oil and Resid Compatibility and Stability*, San Diego, CA, 104-110.
- Pauli, A. T., Grimes, W., Huang, S. C., and Robertson, R. E. (2003). "Surface energy studies of SHRP asphalts by AFM." *Petroleum Chemistry Division Preprints*, 48(14-18).
- Pawlisch, C. A., Macris, A., and Laurence, R. L. (1987). "Solute diffusion in polymers. 1. The use of the capillary column inverse gas chromatography." *Macromolecules*, 20, 1564-1578.
- Pereira, M. R., and Yarwood, J. (1996a). "ATR-FTIR spectroscopic studies of the structure and permeability of sulfonated poly(ether sulfone) membranes .1. Interfacial water-polymer interactions." *Journal of the Chemical Society-Faraday Transactions*, 92(15), 2731-2735.
- Pereira, M. R., and Yarwood, J. (1996b). "ATR-FTIR spectroscopic studies of the structure and permeability of sulfonated poly(ether sulfone) membranes .2. Water diffusion processes." *Journal of the Chemical Society-Faraday Transactions*, 92(15), 2737-2743.
- Robl, T. L., Milburn, D., Thomas, G., Groppo, J., O'Hara, K., and Haak, A. (1991). "The SHRP Materials Reference Library Aggregates: Chemical, Mineralogical, and Sorption Analysis." *SHRP-A/UIR-91-509*, Strategic Highway Research Program, National Research Council, Washington, D.C., USA.

- Salomon, D., and Zhai, H. (Accessed November/2009) "Ranking asphalt binders by activation energy for flow." <http://www.technopave.com/publications/>.
- Sasaki, I., Moriyoshi, A., Hachiya, Y., and Nagaoka, N. (2006). "New test method for moisture permeation in bituminous mixtures." *Journal of the Japan Petroleum Institute*, 49(1), 33-37.
- Schabel, W., Scharfer, P., Kind, M., and Mamaliga, I. (2007). "Sorption and diffusion measurements in ternary polymer-solvent-solvent systems by means of a magnetic suspension balance - experimental methods and correlations with a modified Flory-Huggins and free-volume theory." *Chemical Engineering Science*, 62, 2254-2266.
- Schlotter, N. E., and Furlan, P. Y. (1992). "A review of small molecule diffusion in polyolefins." *Polymer*, 33(16), 3323-3342.
- Shen, Y. R., and Ostroverkhov, V. (2006). "Sum-frequency vibrational spectroscopy on water interfaces: polar orientation of water molecules at interfaces." *Chemical Reviews*, 106(4), 1140-1154.
- Simonyan, A. V., Behrens, H., and Dultz, S. (2009). "Diffusive transport of water in porous feldspar from granitic saprolites: In situ experiments using FTIR spectroscopy." *Geochimica Et Cosmochimica Acta*, 73, 7019-7033.
- Smith, A. L., Ashcraft, J. N., and Hammond, P. T. (2006). "Sorption isotherms, sorption enthalpies, diffusion coefficients, and permeabilities of water in a multilayer PEO/PAA polymer film using the quartz crystal microbalance/heat conduction calorimeter." *Thermochimica Acta*, 450, 118-125.
- Thomas, N. L., and Windle, A. H. (1982). "A theory of case II diffusion." *Polymer*, 23(April), 529-542.
- Tong, H. M., Saenger, K. L., and Durning, C. J. (1989). "A study of solvent diffusion in thin polyimide films using laser interferometry." *Journal of Polymer Science Part B-Polymer Physics*, 27, 686-708.
- Vasconcelos, K. L., Bhasin, A., and Little, D. N. (2010). "Measurement of water diffusion in asphalt binders using the FTIR-ATR technique." 89th *Transportation Research Board Meeting*, Washington, DC.
- Vogt, B. D., Soles, C. L., Lee, E. K., and Wu, W. (2004). "Moisture absorption and absorption kinetics in polyelectrolyte films: influence of film thickness." *Langmuir*, 20, 1453-1458.

- Wei, J. (2009). "Study on the Surface Free Energy of Asphalt, Aggregate and Moisture Diffusion in Asphalt Binder," Ph.D. dissertation, China University of Petroleum, Beijing.
- Weis, D. D., and Ewing, G. E. (1998). "Absorption anomalies in ratio and subtraction FT-IR spectroscopy." *Analytical Chemistry*, 70(15), 3175-3183.
- Wolf, R. V. (1991). *Diffusion In and Through Polymers: Principles and Applications*, Hanser Publishers, New York.
- WRI. (2001). "Fundamental Properties of Asphalts and Modified Asphalts, Volume I: Interpretive Report." *FHWA-RD-99-212*, Western Research Institute, Laramie, WY.
- Wu, S., Pang, L., Mo, L., Chen, Y., and Zhu, G. (2008). "Influence of aging on the evolution of structure, morphology and rheology of base and SBS modified bitumen." *Construction and Building Materials*, doi:10.1016/j.conbuildmat.2008.05.004.
- Zollinger, C. (2005). "Application of Surface Energy Measurements to Evaluate Moisture Susceptibility of Asphalt and Aggregates," M.S. thesis, Texas A&M University, College Station, TX.

APPENDIX A

DEVELOPMENT OF THE FTIR-ATR DIFFUSION MODEL

The diffusion of many liquids is described by Fick's second law, and are termed one-dimensional in situations where the thickness of the sample is much smaller than its width or length. Equation (A-1) is a solution for a 'thin film' under uniform initial distribution and equal surface concentrations, as stated in the boundary conditions below (Crank 1979):

$$t = 0, \quad -L < z < L, \quad C = C_0 \text{ (uniform)}$$

$$t > 0, \quad @ \text{ film surface}, \quad C = C_1 \text{ (constant)},$$

$$\frac{C(z,t)}{C_\infty} = 1 - \frac{4}{\pi} \sum_{n=0}^{\infty} \frac{(-1)^n}{2n+1} \exp\left[-\frac{D(2n+1)^2 \pi^2 t}{4L^2}\right] \cos\left[\frac{(2n+1)\pi z}{2L}\right] \quad (\text{A-1})$$

where,

C_∞ = equilibrium concentration of penetrant in the film; and

D = concentration-independent diffusivity.

To obtain quantitative information from the ATR spectroscopy experiment, the evanescent wave field equation should be combined with the Beer-Lambert law for transmission spectroscopy ($dI = -\epsilon C I dz$). In doing so, it is necessary to assume that only weak absorption occurs. Then,

$$\frac{I}{I_0} = e^{-A} \approx (1 - A) \quad \text{or,} \quad (\text{A-2})$$

$$dI = -I_0 dA \quad (\text{A-3})$$

Substitution of equation (A-3) into the differential form of the Beer-Lambert law and subsequent integration yields:

$$A = \int_0^L \frac{\varepsilon C I}{I_0} dz \quad (\text{A-4})$$

where,

ε = molar extinction coefficient;

I = intensity; and

C = concentration of the absorbing species.

The limits of the integration are reflective of the diffusion of the penetrant through one side of the film. Since intensity $(I) = E^2$, where E is the electric field strength of the evanescent wave, the equation (A-4) can be rewritten for multiple reflection N , as:

$$A = \int_0^L \frac{N \varepsilon C E_0^2}{I_0} \exp(-2\gamma z) dz \quad (\text{A-5})$$

Equation (A-5) is the expression analogous to the Beer-Lambert law for ATR spectroscopy. It directly relates changes in concentration to those in the absorbance spectrum during the experiment. To utilize this technique for evaluating the kinetics of a diffusion process, the physics of spectroscopy theory must be incorporated with a diffusion model.

In order to derive a single expression relating IR absorbance to diffusivity, the term W is defined:

$$W = \frac{A_t}{A_\infty} \quad (\text{A-6})$$

where,

A_t = absorbance at time t ; and

A_∞ = absorbance at infinite time.

Substituting (A-5) in (A-6):

$$W = \frac{\int_0^L \frac{N\varepsilon CE_0^2 \exp(-2\gamma z)}{I_0} dz}{\int_0^L \frac{N\varepsilon C_\infty E_0^2 \exp(-2\gamma z)}{I_0} dz} = \frac{\int_0^L C \exp(-2\gamma z) dz}{\int_0^L C_\infty \exp(-2\gamma z) dz} = \frac{\int_0^L C \exp(-2\gamma z) dz}{J} \quad (\text{A-7})$$

where,

$$J = \int_0^L C_\infty \exp(-2\gamma z) dz$$

Developing J gives,

$$J = \int_0^L C_\infty \exp(-2\gamma z) dz = C_\infty \left[\frac{1}{-2\gamma} \exp(-2\gamma z) \right]_0^L = \frac{C_\infty}{-2\gamma} [\exp(-2\gamma L) - 1] = \frac{C_\infty}{2\gamma} [1 - \exp(-2\gamma L)] \quad (\text{A-8})$$

Substituting equation (A-8) into equation (A-7):

$$W = \frac{\int_0^L C \exp(-2\gamma z) dz}{\frac{C_\infty}{2\gamma} [1 - \exp(-2\gamma L)]} \quad (\text{A-9})$$

The physics of diffusion is incorporated by substituting the concentration term (C) from equation (A-1) into the equation (A-9).

$$W = \frac{\int_0^L C_\infty \left[1 - \frac{4}{\pi} \sum_{n=0}^{\infty} \frac{(-1)^n}{2n+1} \exp\left[\frac{-D(2n+1)^2 \pi^2 t}{4L^2} \right] \cos\left[\frac{(2n+1)\pi z}{2L} \right] \exp(-2\gamma z) \right] dz}{\frac{C_\infty}{2\gamma} [1 - \exp(-2\gamma L)]} \quad (\text{A-10})$$

Equation (A-10) can be simplified to:

$$W = 1 - \frac{\int_0^L \frac{4}{\pi} \sum_{n=0}^{\infty} \frac{(-1)^n}{2n+1} \exp(g) \cos(fz) \exp(-2\gamma z) dz}{J'} \quad (\text{A-11})$$

where,

$$J' = \frac{1}{2\gamma} [1 - \exp(-2\gamma L)];$$

$$g = \frac{-D(2n+1)^2 \pi^2 t}{4L^2}; \text{ and}$$

$$f = \frac{(2n+1)\pi}{2L}$$

Placing the independent parameters outside the integral, yields the following:

$$W = 1 - \frac{4}{\pi J'} \int_0^L \sum_{n=0}^{\infty} \frac{(-1)^n}{2n+1} \exp(g) \cos(fz) \exp(-2\gamma z) dz \quad (\text{A-12})$$

Recalling the law of summation of integrals, equation (A-12) may be rewritten as:

$$W = 1 - \frac{4}{\pi J'} \sum_{n=0}^{\infty} \int_0^L \frac{(-1)^n}{(2n+1)} \exp(g) \cos(fz) \exp(-2\gamma z) dz \quad (\text{A-13})$$

Isolating in equation (A-13) only the terms dependent on z and calling them V :

$$V = \int_0^L \cos(fz) \exp(-2\gamma z) dz \quad (\text{A-14})$$

Equation (A-13) becomes:

$$W = 1 - \frac{4}{\pi J'} \sum_{n=0}^{\infty} \frac{(-1)^n}{(2n+1)} \exp(g)V \quad (\text{A-15})$$

Integrating V by parts:

$$V = \frac{\cos(fz) \exp(-2\gamma z)}{-2\gamma} \Big|_0^L - \int_0^L \frac{\exp(-2\gamma z) f \sin(fz)}{2\gamma} dz \quad (\text{A-16})$$

Evaluating the second term of equation (A-16) using once again the integral by parts:

$$\frac{-f}{2\gamma} \int_0^L \exp(-2\gamma z) \sin(fz) dz = \frac{-f}{2\gamma} \left[\frac{\sin(fz) \exp(-2\gamma z)}{-2\gamma} \Big|_0^L - \int_0^L \frac{\exp(-2\gamma z)}{-2\gamma} f \cos(fz) dz \right] \quad (\text{A-17})$$

Substituting equation (A-17) into equation (A-16):

$$V = \frac{\cos(fL) \exp(-2\gamma L) - 1}{-2\gamma} + \frac{f \sin(fL) \exp(-2\gamma L)}{(2\gamma)^2} + \frac{-f^2}{(2\gamma)^2} \int_0^L \cos(fz) \exp(-2\gamma z) dz \quad (\text{A-18})$$

The remaining integral in equation (A-18) is the same as the one that define V in equation (A-14). Simplifying yields:

$$V \left(\frac{4\gamma^2 + f^2}{4\gamma^2} \right) = \frac{\cos(fL) \exp(-2\gamma L) - 1}{-2\gamma} + \frac{f \sin(fL) \exp(-2\gamma L)}{4\gamma^2} \quad (\text{A-19})$$

Multiplying both sides by $\left(\frac{4\gamma^2}{4\gamma^2 + f^2} \right)$:

$$V = \frac{[-2\gamma \cos(fL) \exp(-2\gamma L) + 2\gamma + f \sin(fL) \exp(-2\gamma L)]}{(4\gamma^2 + f^2)} \quad (\text{A-20})$$

Since $f = \frac{(2n+1)\pi}{2L}$,

$$\cos(fL) = \cos\left[\frac{(2n+1)\pi}{2L} L\right] = \cos\left[\frac{(2n+1)\pi}{2}\right] \quad (\text{A-21})$$

For n=odd, $\cos(fL) = 0$ and for n=even $\cos(fL) = 0$. So the term $\cos(fL)$ can be replaced by zero in equation (A-20). For the sine term,

$$\sin(fL) = \sin\left[\frac{(2n+1)\pi}{2L} L\right] = \sin\left[\frac{(2n+1)\pi}{2}\right] \quad (\text{A-22})$$

For n=odd, $\sin(fL) = -1$ and for n=even $\sin(fL) = +1$. So the term $\sin(fL)$ can be replaced by $(-1)^n$ in equation (A-20).

After the substitutions on sine and cosine in equation (A-20):

$$V = \frac{1}{(4\gamma^2 + f^2)} [2\gamma + (-1)^n f \exp(-2\gamma L)] \quad (\text{A-23})$$

Substituting W , J and V in equation (A-15):

$$\frac{A_i}{A_\infty} = 1 - \frac{8\gamma}{\pi[1 - \exp(-2\gamma L)]} \sum_{n=0}^{\infty} \frac{\exp(g) [(-1)^n 2\gamma + f \exp(-2\gamma L)]}{(2n+1)(4\gamma^2 + f^2)} \quad (\text{A-24})$$

Substituting f and g in equation (A-24) give us the final equation, as described by Fieldson and Barbari (Fieldson and Barbari 1993):

$$\frac{A_t}{A_\infty} = 1 - \frac{8\gamma}{\pi[1 - \exp(-2\gamma L)]} \times \sum_{n=0}^{\infty} \left[\frac{\exp\left[-\frac{D(2n+1)^2 \pi^2 t}{4L^2}\right] \left[\frac{(2n+1)\pi}{2L} \exp(-2\gamma L) + (-1)^n (2\gamma) \right]}{(2n+1) \left(4\gamma^2 + \frac{(2n+1)^2 \pi^2}{4L^2} \right)} \right] \quad (\text{A-25})$$

APPENDIX B

COMPUTING WATER DIFFUSIVITY IN ASPHALT BINDERS USING THE FOURIER TRANSFORM INFRARED – ATTENUATED TOTAL REFLECTANCE (FTIR-ATR) TECHNIQUE

Asphalt Film Preparation

The target film thickness is an important consideration while preparing specimens. There are two possible cases for the specimen film thickness (Figure B-1). The first case is when the film thickness is much greater than the effective depth of penetration, d_p . In this case when a constant boundary condition (100% saturation) is achieved by adding water to the top of the film, water diffusion starts from the upper surface of the film that is beyond the detection range of the FTIR spectra. Therefore, one would have to wait for an undefined and perhaps experimentally unreasonable amount of time until moisture diffuses to within the effective depth of penetration and is detected in the spectra. Change in concentration of water within the film over time is quantified by correcting for the time of arrival of moisture and film thickness. The second case is when the film thickness is less than the effective depth of penetration, d_p . In this case when water is added to the top of the film, a portion of the water over the film as well as the entire film is immediately detected in the spectra. Change in concentration of water within the film over time is quantified by subtracting the initial spectra at time $t = 0$ s from the spectra detected at a specific point in time. In this study, both approaches were used for trial experiments but the later was preferred due to practical considerations.

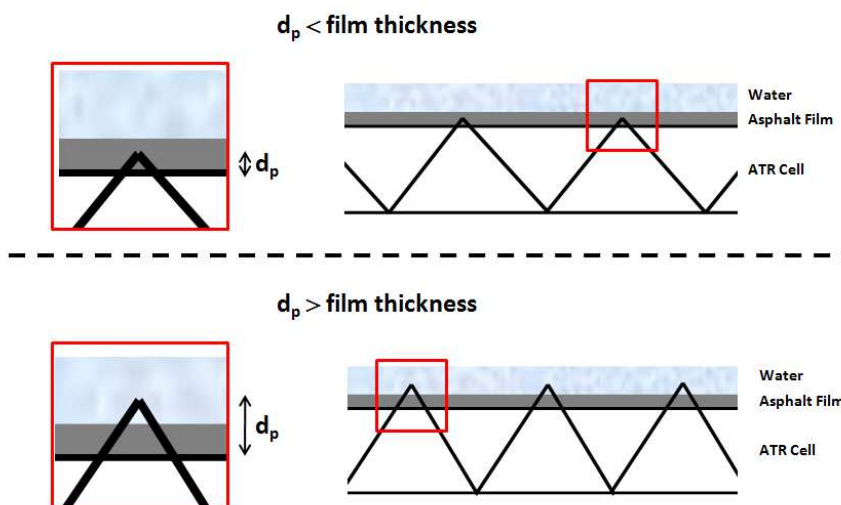


Figure B-1. Two Possible Configurations for the Film Thickness on the Top of the ATR Cell

Another important consideration was not to have a very thin and homogeneous film. Other research studies have shown that the diffusivity of liquids through very thin polymer films is not representative of diffusivity through the bulk (Vogt et al. 2004). However, the limit at which diffusivity changes as a function of film thickness was in the order of tens of nanometers. This study ensured that all films were in the one micron range. Once the thin film samples were prepared, the next important step was to accurately measure the thickness of the thin film.

Asphalt Stock Solution Preparation

- Dissolve 1.5g of asphalt in 11 mL of HPLC grade toluene approximately 12h before use to guarantee that the solvent had dissolved all the asphalt in the container.

Spin Coating of Asphalt Stock Solution in the ATR plate

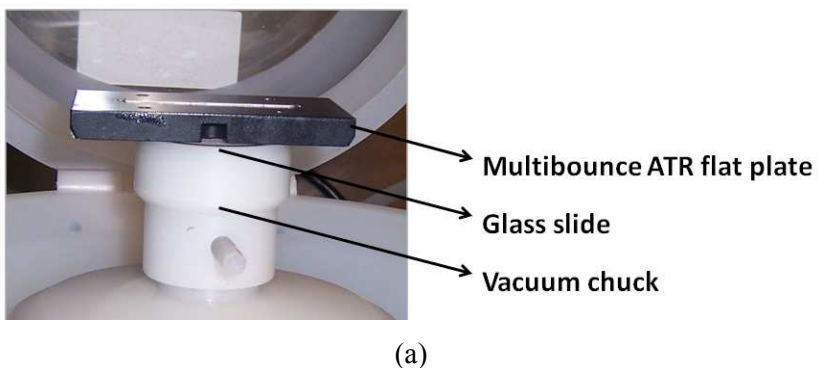
- A spin processor Laurell WS-650S (8.5inch bowl) was used (Figure B-2(a)). The spin processor should be equipped with a vacuum chuck for substrates with the dimensions and weight similar to the ATR plate. Sufficient vacuum to hold the substrate is required to start the motor, and to prevent leakage of chemicals into the vacuum path.

- Cover the stationary seal of the spin coater and prepare a cylinder made of aluminum foil for cleaning purpose (Figure B-2 (b)). Make sure that the aluminum foil does not touch the rotating seal.

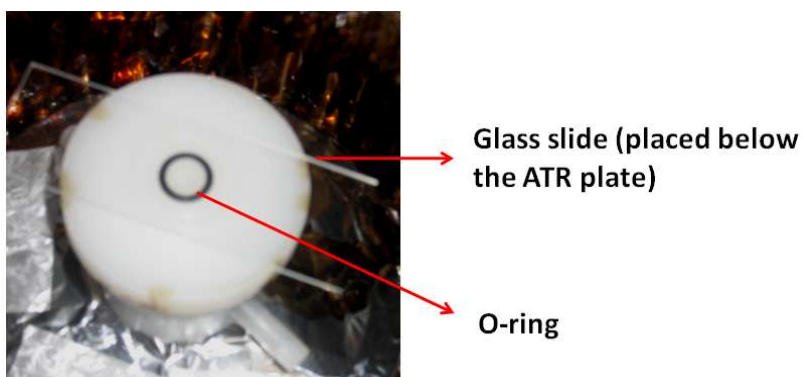


(a) (b)
Figure B-2. (a) Spin Processor, and (b) Covered Stationary Seal

- Attach a glass slide in the bottom part of the Multibounce ATR flat plate to allow the application of vacuum (a regular tape can be used), and place the glass slide and ATR plate on the top of the vacuum chuck (Figure B-3 (a)). Make sure the glass slide is large enough to cover the O-ring completely (Figure B-3 (b)).



(a)
Figure B-3. Configuration of (a) the Glass Slide Attached to the ATR Plate on the Top of the Vacuum Chuck, and (b) the Glass Slide Covering the O-ring



(b)
Figure B-3 Continued

- Adjust the spin coater to rotate at 1000rpm for 10s, as shown in the display in Figure B-4. The substrate should be spin coated two times to ensure complete coverage of the ATR plate by the asphalt solution.

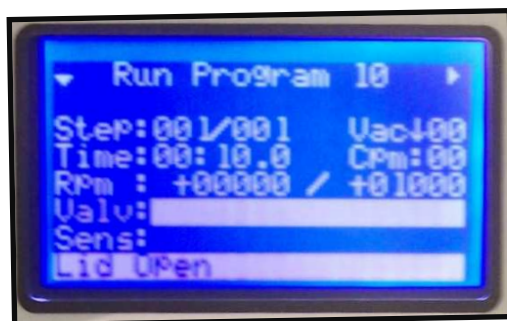


Figure B-4. Spin Coater Display with the Set Speed and Time

- Remove the glass slide from the ATR plate.
- Attach the chamber to the coated ATR plate (Figure B-5). Make sure the film covers not only the ATR crystal, but the whole plate. There should be no spot without asphalt inside the chamber to avoid water transport through the interface asphalt/ATR plate.
- Seal the chamber.

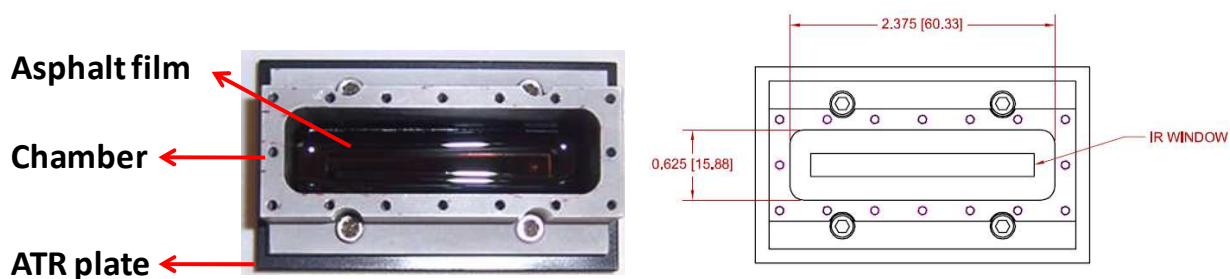


Figure B-5. Chamber Attached to the ATR Plate

Final Preparation of the Asphalt Film

- Connect the ATR plate and chamber to a dry nitrogen purge for 2h to eliminate residual solvent that was used to prepare the film. (Figure B-6).
- Anneal the sample for 1h at 50°C, to eliminate possible micro capillaries in the asphalt film that might have been created due to the vaporization of toluene under nitrogen purge (Figure B-6).

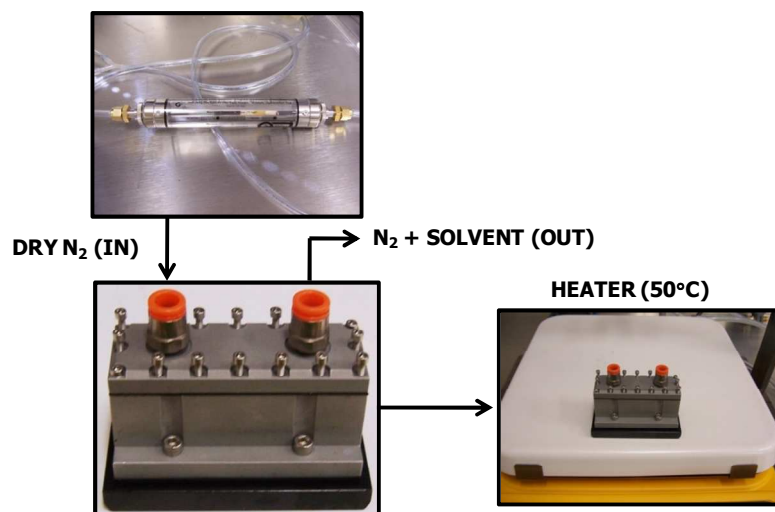


Figure B-6. Illustration of the Dry Nitrogen Purge and Annealing at 50°C

Thickness and Refractive Index of Asphalt Films

The film thickness and the refractive index are input parameters necessary to the analytical model used for determining the water diffusivity in asphalt binders. The ellipsometer was the equipment selected because of its high precision. The Nanofilm EP3-SE was the model utilized (Figure B-7). It is an auto-nulling spectroscopic imaging ellipsometer in the PCSA configuration.

Following is a short description of the sample preparation, test procedure and analysis method used for the ellipsometer.

Sample Preparation

The ATR crystal is transparent and therefore could not be used with the ellipsometer as a substrate to measure the thickness of the asphalt film. Instead, the same procedure was used to cast thin films on silica wafers as substrates. The Si wafer substrate produces more accurate results because of its reflectivity and known optical properties. The roughness of Si wafer and ZnSe crystal and differences in the thickness of the film casted on both surfaces were unlikely to be significant.

- Use the same asphalt solution described in ‘*Asphalt Stock Solution Preparation*’.
- Repeat the spin coating procedure, however instead of using the ATR plate, use 3” Si wafers as substrate (Figure B-7).

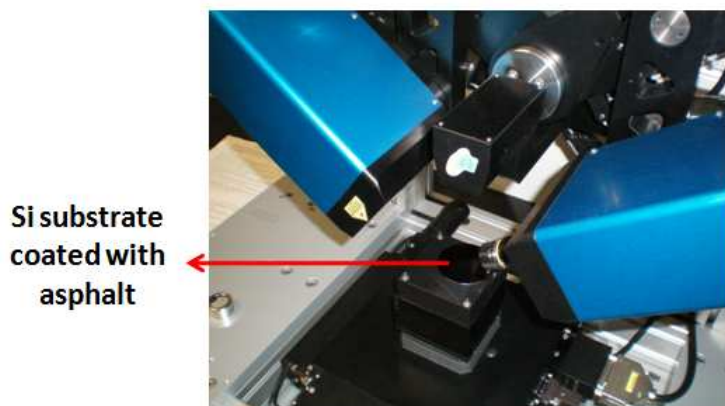


Figure B-7. Nanofilm EP3-SE and the Si Substrate Coated with Asphalt

Test Method

- Turn on the computer, bottom electronics box and monitor.
- Start the EP3 View software. The software begins to initialize the instrument and all motors are reset.
- After initialization the default windows will be displayed. There are the ‘Control and Live Images’ and the ‘Script tree’ window (Figure B-8). The ‘Control and Live Images’ window contains the real-time view of the sample and the control buttons for the

instrument that can be changed (wavelength selection, AoI, shutter, polarizer, etc). The ‘Script tree’ contains function tree with all the available measurement options.

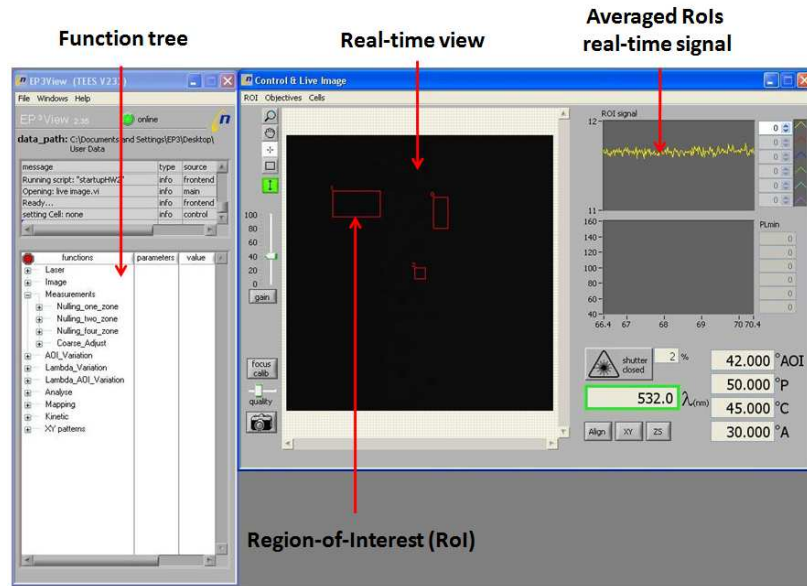
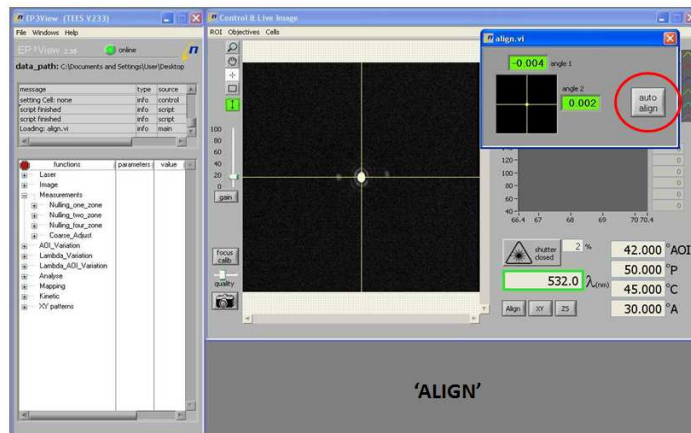


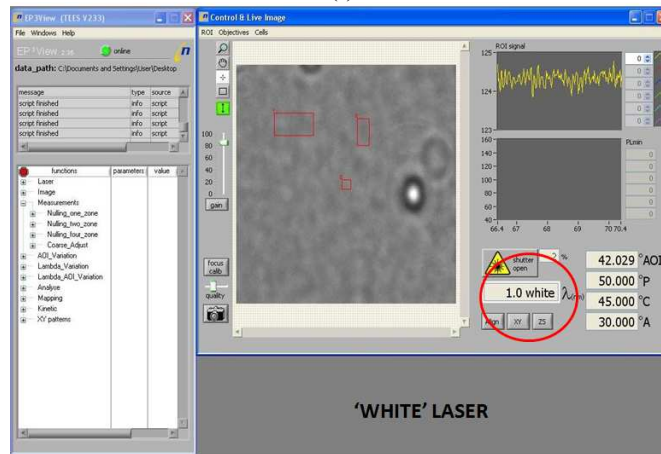
Figure B-8. Default Ellipsometer Window with the ‘Control and Live Images’ and the ‘Script Tree’

- Check that the correct objective is chosen under the ‘objective’ menu. Place the sample (Si substrate coated with thin film of asphalt) on the stage and make sure that the red laser light from the alignment laser is on the sample.
- Click on ‘Align’. By opening the align window the camera automatically switches to the align camera directly over the sample in the middle of the goniometer (Figure B-9 (i)).
- For dark-colored samples (like the asphalt), you may not be able to see an optical image with the default laser (532nm). In this case, click the text field in the ‘Control and Live Image’ window containing the wavelength and scroll down to select ‘white’. The white laser will help you focus your sample in the proceeding steps. When finished, make sure to set the laser wavelength back to 523nm (Figure B-9 (ii)).
- Check the gain and then click the auto align button. This is the initial plane alignment. Close the align window.
- Open the shutter and adjust the laser power to 2%.

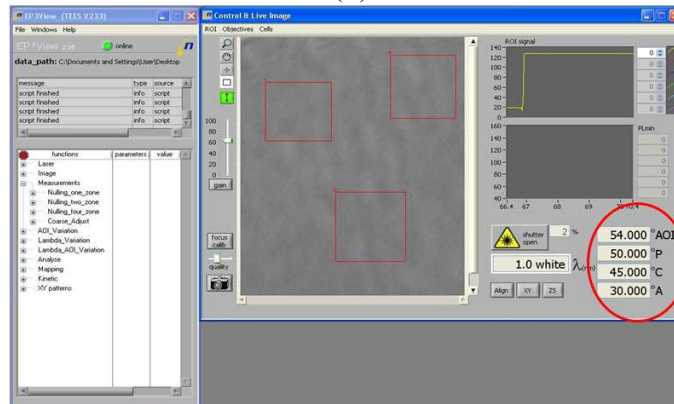
- Select 54° for the angle of incidence (AoI) (goniometer angle), and 50° , 45° and 30° for the polarizer, compensator and analyzer angles, respectively (Figure B-9 (iii)).
- Move the sample stage up and down using the Z-control in order to get the laser spot centered in the live window, and the real time RoI (region of interest) signal maximized.
- At this point you should see your sample, though the image probably will be sharp.
- Check the alignment again and click on the auto-gain bottom to avoid saturation.
- Open the focus/calibration window and use the lower slider to move the objective until your sample is focused.
- Check that 532nm (green) laser reflection is hitting center of objective. If not, realign z until it is.
- At this point the equipment is ready to start the data collection.
- Select at least three RoIs over the areas you want to measure. It is important to check the thickness variations in the sample.
- Select 'Coarse Adjust' from the function tree (Figure B-9 (iv)). This will adjust the analyzer/polarizer angles to a position where the intensity of the reflected polarizer light is minimized in the CCD (charge-coupled-device) camera. This will find the minima of all RoIs.
- Select the 'Lambda Variation' as the measurement script in the function tree. Click on + sign in front of it to expand the three. Click on + sign in front of the nulling four zone to display the parameters. Use the 0-44 steps (359-1050nm), illustrated in Figure B-9 (iv).
- Double click on the script to start measurement.



(i)

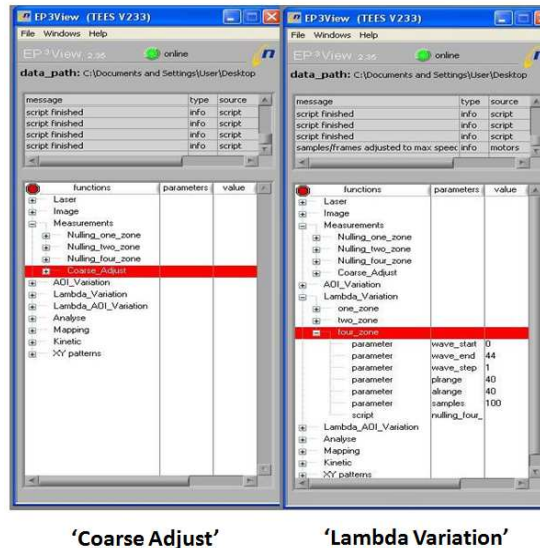


(ii)



(iii)

Figure B-9. Some Steps for the Ellipsometric Measurement

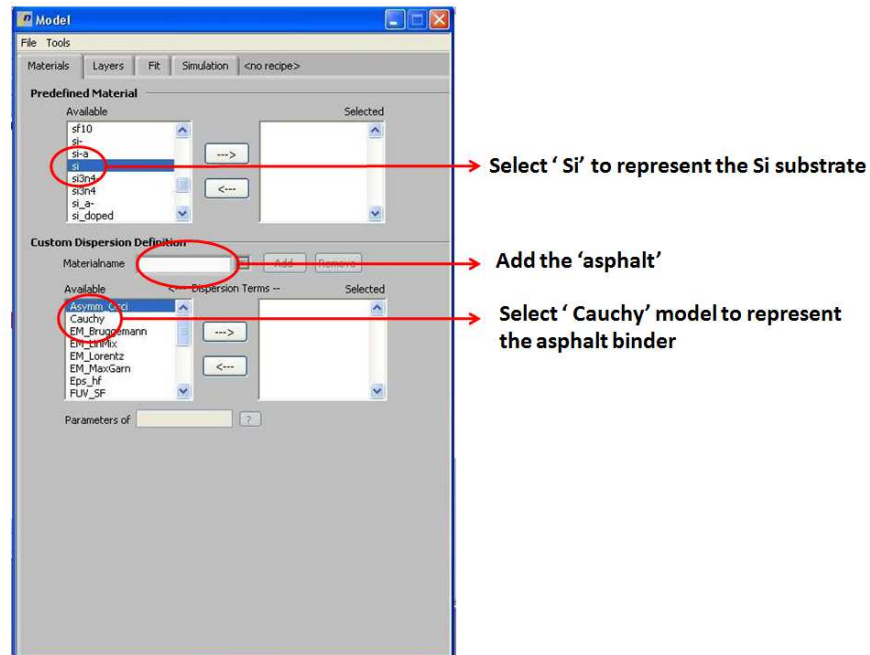


(iv)

Figure B-9 Continued*Analyzing and Modeling the Ellipsometer Data*

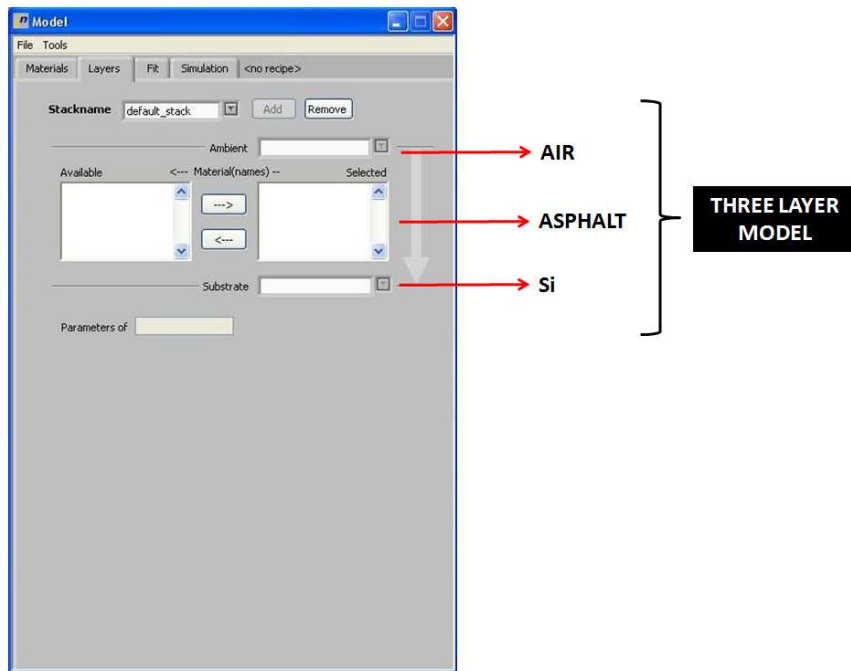
- To analyze the data you need to set up an optical model and fit the measured data to that model. For asphalt samples, and Cauchy function is recommended.
- Mark all the delta and psi results by clicking on the upper left cell, then keep the shift button down and click on the bottom right cell. Make sure before you make the selection you have erased all the lines that have 'NaN' as result.
- Go to 'Tools – Selection to Model' to transfer the results to the model window.
- Open the model window from the EP3 View page.
- Open the 'Materials' tab in the model window (Figure B-10(i)).
- Select Si from the list of predefined materials, add a name for the sample you are evaluating ('asphalt X', for example), and select the Cauchy model to represent the asphalt sample (Figure B-10(i)).
- Move to the 'Layers' tab and choose air as the ambient, 'asphalt X' as the material, and Si as the substrate (Figure B-10(ii)).
- Left click on 'asphalt X' in the selected list and type the estimated range of thickness in the 'thickness' control.
- Go to the 'Fit' tab and in the fit parameters box, click on the line you want to edit, press 'edit' and define the thickness range of your fit (Figure B-10(iii)).

- Press the fit button in the middle of the window and the results will appear in the lower spreadsheet.

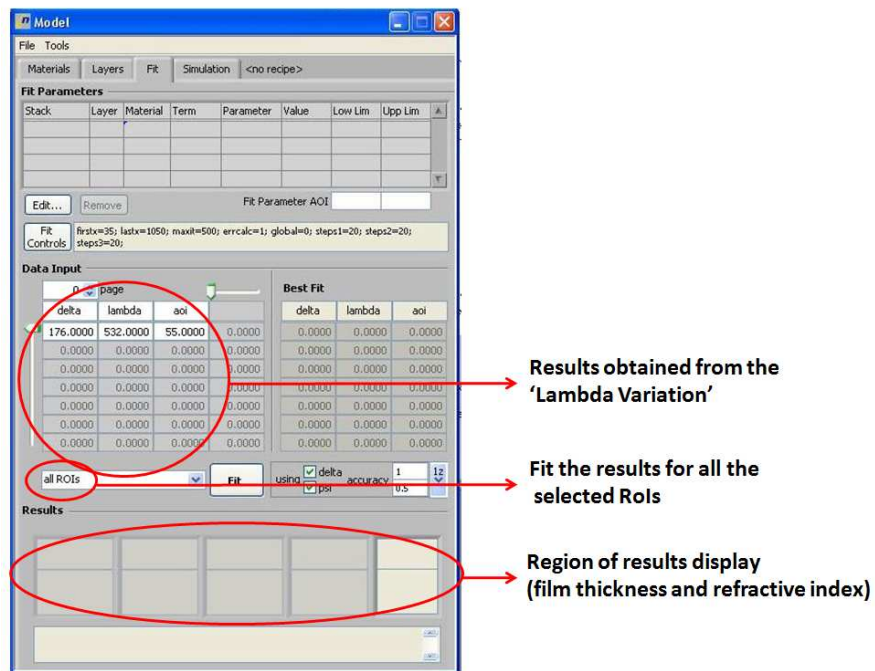


(i)

Figure B-10. Some Steps of the Fitting Process for the Ellipsometric Measurement



(ii)

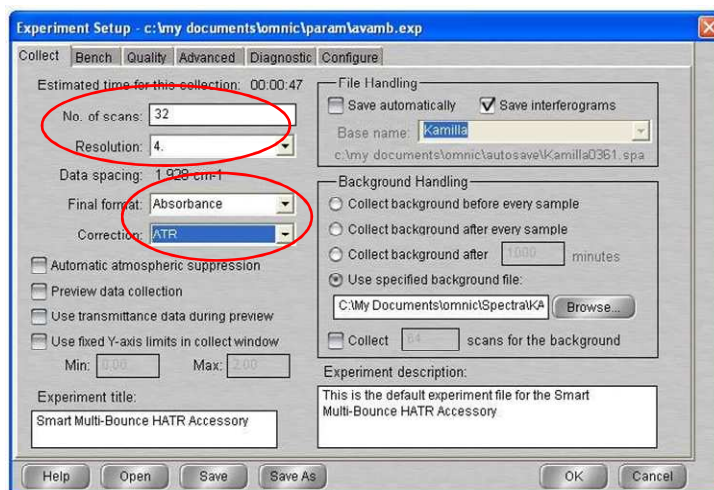


(iii)

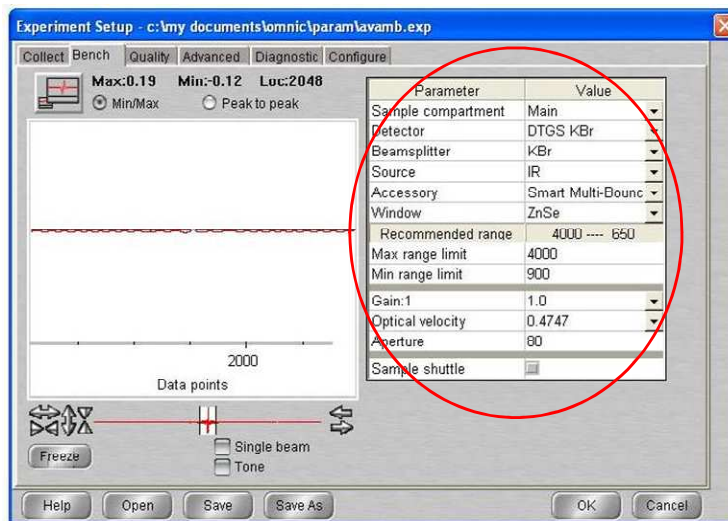
Figure B-10 Continued

FTIR-ATR Test Procedure

- Before start the experiment, check the Setup with the parameters illustrated in Figure B-11.



(i)



(ii)

Figure B-11. FTIR-ATR – ‘Experiment Setup’ Window

- The IR spectrum is displayed in Absorbance unit. It represents how much of the original IR intensity passes through the sample. In order to calculate this, we first need to know the IR intensity with no sample, so we run a background, illustrated in Figure B-12.

Make sure the background was collected before start the procedure described in ‘Asphalt Film Preparation’.

- Save the background to use as reference in the following sample collections.

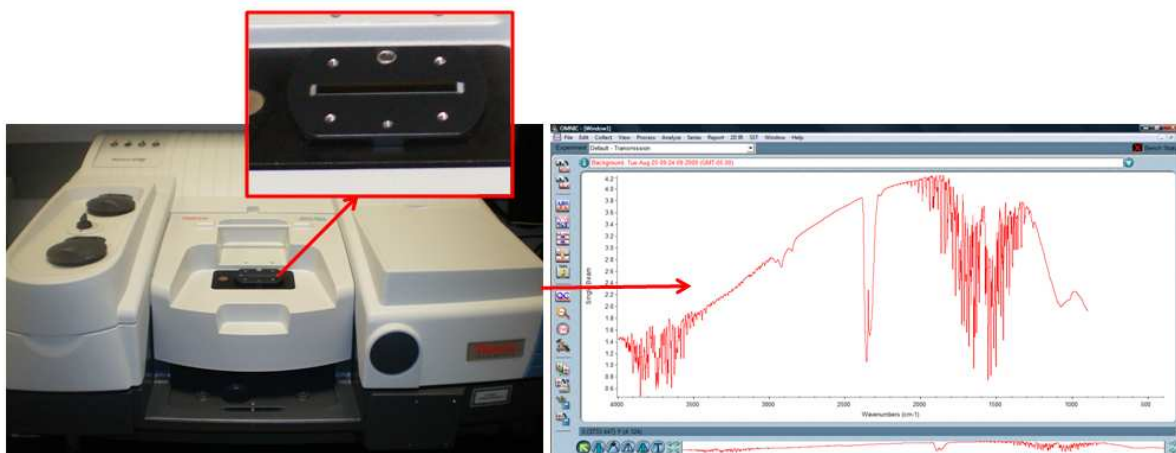


Figure B-12. FTIR-ATR - Illustration of Background Collection

- After the background was collected and saved, you proceed to the asphalt film preparation as previously described.
- Collect the spectra of the asphalt film before add water into the chamber. This spectrum will be subtracted from the following spectra after the water is added to the system.
- With the ATR plate placed on the FTIR machine and ready to sample collection, add 10mL of HPLC water into the chamber. It will create a layer of water of approximately 15mm above the asphalt film.
- Collect the sample spectra right away. This will be considered the $t=0$.
- For the first hour, collect the spectra every 2-10min, then for the next 10h space the collections to every 30min-1h. After 12h of test, the rate of increase in the water peak (described in the next section) decrease considerably, and the spectra collection can be done just once or twice per day. This is valid for film thickness in the order of $1\mu\text{m}$. Figure B-13 illustrates a series of sample collections.

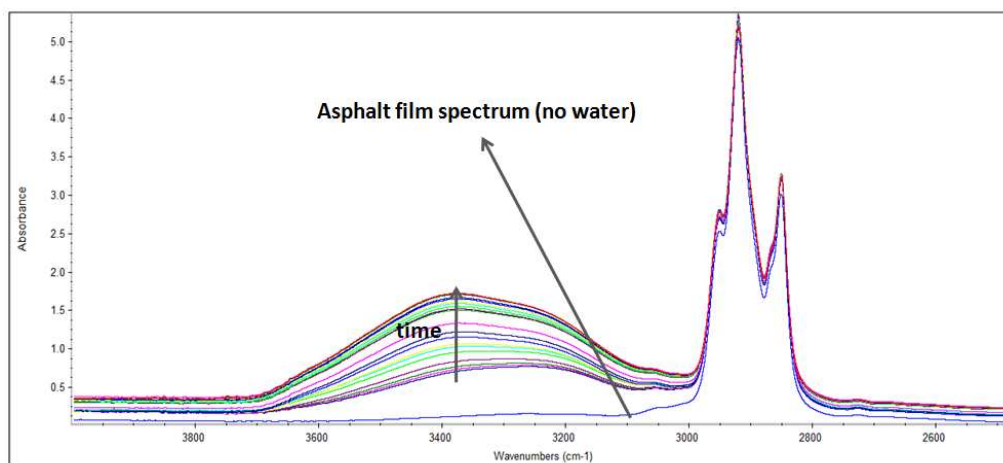


Figure B-13. FTIR-ATR - Illustration of Sample Collection with Time

- Subtract the asphalt spectrum from all the spectra that followed the water addition into the chamber, as illustrated in Figure B-14.

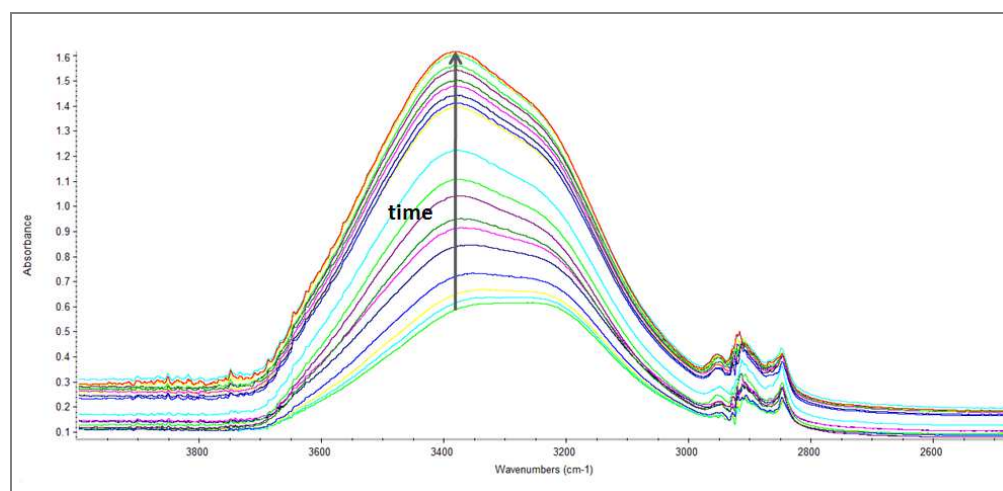
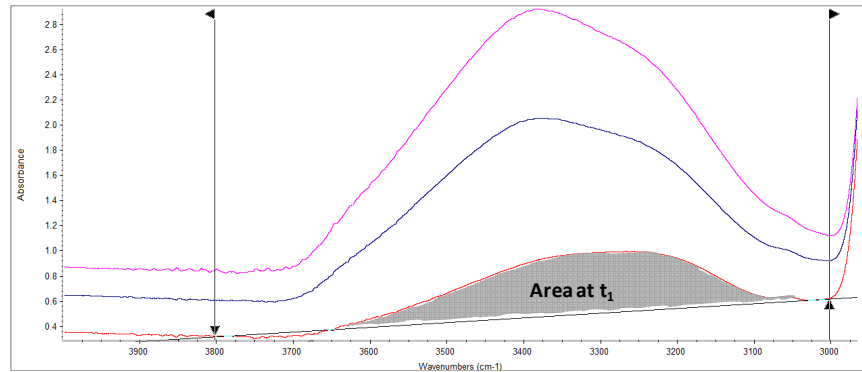


Figure B-14. Spectra after Subtraction of Asphalt without Water

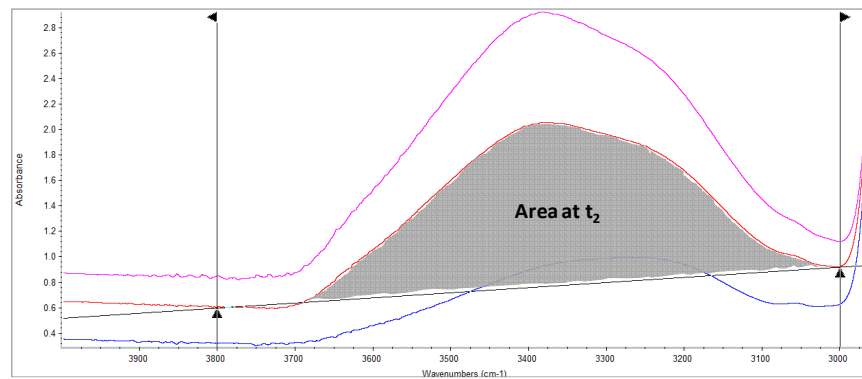
Analysis Approach

The water absorption bands are related to molecular vibrations involving different combinations of the three fundamental vibration transitions: (i) ν_1 (symmetric stretch mode at 3277cm^{-1}), (ii) ν_2 (bending mode at 1645cm^{-1}), and (iii) ν_3 (asymmetric stretch mode at 3490cm^{-1}). The quantitative analysis is performed using the corrected area between 3000 and 3800 cm^{-1} , as

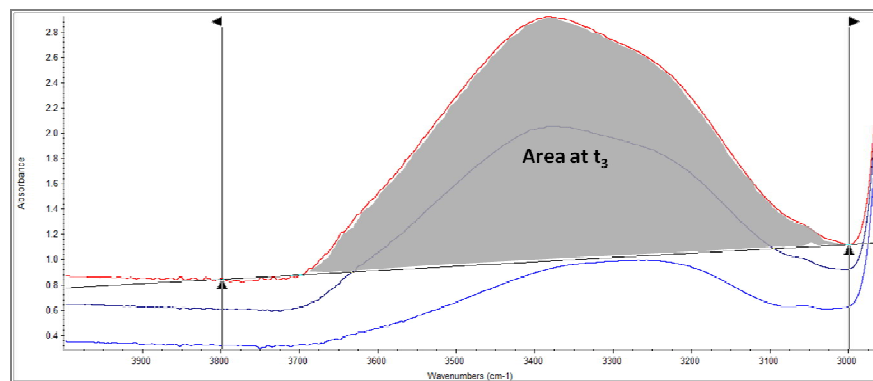
illustrated in Figure B-15. The increase of the area with time was used to quantify the increase in water concentration into the asphalt binder.



(i)



(ii)



(iii)

Figure B-15. Region of Analysis used to Quantify Change of Water Concentration into the Asphalt Binder with Time

- Calculate the areas illustrated in Figure B-15 and plot the results versus time (data illustrated in Figure B-16).
- Fit the data using the Dual Mode Diffusion Model*.
- Repeat the procedure for at least three replicates per asphalt.

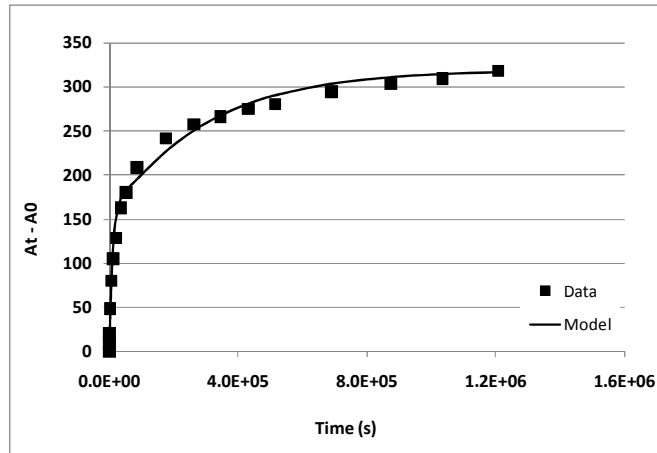


Figure B-16. Data and the Dual Mode Diffusion Model

* Fieldson and Barbari (1993) initially proposed a model correlating the absorbance data obtained by the FTIR-ATR with the total instantaneous mass of the diffusant within the film. Pereira and Yarwood (1996b) adapted this model to the so called ‘Dual Mode Diffusion Model’. The analysis considers that the cumulative diffusion of water through thin films of asphalt binder does not follow Fick’s law. Instead, water diffuses following a dual sorption mode, where each mode of sorption individually follows Fick’s law. In this model it is assumed that a fraction of the water molecules (x_1) is partially mobile (rapid absorption onto the surface sites), and the other fraction ($1 - x_1$) is completely mobile and can diffuse into the asphalt matrix freely (subsequent diffusion into the bulk materials). Thus the expression for describing this model contains two diffusion coefficients:

$$\frac{A_1 - x_1 A_0}{x_1 (A_{eq} - A_0)} = 1 - \frac{8\gamma}{\pi [1 - \exp(2l\gamma)]} \sum_{n=0}^{\infty} \left[\frac{\exp\left(\frac{-D_1 (2n+1)^2 \pi^2 t}{4l^2}\right) \left[\frac{(2n+1)\pi}{2l} \exp(-\gamma 2l) + (-1)^n (2\gamma) \right]}{(2n+1) \left(4\gamma^2 + \left(\frac{(2n+1)\pi}{2l} \right)^2 \right)} \right] \quad (\text{B-1})$$

$$\frac{A_2 - x_2 A_0}{x_2 (A_{eq} - A_0)} = 1 - \frac{8\gamma}{\pi [1 - \exp(2l\gamma)]} \sum_{n=0}^{\infty} \left[\frac{\exp\left(\frac{-D_2 (2n+1)^2 \pi^2 t}{4l^2}\right) \left[\frac{(2n+1)\pi}{2l} \exp(-\gamma 2l) + (-1)^n (2\gamma) \right]}{(2n+1) \left(4\gamma^2 + \left(\frac{(2n+1)\pi}{2l} \right)^2 \right)} \right] \quad (\text{B-2})$$

where, D_1 and D_2 are the diffusivities (or diffusion coefficients) components of the dual mode diffusion model. After rearranging Equations B-1 and B-2 as a function of A_1 and A_2 , they can be added to produce the total absorbance at time t ($A_1 + A_2 = A_t$). The values of x_1 and x_2 are related to the proportion of the partially and totally mobile molecules ($x_1 + x_2 = 1$). The value of x_1 and two separate diffusion coefficients (D_1 and D_2) are then derived from the absorbance data.

APPENDIX C

INFLUENCE OF THE PHYSICAL STATE OF WATER IN THE DIFFUSION IN ASPHALT BINDERS

Introduction and Background

There are three potential ways by which moisture can reach the asphalt-aggregate interface: (i) defect on asphalt coating, (ii) residual moisture present into the aggregates, and (iii) diffusion through the asphalt/mastic (Figure C-1). The diffusion coefficient is dependent on the rate of moisture infiltration towards the asphalt-aggregate interface, and is an indicator of the time scale over which the moisture damage occurs.

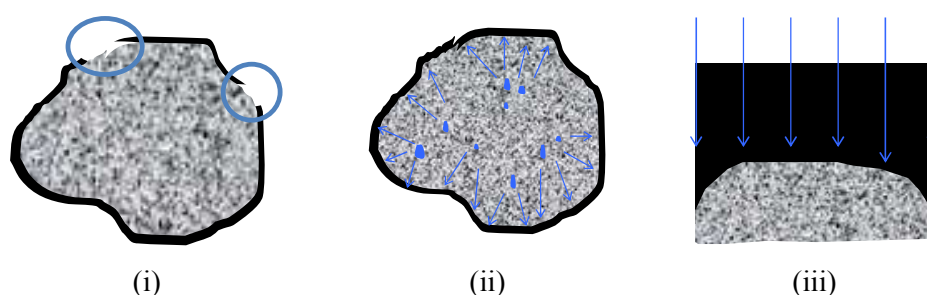


Figure C-1. Potential Forms by which the Moisture can Reach the Asphalt/Aggregate Interface: (i) Defect on Asphalt Coating, (ii) Wet Aggregates, and (iii) Diffusion through the Asphalt/Mastic

Different experimental setups have been used to measure moisture diffusion or permeation in asphalt materials. However, the influence of the physical state of water in the diffusion measurements has yet to be analyzed in more detail. Some studies have considered water in the liquid state (Cheng et al. 2003; Kassem et al. 2006; Nguyen et al. 2005; Wei 2009); others controlled the relative humidity of the environment in contact with the sample to simulate water in the vapor or molecular form (Arambula et al. 2009; Kringos et al. 2008a; Sasaki et al. 2006).

The three diagrams below (Figure C-2) illustrate the distinct arrangement patterns of water molecules as they change their physical state from ice to water to gas. Frozen water molecules arrange themselves in a particular highly organized rigid geometric pattern that causes the mass of water to expand and to decrease in density. In the liquid phase, water molecules

arrange themselves into small groups of joined particles. The fact that these arrangements are small allows liquid water to move and flow. Water molecules in the form of a gas are highly energized. This high energy state sets the molecules in continuous movement reducing the likelihood of the formation of bonds between individual molecules.

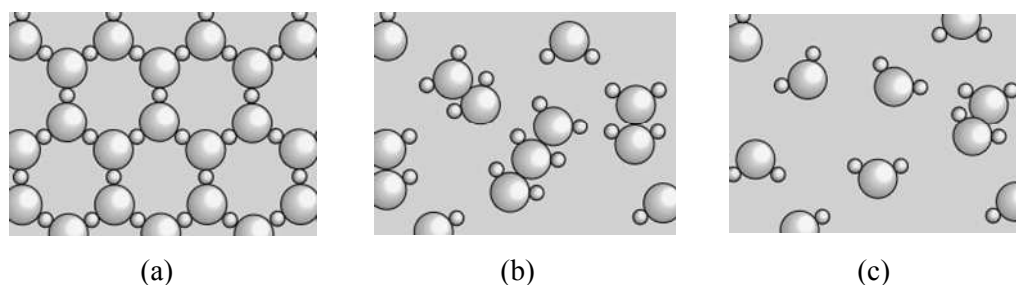


Figure C-2. Arrangement Patterns of Water Molecules at Different Physical States: (a) Ice, (b) Liquid, (c) Vapor

The literature describes water diffusion in several types of polymeric materials. Previous research proved that for liquids in polymeric materials, sorbed volumes can be 10 to 20% or even higher, compared to gas-polymer systems where sorbed volumes are vanishingly small in most cases (Wolf 1991). According to Wolf, liquids open up the structure, with the result that the absolute flux rates through a membrane can be 2 to 3 orders of magnitude higher for a liquid than for a non-condensable gas. The water molecule has the ability to form hydrogen bonds with other water molecules and/or polar groups in the polymer. The diffusion coefficient may increase with increasing concentration, for hydrophilic polymers, or vary inversely for hydrophobic polymers.

However the authors have not been able to find studies referenced in the literature that compare the diffusion coefficient for the same material, using the same experiment setup, but varying the physical state of water only. We do know that water spectrum has very different configuration in the ice, liquid and vapor states, and this produces completely different spectra when subjected to molecular vibration (Ewing et al. 2003). The objective of this paper is to use the Fourier Transform Infrared – Attenuated Total Reflectance (FTIR-ATR) technique to evaluate water (under liquid and vapor form) diffusion in asphalt binders. The technique allows the differentiation between both modes of moisture transport.

FTIR-ATR Spectra of Water in Liquid and Vapor Form

FTIR-ATR spectroscopy has been used with increasing frequency to examine diffusion in polymers, with investigations covering a diverse array of applications. It is a technique that sets itself apart from other techniques with its ability to sensitively distinguish between different chemical species by providing molecular-level contrast between solutes and polymers based on absorbing light at different wavelengths or vibrational bond energies.

The water absorption bands are related to molecular vibrations involving different combinations of the three fundamental vibration transitions: (i) ν_1 (symmetric stretch mode at 3277cm^{-1}), (ii) ν_2 (bending mode at 1645cm^{-1}), and (iii) ν_3 (asymmetric stretch mode at 3490cm^{-1}), all illustrated in Figure C-3. The dipole moments change in the direction of the movement of the oxygen atoms as shown by the arrows.

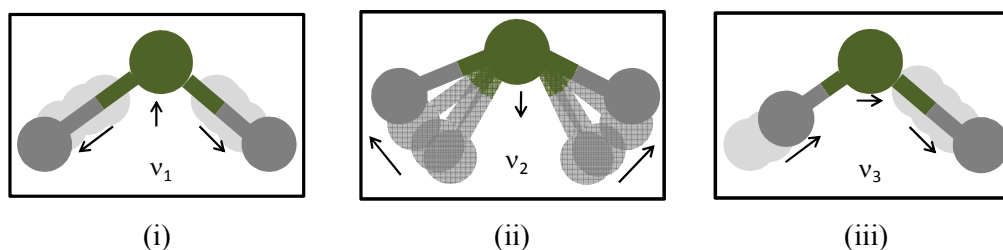


Figure C-3. Fundamental Vibration Transitions: (i) Symmetric Stretching, (ii) Bending, and (iii) Asymmetric Stretching

The water molecule has a very small moment of inertia on rotation which gives rise to rich combined vibrational-rotational spectra in the vapor containing many spectral lines. In the liquid, rotations tend to be restricted by hydrogen bonds, giving the librations (vibrations before coming to a total rest). Also, spectral lines are broader causing overlapping of many absorption peaks. Figure C-4 illustrates the water spectra in the vapor and liquid form at different temperatures. Ewing et al. (2003) presented the spectra for water and vapor at 25°C , Figure C-5, and the results were similar to the results presented in Figure C-4. Increased strength of hydrogen bonding, observed from the vapor to the liquid state, typically shifts the stretch vibration (represented in the region around 3400cm^{-1}) to lower frequencies with greatly increase intensity in the absorbance results (Figure C-5).

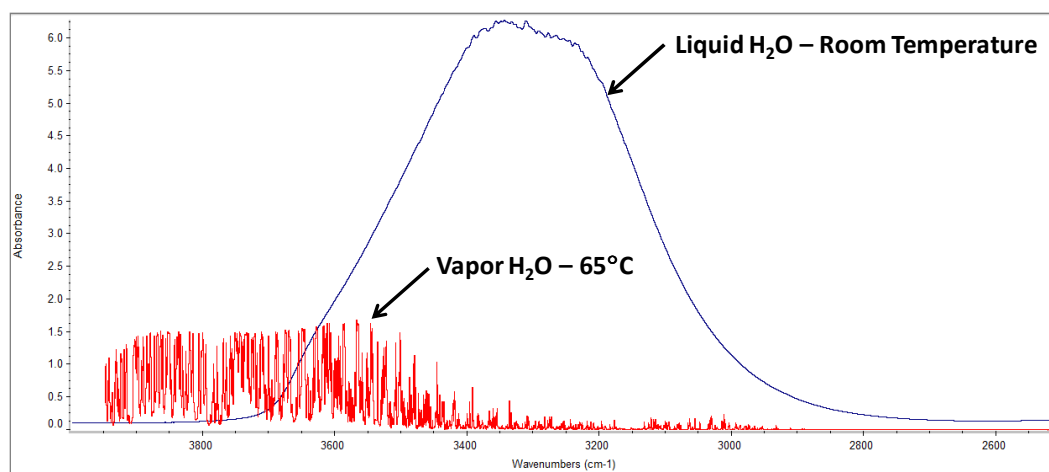


Figure C-4. Comparison of Water Spectra in Vapor and Liquid Form (Source: Termo Fischer Scientific)

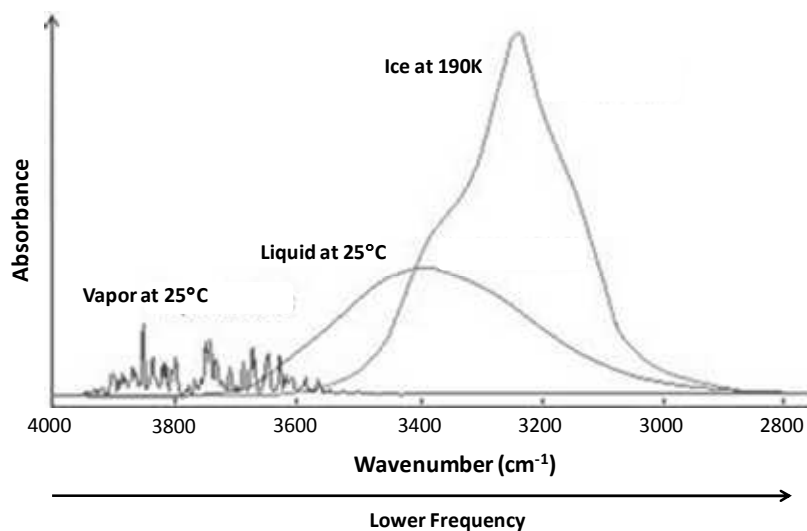


Figure C-5. Illustration of Water Spectra in Different Physical States, Adapted from Ewing et al. (2003)

Hydrogen bonds in liquid water have a broad, smooth, single-peaked distribution of strengths which gradually shifts with temperature. An increase in temperature causes a gradual shift in the direction of the vapor frequency (Figure C-5). At one end of the distributions are hydrogen bonds having strengths comparable with those of hydrogen bonds in ice (Bertie et al. 1969). At the other end are very weak hydrogen bonds, which correspond to the small but appreciable absorption at frequencies approaching those of non-hydrogen-bonded (or free) OH.

These extremes according to Falk and Ford (1966) do not correspond to distinct molecular species.

The frequency of OH stretching vibrations is known to decrease in a regular manner with the strength of hydrogen bonding, while frequencies of bending vibrations increase upon hydrogen bonding but the shifts are much smaller (Falk and Ford 1966). Du et al. (1993) used an infrared technique to obtain the OH stretch vibrational spectra of water at the vapor/water interface. The results presented indicate that more than 20% of surface water molecules have a non-hydrogen-bonded OH (free OH bond) pointing out of the liquid and the other OH, hydrogen bond, pointing into the bulk liquid. The surface vibrational spectra generally exhibit a set of characteristic features indicating that the water molecules form a hydrogen-bonding network which is more well ordered than the bulk. This is more or less expected based on the measured values of the surface tension of water (Shen and Ostroverkhov 2006). Benjamin (1994) also supported the existence of free OH bonds at the surface and showed that the broad peak near 3400cm⁻¹, which corresponds to the OH stretching mode in bulk water, is split into two peaks for water at the surface. The new peak at 3700cm⁻¹ corresponds to free OH bonds. At the vapor/liquid interface, the molecules face an environment on the vapor side with no neighboring molecules to complete the hydrogen bonded to. No matter how a water molecule orients itself at the interface, one hydrogen bond with neighboring molecules is necessarily broken. Du et al. (1993) also studied the temperature dependence of the vapor/water interface spectrum, and based on the data presented, there is no significant change over the temperature range from 10 to 80°C.

Experimental Design

This section presents the experimental design used in this study as well as a description of the materials used, the specimen fabrication processes and the testing and analysis methodology.

Materials and Specimens Fabrication

Three asphalt binders were selected from the Strategic Highway Research Program (SHRP) Materials Reference Library (MRL): AAD is a PG 58-22 grade California Coastal, AAF is a PG 64-10 from W Texas, and ABD is a PG 58-10 California Valley (Jones IV 1993).

Two specimens' configurations are under evaluation: (i) the infrared depth of penetration that exceeds the thickness of the asphalt film, and (ii) the infrared depth of penetration within the asphalt film, or that does not exceed the thickness of the asphalt film

(Figure C-6). Up to this point of the investigation, only liquid water has been considered. Figure 2-2, Section 2, demonstrates the chamber that holds the substrate, the asphalt film and the water. These configurations were used to investigate the rate of diffusion of semi-ordered water molecules (representing the liquid water) and the random water molecules (representing the water vapor at ambient temperature) through the asphalt film.

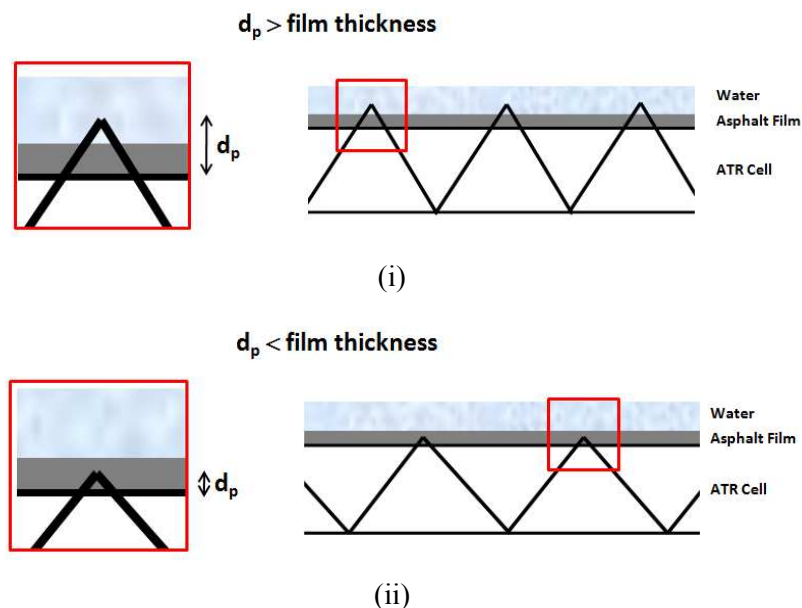


Figure C-6. Film Thickness Configurations used in the Experiments

In the configuration presented in Figure C-6(i), the film thickness has approximately $1\ \mu\text{m}$. The samples were prepared using stock asphalt solutions and the spin coater, according to the procedure described by Vasconcelos et al. (2010). In the second configuration, Figure C-6(ii), neat asphalt binders were heated up to 100°C and pored above the ATR plate (the chamber to hold the water was already attached to the plate). The film thickness could not be measured using the Ellipsometer as the films produced according to configuration (i). Ellipsometer represents a powerful optical tool for studies of organic layers. Given its high precision, this tool can only lead to reliable measurements for films with a maximum of approximately $1\ \mu\text{m}$. For this reason, the film thickness in configuration (ii) was estimated based on the gasket thickness, which has approximately 1mm . In both configurations, the test temperature was kept constant at approximately 24°C . The procedure to determine the diffusivity of water through these binders is described in the following subsections.

Test Method and Analysis Approach

As previously described, the FTIR-ATR has the capacity to differentiate water molecules in different physical states. The detailed test method can be found in a previous publication (Vasconcelos et al. 2010). The region of sample collection should cover at least the frequencies where both physical states of water can be observed, between 3000 and 4000 cm^{-1} (wavenumber). In order to also monitor possible changes in the asphalt binder composition due to the contact with water, the spectra are collected from 900 to 4000 cm^{-1} .

According to the diffusivity results obtained using configuration (i) (Vasconcelos et al. 2010), several months will be required before the liquid water signal can be quantified if 1mm film thickness is used. The intention in use thicker films is in quantify the water vapor diffusion (maintaining room temperature along the test). The authors believe that the water molecules in the vapor state will diffuse faster than the liquid water. Two regions are being evaluated based on the FTIR-ATR spectra acquired: (i) the region representing the liquid water, 3100-3700 cm^{-1} , and (ii) the region representing the water vapor, 3800-4000 cm^{-1} . Figure C-7 illustrates how the infrared depth of penetration varies with the wavenumber (determined using Equation 2-3 in Section 2). In order to determine the diffusivity of liquid water and water vapor in asphalt binders, this difference in infrared depth of penetration should be considered in the Dual Mode diffusion model.

In the analysis procedure, the initial spectrum of the asphalt binder films (without water) was not subtracted from the subsequent spectra after water was added into the chamber. According to Weis and Ewing (1998), large absorption anomalies can be found in the subtraction of the spectra containing strong absorption lines, that is the case for the water in the vapor (or molecular) form. One cause of this anomaly is the part-per-million errors in the wavenumber of the reference laser, which can introduce large errors in subtraction spectra by introducing error into the wavenumber scale of the spectra (Weis and Ewing 1998). This phenomenon is more pronounced when evaluating the region of moisture (or water vapor) manifestation.

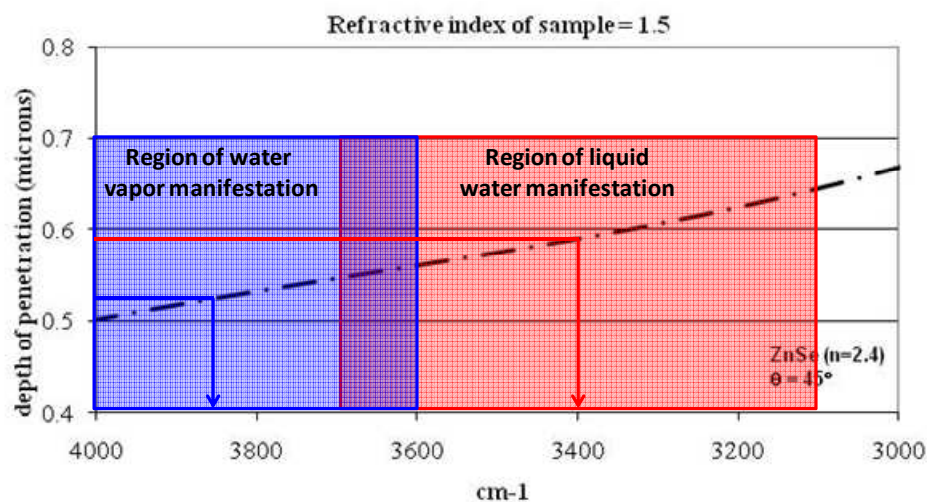
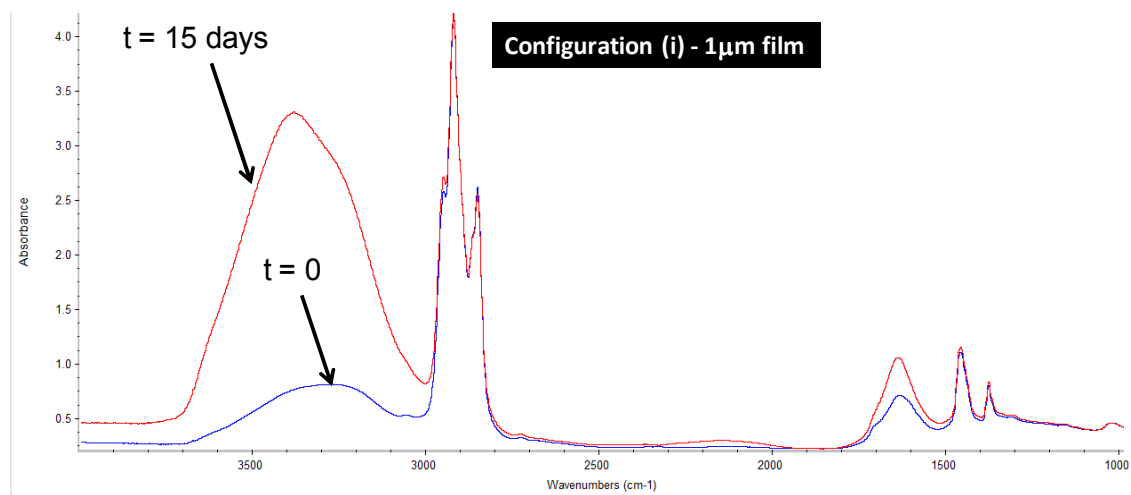


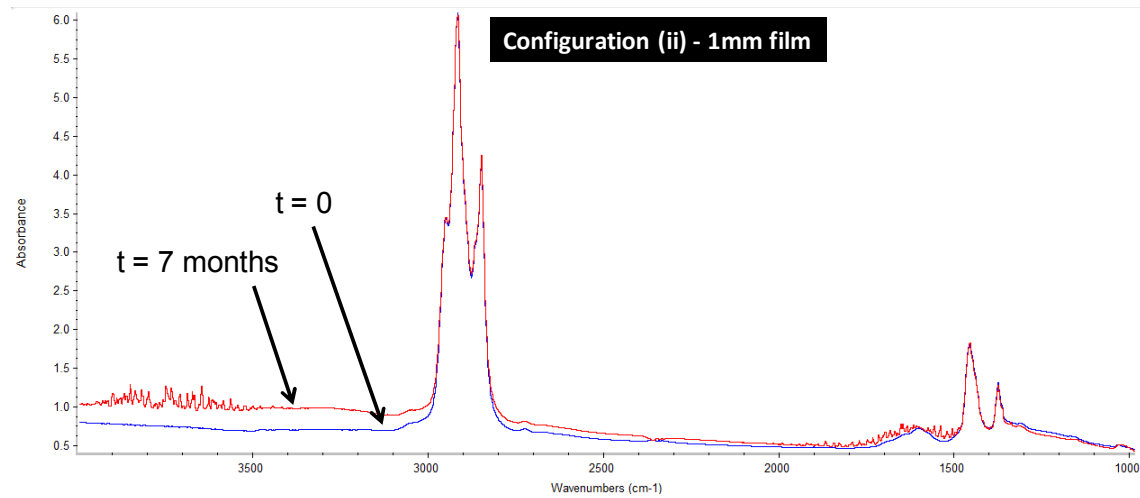
Figure C-7. Difference in the Depth of Penetration in Both Regions Evaluated (ZnSe Crystal with $\theta=45^\circ$, and Refractive Index of Asphalt Assumed 1.5)

Partial Results

Figure C-8 illustrates the first and the last spectra obtained using both configurations. The sample in configuration (ii) is still being monitored, since the pronounced peak characteristic of liquid water has not yet been observed, and the water vapor characteristic absorbance, is still changing with time. Figures C-9 and C-10 present data of absorbance versus time for configuration conditions (i) and (ii), respectively. Side (a) of the respective figures presents data for liquid water and side (b) presents data for water vapor, in both Figures. These are still preliminary results for one replicate of only one asphalt binder. The objective is to quantify the diffusivity for both water physical states, using the FTIR-ATR technique, for three asphalt binders (already in test).



(i)



(ii)

Figure C-8. Partial Results Obtained for Film Thickness in Both Configurations Presented in Figure C-6

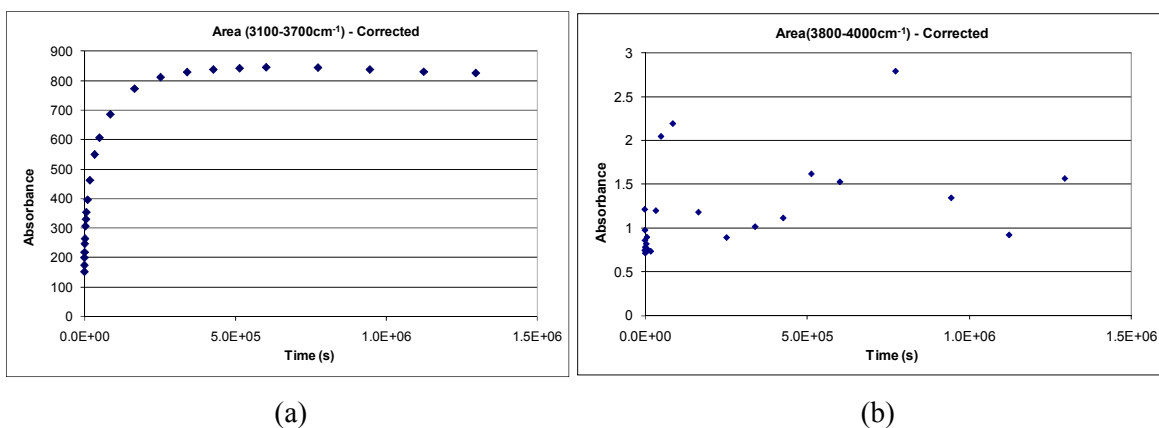


Figure C-9. Partial Results of Absorbance with Time for Asphalt AAD – Configuration (i), (a) Liquid Water Region, and (b) Water Vapor Region

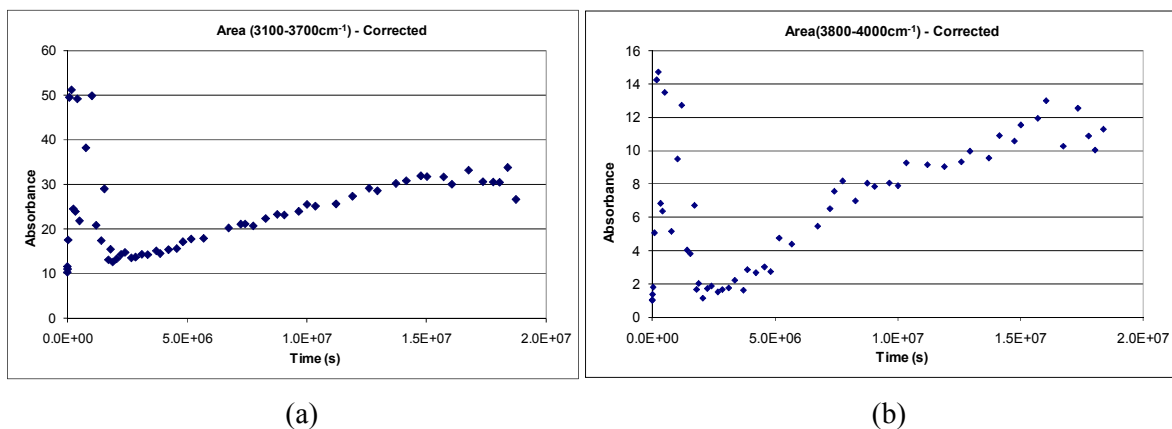


Figure C-10. Partial Results of Absorbance with Time for Asphalt AAD – Configuration (ii), (a) Liquid Water Region, and (b) Water Vapor Region

VITA

Kamilla Lima Vasconcelos received her Bachelor in Civil Engineering degree from the Universidade Federal do Ceará in March 2003. In 2004 she received her Master of Science degree in transportation engineering (with emphasis on highway infrastructure and materials) at the same university. In 2005, she joined Texas A&M University and received her Ph.D. degree in May 2010. Her permanent address is:

Rua José Vilar 910, apt 1702 - Meireles

Fortaleza, CE

Brazil

kamilla.vasconcelos@gmail.com